Numerical Modelling of Groundwater Flow at Mogalakwena Subcatchment, Limpopo Province: Implication for Sustainability of Groundwater Supply

by

Manare Judith Marweshi

Thesis Submitted in fulfilments of the Requirements for the Degree of

Master of Science

in

Geology

in the

Faculty of Science and Agriculture
School of Physical and Mineral Sciences
(Department of Geology and Mining)

in the

University of Limpopo

Supervisor: Prof AZ Tessema

2022

Declaration

I, Manare Judith Marweshi, hereby declare that the work contained in this thesis submitted to the Department of Geology and Mining in the University of Limpopo, for an MSc Degree in Geology, is my original work and has not been previously submitted in this University or any other institution of higher learning and all reference materials contained therein have been fully and accordingly acknowledged.

Signature 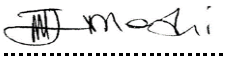

Date 15 December 2021

Acknowledgements

My heartfelt gratitude to my supervisor Prof AZ Tessema for his dedication, guidance, encouragement, support, and patience throughout this research project. Special thanks to Council for Geoscience (CGs) for their financial assistance. I would like to pass my sincere gratitude to Mogalakwena Municipal Officials (Mr Phago KW, Mr Molefe M, Mr Mashishi LJ and Mr Nkwana MP) for their cooperation in permitting me access to the municipal boreholes and ensuring that the fieldwork is successful. I would like to equally thank the municipal representatives (Mr Maaka SJ and Mr Masenya MM) for accompanying me to the field, not overlooking all the pump operators for their cooperation in unlocking the boreholes. I would like to thank Mr Butler MJ and his colleagues at Ithemba Labs for assisting with isotopes laboratory analysis. I am grateful to all my friends, family, and colleague (Mohale Gladness) for their support and motivation throughout this project. Finally, Special appreciation to my mother Marweshi Mpokwane Josephine for her everlasting love, support, and daily encouragements.

Above all, I am thankful to God Almighty for the strength and good health throughout this research project.

Abstract

The Limpopo Province is largely underlain by crystalline basement rocks, which are characterised by low porosity and permeability. The climate in this province is arid to semi-arid, with scarce surface water for domestic and industrial use. As a result, groundwater is the prime source of fresh water supply for various uses. The complex geology, the impacts of climate change and man-made interactions with groundwater and surface water are the main threat to the availability of a sustainable source of fresh water in the province. In addition, despite substantial research efforts conducted by academic institutions and government organisations, there is still a gap in understanding quantitatively the dynamics of the hydrological systems in large parts of the Limpopo Province. The present study is therefore focused on the investigation of hydrological stresses that are applied to groundwater and surface water in one of the catchments situated in the Limpopo Province.

In this study, a three-dimensional steady-state numerical model of groundwater flow was carried out at Mogalakwena Subcatchment, which is situated in the western sector of the Limpopo Province. The area is situated approximately 40 km northwest of Mokopane and 50 km west of Polokwane town. The research aims to understand the dynamics of the exchange between surface water and groundwater, and to assess the influences of these processes on the sustainability of water supply in the area. Hydrologically, the area falls within the boundaries of the Mogalakwena River Catchment, which forms part of the Limpopo River Basin.

Previous studies suggest that there is a continuous decline in groundwater levels in the study area due to extensive use of groundwater for mining, irrigation, and domestic purposes. Furthermore, continued climate changes have altered the rainfall events during the last couple of decades, which consequently had an impact on groundwater recharge, quality, and availability. In addition, the complex geology of the area has an impact on the aquifers' productivity resulting in variability in borehole yields throughout the study area.

To achieve the aims of the research project, a three-dimensional steady-state numerical model of groundwater flow was implemented using MODFLOW NWT and ModelMuse

graphical user interface. The model domain covers an area of 5896 sq. km and was discretised with a grid cell size of 200 m by 200 m. The MODFLOW Packages used include DIS, UPW, RCH, EVT, WEL, GHB, RIV and UZF as well as the ZONEBUDGET. The conceptual model of groundwater flow consists of two layers, and it was developed based on drillhole logs, hydrochemical data, environmental isotopes, geological, digital terrain models, and other spatial data relevant for the conceptualisation of boundary conditions and hydrological stresses.

The results of the steady-state simulation of groundwater flow show that recharge contributes 99.6% of inflow, followed by river leakage (0.36%) and GHB (0.08%). Among the outflow components, surface runoff takes the lion's share (83.3%), followed by evapotranspiration (16.6%) and river leakage 0.02%. The zone budget was implemented to evaluate the interaction between surface water and groundwater by quantifying the amount of water that flows from one zone to the other. This was achieved by assigning zone numbers to the objects that represent boundary conditions (e.g., aquifer, river and dam). Zone 1, 2 and 3 were assigned to the aquifer, river and dam, respectively. The results indicate that the rivers gain more water than they supply to the aquifer. Similarly, the Glen Alpine Dam gain more water from the aquifer than it supplies to the aquifer. This implies that the interaction between surface water bodies such as rivers and dams have a significant impact on the aquifer, which consequently partly contributed to the shortage of water in the area.

A predictive analysis of the aquifer's response to an increase in abstraction rate, evapotranspiration rate and a decrease in recharge was carried out to investigate the future fate of water availability in the study area. The results suggest that as recharge decreases, the river inflow slightly increases to compensate for the declining water level due to the river stage exceeding the piezometric surface. In addition, the decrease in recharge rate is accompanied by a slight decrease in both surface runoff and evapotranspiration rate. Thus, a decline in recharge causes a significant drop in piezometric surface relative to the evapotranspiration extinction depth, which ultimately decreases the rate of evapotranspiration. Similarly, a decrease in recharge rate lowers the depth of the water level below the river stage, which consequently triggers water

exchange from Mogalakwena River to the aquifer. In general, the water balance shows that as recharge decreases by 20% or more, the outflows exceed the inflows resulting in a continuous drop in water level, which may ultimately risk the availability of groundwater in the area.

Table of Contents

List of Figures

List of Tables

Chapter One: Introduction

1.1 Background

Groundwater is the utmost reliable source of fresh water in South Africa compared to surface water due to its high quality, protection from harmful microbial and chemical pollutants, and less impact from long-term drought resulting from climate change (Aral and Taylor, 2011). As a result, groundwater has become very important for domestic water use and industrial activities. The demand for fresh water in the Limpopo Province has significantly increased during the last two decades, resulting in a decrease in water levels owing to overexploitation of groundwater (Tewari and Kushwaha, 2008; Odiyo and Makungo, 2012). Surface water such as rivers also dried out due to groundwater-surface water interaction, i.e., groundwater loses to surface water and vice versa, making groundwater scarce (Aral and Taylor, 2011). Besides the ongoing increasing water demand, natural factors such as climate change, the complexity of the geology and variability of topographic relief, among many other factors have negatively impacted groundwater availability in the Limpopo Province.

The Limpopo Province is largely covered by hard crystalline rocks, which are characterised by limited permeability and porosity (Holland and Witthüser, 2011; Tewari and Kushwaha, 2008; Odiyo and Makungo, 2012). The groundwater availability in such types of rocks is typically controlled by the presence of thick weathered materials that overlies a layer consisting of interconnected fractures, which owe the name to ‘fractured crystalline basement aquifer’ (Holland and Witthüser, 2011). A large part of the province is underlain by the Archean granites, greenstone belts, high-grade metamorphic rocks of the Limpopo Mobile Belts, and volcano-sedimentary rocks of variable age. Thus, the complex geology, climate change, and man-made interaction with surface water and groundwater have contributed to the scarcity and vulnerability of groundwater in this province. In addition, many farmers use groundwater to irrigate their land to improve crop yield during the dry season. Furthermore, in arid areas where rainfall is low and unpredictable, groundwater is the only source of water supply for industrial activities including mining, agriculture as well as domestic water use.

In addition to the complex geology, the Limpopo Province is characterised by a contrasting morphology ranging from flat terrain to rugged and mountain ranges (Cai et al., 2017). The topography in the province is categorised into three distinct regions, which influence the climate (Holland and Witthüser, 2011; Cai et al., 2017). These are:

I. Lowveld region-arid and semi-arid climate,
II. Middle-veld region-semiarid,
III. Escarpment region-subhumid climate.

The climate in the Limpopo Province is sub-tropical to dry savanna, with highly variable precipitation, varying from 200 mm/a in the dry western part to 600 mm/a in the eastern part of the province (Holland and Witthüser, 2011). The climate is largely influenced, among other things, by the continental tropical convergence zone which has a direct impact on the occurrence of water resources in many parts of the province (Holland and Witthüser, 2011). The current changes in climatic conditions have resulted in increased temperatures which causes water stresses as rivers and dams levels drop due to low rainfall and high evaporation rates. During the last two decades, an increase in the development of various sectors such as agriculture and mining coupled with population growth exacerbated the demand for water use. In addition, besides the increased water demands exceeding the supply, the province lacks proper management of the existing water systems.

The Department of Water and Sanitation (DWS) in collaboration with academic institutions has carried out several hydrogeological studies focusing on factors that control the productivity of crystalline basement aquifers in the Limpopo Province (e.g., Holland and Witthüser, 2011). However, there is a knowledge gap regarding the impacts of natural processes such as surface water and groundwater interactions and the changing climate on the sustainable supply of groundwater due to limited studies. For example, if groundwater is continuously utilised and the amount of abstraction exceeds its recharge, the water table significantly declines, which may eventually lead to a dry well. Quantitative analysis of the water budget ensures management, protection, and sustainable use of groundwater. The present study is therefore intended to assess and understand the

hydrogeological system of the Mogalakwena Subcatchment, which is situated in the western part of the Limpopo Province.

1.2 Overview of Study Area

Mogalakwena Subcatchment is located within the Waterberg District, in the western part of the Limpopo Province, covering five local municipalities, namely, Aganang, Blouberg, Lephalale, Modimolle, and Mogalakwena (Figure 1.1). The study area is located 40 km northwest of Mokopane town, bounded between longitude 27.65^{o} E and 29.34^{o} E and latitude 24. 70^{o} S and 22.4^{o} S. The area is subdivided into 14 Quaternary Catchments which include A61H, A62H, A62E, A62F, A63B, A63A, A62J, A62G, A62D, A62C, A62B, A61G, A62A and A61J. Out of the 14 Quaternary Catchments, eight of them were selected for a detailed assessment of the groundwater system through numerical modelling of groundwater flow.

Hydrogeologically, the area falls within the boundary of the Mogalakwena River Catchment, which is one of the major watersheds in the Limpopo Province. There are two major dams, namely, the Doorndraai Dam in the upper reach, while the Glen Alpine Dam is situated in the lower reach of the Mogalakwena River (Figure 1.1). The Doorndraai Dam supplies water for mining, irrigation, and domestic water use, while the Glen Alpine dam largely supplies water for irrigation purposes. Both dams are supplied with water by the Mogalakwena River, which enters the study area from the south and discharges to the north. The river flows north-north-easterly bisecting the study area into the eastern and western sectors. The Mogalakwena River is one of the major perennial tributaries of the Limpopo River occupying approximately 9 400 km^{2} drainage basin.

The geology of the Mogalakwena Subcatchment is relatively heterogeneous and complex. The area is underlain by fractured Archean crystalline basement rocks and granitic rocks of the Bushveld Complex, and porous sedimentary rocks of the Waterberg Group. The geology greatly influenced the topography in the area, in that the slopes are generally flat with hilly areas associated with the Bushveld Complex and Waterberg Group (Figure 1.1).

The study area is characterised by semi-arid climatic conditions receiving a low summer rainfall ranging from 300 mm to 650 mm per annum with maximum temperatures of 33^{o} C (Dube et al., 2020; Dippenaar et al., 2009). The semi-arid climate coupled with high evaporation rates is massively contribute to water scarcity in the area (Dube et al., 2020; Dippenaar et al., 2009). The major economic activities are mining and agriculture, which considerably contribute to increased water demand (Busari, 2008).

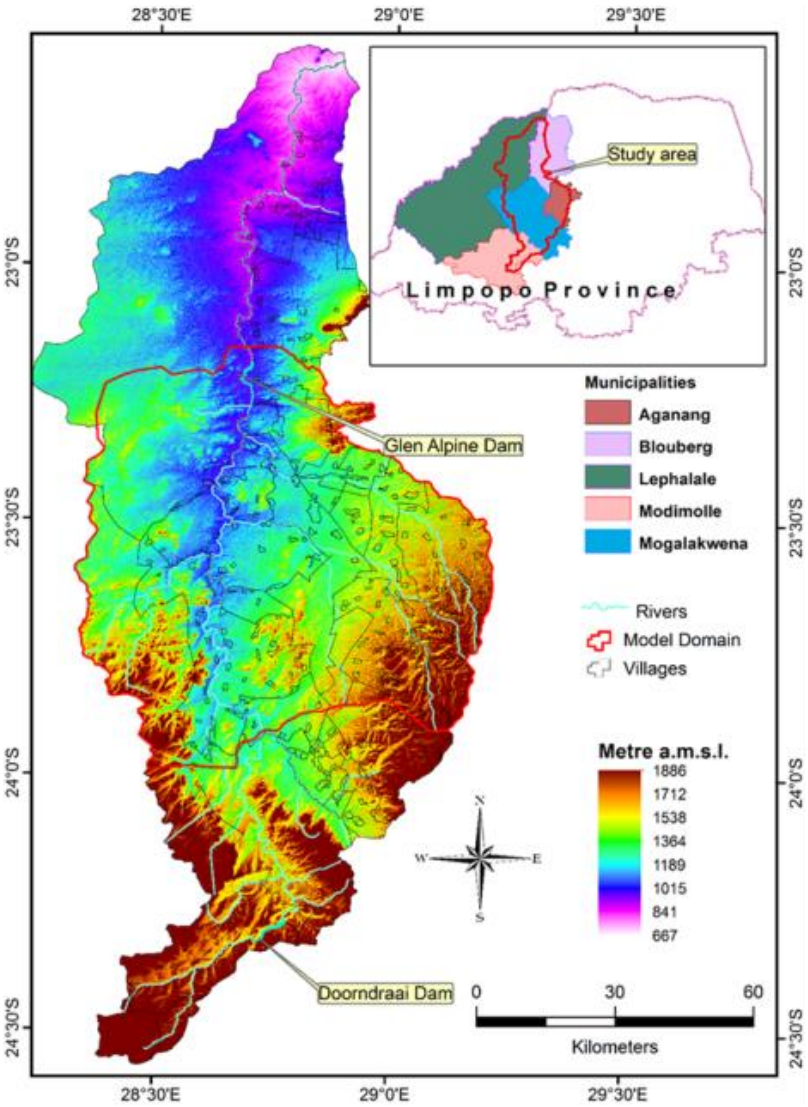

Figure 1.1: Location map of the Mogalakwena Subcatchment showing the two major dams, rivers, and villages. The area shown by the red polygon defines the boundary of the proposed area for the implementation of a numerical simulation of groundwater flow. The inset map shows the study area within the five local municipalities in the Limpopo Province.

1.3 Research Problem

Groundwater is the most reliable natural resource for water supply in both urban and rural areas in the Limpopo Province (Dube et al., 2020). However, during the last decade, climate change has resulted in low rainfall events, which consequently affected groundwater recharge, quality, and availability in various parts of the province. These created challenges, and a tremendous threat to water availability and quality that negatively impacted the continued provision of adequate and safe potable freshwater. The impacts of climate change and high groundwater abstraction attributed to increased population growth have triggered the exchange between surface water and groundwater, which consequently contributed to water scarcity in the Limpopo Province.

Mogalakwena Subcatchment is no exception, there is a substantial decline in groundwater levels in the area in response to the extensive groundwater use for mining, farming, and domestic purposes exceeding groundwater recharge (Broadhurst, 2019; Busari, 2008; Busari, 2009; Fourie, 2016). The declining groundwater levels contributed to an imbalance among hydrologic stresses as the abstraction rates exceeded groundwater recharge (Oljira, 2006). Aquifer response to overexploitation and climate change on water resources need a quantitative examination to ensure the sustainable water supply in the area.

In addition to the declining water levels, the area is characterised by complex geology, which is not well understood from a hydrogeological perspective. The complexity of geology and its impacts on aquifer productivity varies from one environment to another. Due to the differences in aquifers' properties, the borehole yields at Mogalakwena Subcatchment vary widely. Therefore, a detailed hydrogeological study is required to understand the aquifers' productivity and sustainable yield.

In response to the growing demand for water in the subcatchment, The Department of Water and Sanitation (DWS) initiated chain water transfer schemes. The DWS has formulated a water management plan whereby different dams are strictly allocated to certain regions for water supply depending on their capacity. In the process, Doorndraai Dam and groundwater partially supply water to Mokopane, Mogalakwena Platinum Mines and surrounding settlements in the study area (Lombaard et al., 2015). The Glen Alpine

Dam mainly supplies water to the emerging farms and the surrounding villages (Lombaard et al, 2015). Additional water is sourced outside the study area from the Flag Boshielo, Roodeplat, Donkerpoort and Welgevond Dams to supply Mogalakwena mine, Modimolle region, Mokgopong and surrounding farms, respectively (Lombaard et al., 2015).

Despite the measures currently in place to mitigate water shortage by the DWS, there is inadequate understanding of the groundwater system in the area. The impacts of climate change on surface water and groundwater coupled with the overuse of water are not well understood. Thus, there is an urgent need for undertaking a quantitative analysis of the stresses that are applied to the hydrological system. This will help to mitigate the prevailing water scarcity and ensure the best management practices that enable the sustainable use of this valuable resource in the area (Roefs, 2001). Estimation of the current groundwater resource is required to ensure proper planning and water management that enable sustainable use of water without adversely affecting future demand.

1.4 Motivation

There are several villages in the study area, which largely depend on Glen Alpine and Doorndraai Dams and Mogalakwena River for crop production and domestic water use. In addition, several boreholes were drilled for rural water supply by the five local municipalities and the DWS. According to the hydrogeology concept, the Doorndraai and Glen Alpine Dams and the Mogalakwena River are anticipated to exchange water with the underlying groundwater aquifers. The exchange can be due to change in the piezometric surface of the aquifers and the river stage, including the fluctuation of the dams' water level that allows water flux from one system to another. In addition, the conductance of the sediments that form the riverbed and bottom of the dams is essential in allowing the exchange between surface water (rivers and dam) and groundwater. These processes of exchange of surface water (rivers and dams) with groundwater are largely driven by natural processes such as climate change, local geology (the type of rocks), and anthropogenic activities (excessive use of groundwater and change in land use, among others).

The long-term interaction between the two broad categories of water systems in the area can have a significant impact on the availability and sustainability of the water supply. This is because any hydrologic stress applied to surface water will have a direct impact on groundwater, or vice versa (Anderson et al., 2015). This research project is therefore crucial to assess and evaluate the exchange between the surface and groundwater to understand the impact of these processes on the future fate of groundwater and surface water availability and sustainability in the area.

A review of the available literature shows loopholes in the hydrogeological understanding of the sustainability of groundwater supply within the Mogalakwena Subcatchment (for example, Holland and Witthüser, 2011). This is due to the complexity of the hydrogeological characteristics of the Subcatchment and the lack of availability of suitable data to model the flow of groundwater in the underlying rock formation.

Currently, several platforms and computer codes for the simulation of groundwater flow with varying degrees of capabilities are available for researchers and hydrogeological practitioners. Such platforms and simulation tools for groundwater flow modelling help to understand and evaluate the dynamics of the interaction between surface water and groundwater. The present study is therefore intended to apply numerical modelling of groundwater flow to quantify and assess the prevailing stresses that are applied to the hydrological system in the area. The results of the model will allow evaluation of the interaction between the aquifer and surface water and the aquifers' response to changes in climate, and excessive abstraction (Regli et al., 2003). In addition, the results will enable us to forecast future scenarios that are associated with water use and climate change, thus making the management and sustainable utilisation of groundwater and surface water possible.

1.5 Research Aims and Objectives

The study aims to achieve the following:

I. To understand the dynamics of the exchange between groundwater and surface water and evaluate its impacts on the sustainable supply of water resources,

II. To investigate the control of groundwater availability and identify areas suitable for borehole drilling,

III. To identify the main factors that contributed to the degradation of groundwater quality.

The objectives of the study are to:

I. process spatial data that are relevant for the determination of groundwater flow direction, source, and sink,

II. generate water balance and assess the flux between various boundary conditions,

III. compile water-level data at monitoring wells,

IV. process spatial data that are required for building boundary conditions,

V. estimate hydraulic parameters (e.g., hydraulic conductivity and transmissivity) of the aquifers that are required for modelling groundwater flow,

VI. process borehole log data that is relevant for the determination of MODFLOW Layer Groups (hydrostratigraphic units) thereby defining confined, unconfined, and convertible layers,

VII. compile climate data such as rainfall, temperature, and evapotranspiration that are relevant for numerical simulation of groundwater flow,

VIII. process topographic, borehole data, land cover, soil, and lithological data that enable the definition of hydraulic conductivity zones,

IX. process geological data, lineaments, soil, land cover, slope and stream density to produce groundwater potential map.

1.6 Research Questions

I. How does surface water-groundwater interaction affect water balance dynamics?

II. How will the status of groundwater affect the livelihood of Mogalakwena Subcatchment communities in future?

Chapter Two: Literature Review

2.1 Introduction

Groundwater is the fundamental natural resource and alternative solution to the current water challenges in South Africa. A proper understanding of the groundwater system is required to ensure water management and protection. Several studies were conducted on groundwater quality at the Nyl/Mogalakwena River during the last two decades, mostly focussing on aquatic life (Phungula, 2018). However, there are limited studies related to quantitative analysis of the hydrological stresses that apply to groundwater and surface water. In the following section, the summary of water use and challenges are presented based on the previous studies.

2.2 Water Challenges and Use

Mogalakwena Subcatchment is the most industrialised and densely populated area within the Limpopo Water Management Area (Lombaard et al, 2015). The demand for groundwater has recently increased around Mokopane town due to emerging platinum mines (Busari, 2008). The increase in abstraction rates was recorded between the years 1995 and 2002 resulting in a decline in groundwater levels (Busari, 2008). The excessive abstraction of groundwater alters the water balance by depleting base flow, inducing transmission losses and a decline in evapotranspiration through the root zone (Lombaard et al., 2015). Furthermore, the dewatering processes at the mines also affect the interaction between groundwater and surface water (Lombaard et al., 2015).

Mogalakwena Subcatchment receives unevenly distributed seasonal rainfall, which is coupled with high evaporation rates resulting in water shortages (Zhu and Ringer, 2012; Moalafhi et al., 2017). According to Roefs (2001), the study area receives a five-year rain cycle, i.e., dry for five years followed by wet for five years. These rainfall patterns cause an imbalance in the groundwater system as abstraction rates exceed recharge rates, particularly during the dry cycle of rainfall events, which consequently resulted in a decline in groundwater level (Busari, 2008).

The rapid population growth, agricultural activities, and expansion of mines are a threat to groundwater and surface water resources (Moalafhi et al., 2017). Anthropogenic activities such as land use, abstraction for domestic use, and irrigation influence surface runoff and evaporation, which consequently have an impact on groundwater resources. In addition, the rural population largely depend on groundwater, particularly during the dry season putting additional stress on the aquifer system (Lombaard et al., 2015).

2.3 Groundwater Modelling

A model is defined as a simplified representation of a complex natural world used to interpret and understand environmental issues with a complex interaction of various variables in a system (Anderson et al., 2015; Elango, 2005). Groundwater models are utilised worldwide on different hydrogeological conditions, mainly to answer questions concerning groundwater management (Elango, 2005; Kumar, 2013). In the past years, groundwater models have been used globally as reliable tools to investigate the impacts of groundwater abstraction on the environment, surface water-groundwater interactions and predict future stresses on groundwater system (Gebere et al., 2021).

The increasing population rate and changes in climate coupled with complex geology greatly impacts groundwater availability in the Limpopo Province. The application of groundwater models has been the best approach to understand the dynamics of the groundwater system. However, numerical models demand a lot of data and the simplification of the natural system need a good understanding of the groundwater system (Anderson et al., 2015). A review of the available literature shows loopholes in the hydrogeological understanding of the sustainability of groundwater supply within the Mogalakwena Subcatchment (for example, Holland and Witthüser, 2011).

Hydrogeologists use groundwater flow models to investigate hydrologic systems and develop water management strategies (Reilly and Harbaugh, 2004). Groundwater models are utilised worldwide to understand groundwater systems, estimate the properties of aquifers, and have an insight into understanding the past, present, and future scenarios (Reilly and Harbaugh, 2004). Kumar (2013), further highlighted the following advantages of groundwater modelling:

I. improvement of understanding of the hydrogeological system and aquifers' behaviour by combining historical and present aquifer information,
II. assessment of groundwater resources (recharge, discharge, and storage system)/ water balance,
III. aid in decision-making concerning groundwater resources and implementation of groundwater management strategies,
IV. prediction of the possible fate and movement of contaminants for risk evaluation,
V. it enables the designing and development of groundwater rehabilitation measures.

2.4 Development of a Groundwater Flow Model

Groundwater flow models are constructed by following a certain sequence of essential steps. As highlighted by Anderson et al. (2015) and shown in Figure 2.1, flowcharts can be used to provide a summary of the steps that are required for the groundwater flow model. The initial step of any groundwater model involves the identification of the problem which involves literature review, preliminary analysis of existing data, and field data collection (Reilly and Harbaugh, 2004). The determination of the problem enables the modeller to identify and state the purpose of the groundwater model (Anderson et al., 2015).

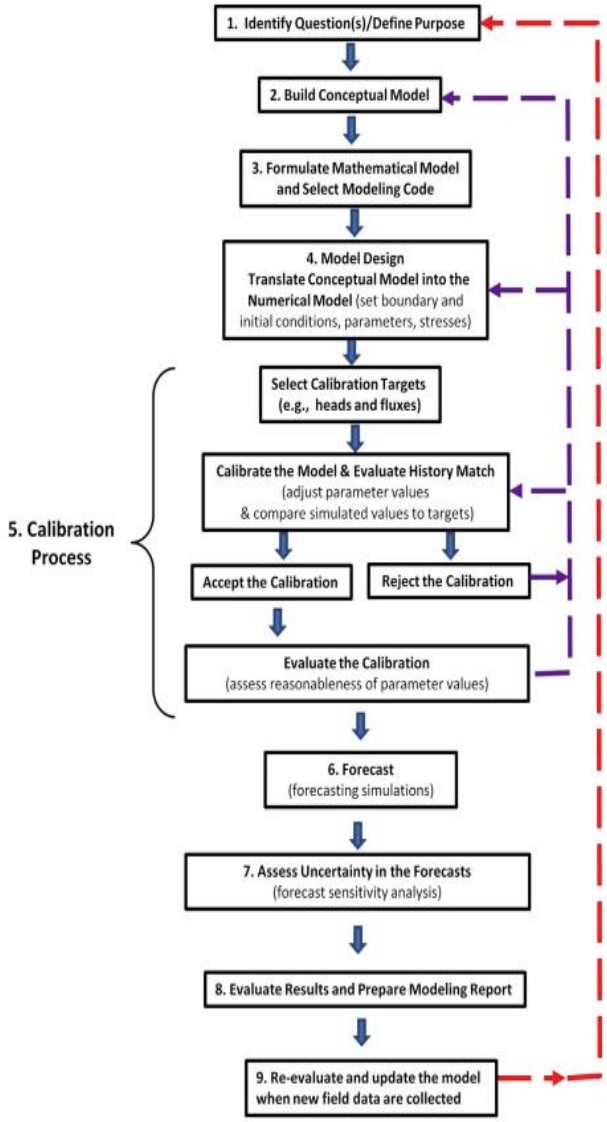

Figure 2.1: Simplified workflow of groundwater modelling (after Anderson et al., 2015).

2.4.1 Conceptual Model

A conceptual model is a descriptive element of a groundwater flow system that considers associated surface water bodies, hydrostratigraphic units and system boundaries (Anderson et al., 2015). The development of a conceptual model provides the framework for the implementation of a numerical model that enables solving complex hydrogeological problems (Anderson et al., 2015). The conceptual model also includes

estimations of groundwater budgets and may require field observations to overcome any uncertainties (Anderson et al., 2015). According to Bear et al. (1992), a conceptual model may include the following: geometry of target area, geology, flow regime, water properties, sources and sinks of water, initial conditions in the considered domain and boundary conditions of the area of interest, which interact with the aquifer system. Below is the summary of the contents of the most important parameters of the conceptual model:

I. Hydrostratigraphy

Hydrostratigraphy involves the characterisation of the stratigraphy, thickness, and lateral extent of hydrostratigraphic units, structural and geomorphologic discontinuities, and classification of aquifer type (Merz, 2012). According to Elango (2005), any geological information acquired from the borehole logs should be translated to information related to the water-bearing formation and non-water bearing formation. The type of aquifer controls the storage, water flow and solute transport throughout the model domain (Merz, 2012). The determination of hydraulic properties and specific yields of the aquifers is important to understand the homogeneity/heterogeneity of the aquifers within the targeted area (Merz, 2012).

II. Model Boundaries

The conceptual model involves the establishment of the boundaries where groundwater flow exits as well as inflow into the aquifer system (Merz, 2012). Boundary conditions are the key components of the mathematical model and have a strong influence on the direction of flow calculated from the steady-state and transient models (Anderson et al., 2015). Boundary conditions specify the interaction between the aquifer system and the environment (Elango, 2005). These boundaries control the flow direction and influence the water balance of the numerical model. These include regions where the flow of water enters or exits the hydrogeological system of the model domain (Merz, 2012). The geometry of the boundary should be delineated and the definition of the process occurring at the boundary (recharge/discharge) is essential (Merz, 2012). These boundary conditions are determined from geologic, topographic and piezometric maps of the study areas (Anderson et al., 2015).

III. Stresses

Hydrogeological stresses can result from both climatic and anthropogenic including pumping, recharge, and evapotranspiration (Merz, 2012). Parameters to be considered include volumetric flow rates, constants/fluctuations over time, and the spread of monitoring stations (Merz, 2012). Hydrometeorological data including long term rainfall patterns, surface runoff, soil thickness, evapotranspiration and infiltration rates are required to understand groundwater recharge (Elango, 2005).

2.4.2 Mathematical Model

Mathematical models indirectly describe the physical processes and boundary conditions of groundwater systems through definitive equations (Kumar, 2013). The mathematical model comprises partial differential equations with appropriate boundary and initial conditions expressing conservation of mass and Darcy's law as well as describing continuous variables within the model domain (Elango, 2005). The governing equations express similar information of hydrogeological processes occurring within the model domain as the conceptual model (Bear et al., 1992). Bear et al. (1992), indicated that a mathematical model comprises of the following information: geometry of the area of interest, equation expressing the water balance, flux equation relating the fluxes of the considered extensive qualities to the state variable of the problem, the equation defining the behaviour of fluids and solids, equation expressing initial and boundary conditions.

2.4.3 Numerical Model

Numerical models are widely utilised to assess the impacts of water stresses such as pumping on the aquifer and simulate groundwater balance in complex hydrological systems. Numerical models are derived from the conceptual model and involve designing the grids/mesh, assigning values of hydrologic stresses and aquifer parameters, selecting time steps, setting boundaries for transient models, and setting initial conditions (Anderson et al., 2015). The numerical model is run with the initial setup of input parameters assigned from the conceptual model (Anderson et al., 2015). The following are the advantages of numerical modelling (Kareem, 2018; Loudyi, 2005):

I. ability to simulate complex hydrogeological systems,
II. capability to simulate multi-dimensional groundwater systems,
III. simulation of both spatial and temporal distributions of various model outputs,
IV. coordination of both steady-state and transient conditions,
V. harmonisation of spatial variability of the input parameters,
VI. fast, accuracy and reliability of model calculations,
VII. incorporation of complex boundary conditions.

Numerical models comprise five techniques, namely finite difference, boundary element, integrated finite difference, finite volume, and finite element methods (Loudyi, 2005). Finite element and finite difference methods are the commonly used approaches; the two methods consist of nodal superimposed over the model domain (Anderson and Woessner, 1992). However, the finite element uses irregular arrays of elemental units to understand the dynamics of the system using triangular techniques, while the finite difference uses regular rectangular grids (Anderson and Woessner, 1992). Furthermore, the finite element defines the variation of the head within the element using interpolation function, while finite-difference defines the head of the nodal points based on either a block-centered or mesh-centered grid (Anderson and Woessner, 1992). The finite difference method is used in MODFLOW; thus, the model transforms differential equations into algebraic equations through spatial discretisation of the hydrogeological domain (Zdechlik, 2016).

2.4.4 Model Calibration

The calibration process is essential for the establishment of the legitimacy of both conceptual and numerical models (Anderson et al., 2015). This process involves the adjustment of model input parameters to have a better correlation between observed and simulated heads (Reilly and Harbaugh, 2004). The calibration model can be operated manually or automatically through linear regression statistical techniques (Reilly and Harbaugh, 2004).

2.4.5 Sensitivity Analysis

Sensitivity analysis is the assessment of the model's input parameters to understand how the model's output (heads and flows) parameters are affected while applying incremental changes to the input parameters (Reilly and Harbaugh, 2004). The process enables the modeller to determine parameters that should be accurately defined and the parameter which is already accurately determined (Konikow, 1996). Sensitivity analysis involves changing model parameters in realistic quantities and observing relative changes in model response (Elango, 2005). The sensitivity analysis aims to quantify the impacts of uncertainties in an approximation of model coefficient including boundary conditions, aquifer parameters and stress (Loudyi, 2005). Parameters that are more sensitive to the model require further characterisation and additional data can be sourced from the field (Kumar, 2013; Konikow, 1996). In the absence of fieldwork, sensitivity analysis assists in evaluating the reliability of the model by providing a range of uncertainty and error in the input data (Konikow, 1996).

Chapter Three: Description of the Study Area

3.1 Introduction

Detailed studies on geology, morphology, climate, land cover and land use are required to understand the control of groundwater movement and its availability. This is because factors such as lithology, Morphology, surface water and lineaments control the occurrence of groundwater (Holland and Witthüser, 2011). In the following sections, these features are summarised to understand their influence on aquifer availability and productivity in the area.

3.2 Geology

The geology of Mogalakwena Subcatchment is classified into six broad lithological domains, namely, Archean granites, Transvaal Supergroup, Bushveld Igneous Complex, Soutpansberg Group, Waterberg Group, and Karoo Supergroup. The Goudplaast and Hout River Gneisses cover the southeastern parts of the area and vary from homogeneous to strongly layered; from fine-grained to pegmatoidal, and from leucocratic to dark grey, suggesting local incipient anatexis (Robb et al., 2006) (Figure 3.1). The gneisses were intruded by Moletsi, Utrecht, Matlala, and Mashashane granites which occur as batholiths and plutons (Holland, 2012). The northern parts of the Mogalakwena Subcatchment are marked by Alldays Gneiss of the Central Zone of the Limpopo high-grade metamorphic belt.

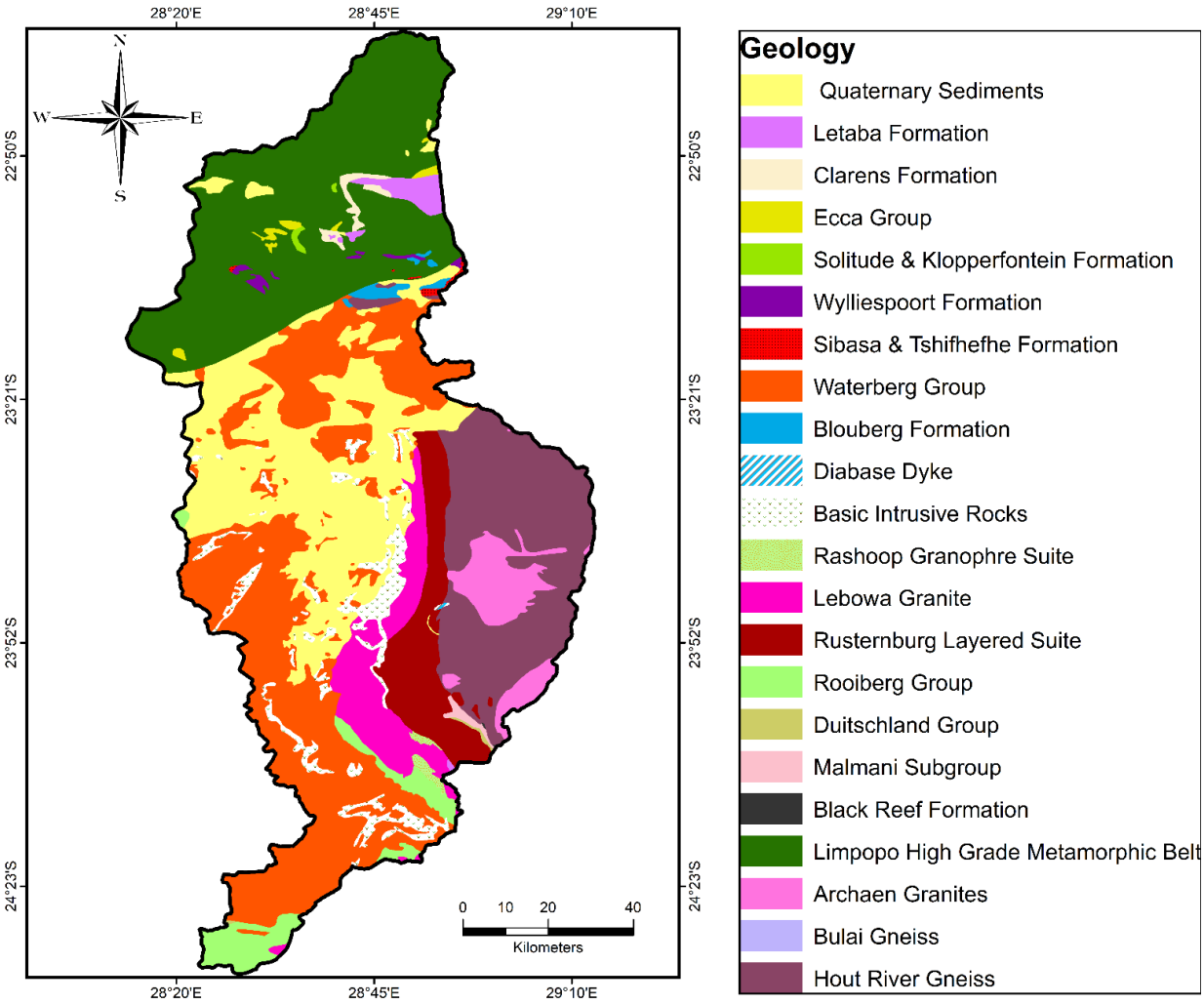

Figure 3.1: Geological map of the study area showing different lithologies.

In the study area, the Transvaal Supergroup volcanic and sedimentary rocks of the overlie the Hout River Gneiss and the granite intrusive rocks (Hartzer, 1995). The basement of the Transvaal Supergroup is marked by the Blackreef Formation consisting of quartz arenites with lesser conglomerates and subordinate mudrocks (Eriksson et al., 2006). Dolomitic rocks of the Malmani Subgroup of the Chuniespoort Group and conglomerates of Duitschland Formation of the Pretoria Group in the southeastern parts of the area. The lavas of the Rooiberg Group (Kwaggasnek and Schrikkloof Formation) overlie the Pretoria Group (Schweitzer et al., 1995). The Pretoria Group was intruded by the Rustenburg Layered Suite of the northern limb of the Bushveld Complex later and uplifted the

Rooiberg Group lithologies (Eriksson et al.,1995). According to Eriksson et al. (1995), rocks of the Rustenburg Layered Suite and Rooiberg Group were intruded by younger rocks such as the Lebowa Granites of the Bushveld Complex.

Two formations of the Soutpansberg Group, namely Sibasa and Williespoort are distinct in the study area (Figure 3.1). Groundwater occurrence in these rocks is associated with well-sorted sandstones and along with the contact between the dykes and the host rocks. (Bumby et al.,2004). The Soutpansberg Group is overlain by the sedimentary rocks of the Waterberg Group consisting of various types of sedimentary and volcanic rocks. Swaekhoek Formation is well preserved in limited areas within the Nylstroom protobasin along the Thabazimbi-Murchison Lineament (TML). The Waterberg Group rocks cover the southwestern and central parts of the study area (Figure 3.1). Groundwater occurrence within these rocks is restricted to the sandstones and fractured volcanic rocks.

The Waterberg Group rocks are overlain by the Karoo Supergroup lithologies, which include the Ecca Group and Clarens Formation. The central part of the Mogalakwena Subcatchment is largely covered by the Quaternary sediments consisting of sand, shales, and siltstones (Figure 3.1). The borehole logs in this area indicate that the thickness of the sediment extends up to a depth of 100 m. Table 3.1 and Figure 3.1 show the geology and stratigraphy of the Mogalakwena Subcatchment, respectively.

In general, the study area is comprised of complex lithological units varying from high-grade metamorphic rocks to Quaternary sediments, which owe the complexity of aquifer types ranging from inter-granular to fractured aquifer systems. Thus, as outlined by Holland and Witthüser (2011), the occurrence of groundwater in the Mogalakwena Subcatchment depends on the following parameters:

I. the depth and nature of regolith,
II. the development of fractures and fault zones,
III. the existence of highly permeable zones such as well sorted sandstones and alluvial deposits along major rivers.

Table 3.1: A geological history of the major igneous/metamorphic/ sedimentary events in the Mogalakwena Subcatchment (McCarthy and Rubidge, 2005; Barker et al., 2006; Robb et al., 2006; Eriksson et al., 2006 and Kramers et al., 2006).

Units		**Lithologies**	**Age**
Quaternary sediments		Sandstone	+/-65 Ma
Letaba Formation		Basalt	+/-180 Ma
Karoo Supergroup	Clarens Formation Ecca Formation	Sandstone, mudstone	250-180 Ma
Waterberg Group		Arenites, Conglomerates Mudrocks	2060-1700 Ma
Soutpansberg Group		Lava	
Bushveld Complex	Lebowa Granite Rashoop Group Rusternburg Layered Suite	Granites Gabbro, Norite, Clinopyroxene, Hartzburgite	~2050 Ma
Rooiberg Group	Schrickkloof Formation Kwagasknek Formation	Rhyolite	2061-2052 Ma
Transvaal Supergroup	Duitschland Formation Malmani Group	Carbonates conglomerate Dolomites	2612-2432 Ma
Blackreef Formation		Conglomerate Shale	~2650 Ma
Limpopo High-Grade Metamorphic Belt	Gumbu Group, Malala Drift Suite, Alldays Gneiss Messina Suite	Gneisses	2,0 Ma-3,15 Ma
Archaean Granite	Mashashane, Matlala, Utrecht and Moletsi Granites	Granites	Neoarchaean intrusions (2800-2500 Ma)
Goudplaast-Hout River Gneiss		Gneiss	Palaeoarchaean intrusions (3600-3200 Ma)

3.3 Structural Geology

Fractures are important linear features controlling groundwater occurrence. They occur as joints, folds, fissures, and faults, and they originate from the brittle deformation of rocks at the upper crustal level. Folds are produced by ductile deformation, and they are exhibited as anticlines and synclines. The identification of these structures is important for the selection of target zones for detailed groundwater exploitation. The spacing, aperture, orientation and interconnection of the lineaments play a critical role in the movement and occurrence of groundwater in fractured rocks (Preeja et al., 2011).

Figures 3.2 and 3.3 show the expression of major lineaments on the aeromagnetic map of the Mogalakwena Subcatchment. The lineaments are oriented ENE-WSW and NW-SE as shown on the aeromagnetic maps of the area (Figures 3.2A and 3.2B). Some of these lineaments portray a NE-SW trend, which appears to be influenced by the trend of the Thabazimbi-Murchison Lineament (TML) as outlined by Holland (2012). The ENE-WSW striking lineaments are associated with intense shearing within the Southern Marginal Zone of the Limpopo Mobile Belt. The shear zone is characterised by northward steeply dipping (270°) with a reverse sense of movement, which collectively forms the Hout River Shear Zone, Matoks, and Petronella Shear Zone that are linked together by near-vertical, north-trending strike-slip fault systems (Holland, 2012).

The study area forms part of the northern lobe of the Bushveld complex which intruded the Transvaal Supergroup. In addition, the study area is proximal to the Southern Marginal Zone of the Limpopo Mobile Belt, which consists of several east-west striking shear zones, folded and faulted structures along which secondary porosity is expected to occur. During the emplacement of the Bushveld Complex, the Transvaal Supergroup was subjected to lateral and vertical compressional forces resulting in localised shearing along the contact zones and faulting, which consequently develop secondary porosity.

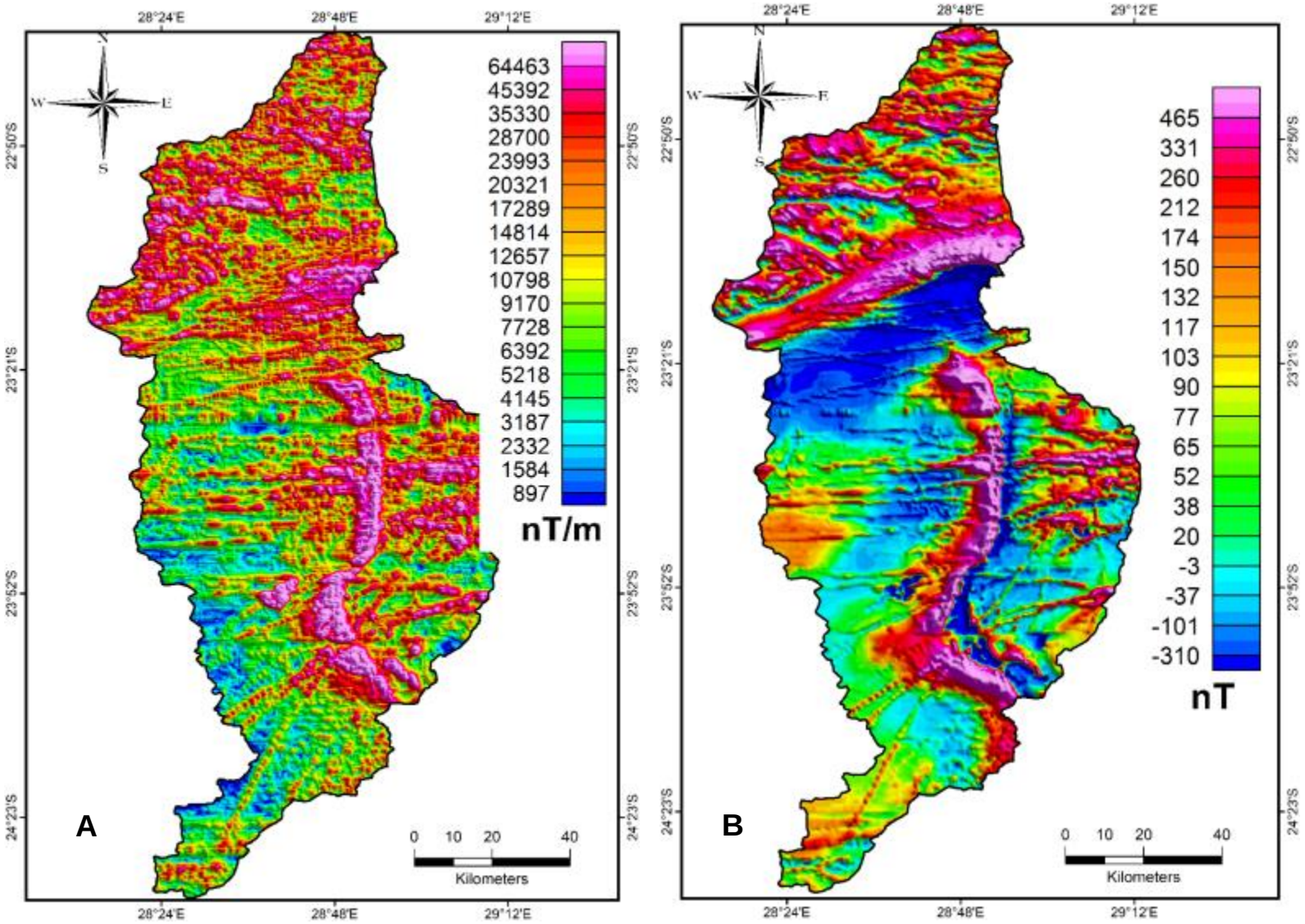

Figure 3.2: Total magnetic intensity (A) and Analytical Signal Magnetic (B) maps of the area.

This suggests that there are several crustal-scale faults, shear zones and folds, which predate and postdate the emplacement of the Bushveld Complex within the study area. The evidence for faulting and folding in this region can be supported by the linear features shown on the aeromagnetic maps (Figures 3.2 and 3.3). Most of these linear features are striking E-W, NNE-SSW and minor NW-SE and NE-SW striking lineaments (see the rose diagram shown in Figure 3.3B). The E-W and NNE-SSW lineaments are the most prominent, though N-S and NW-SE striking structures are observed (Figures 3.2 and 3.3). These structures are generally essential for the development of secondary porosity or fractured and weathered aquifer systems within the crystalline rocks that consist of intrusive and extrusive igneous rocks.

The continuity of the Bushveld Complex in the study area is interrupted to the north by the Palala Shear Zone. As suggested in the previous studies, the Thabazimbi-Murchison Lineament (TML) separates the northern limb of the Bushveld Complex from the western and eastern limbs (Holland, 2012). The major faults in the southern parts of the Mogalakwena Subcatchment are the northeasterly striking Ysterberg and east-west striking Zebediela Faults (McCarthy, 2011). The Zebediela Fault is part of TML, whereas Ysterberg Fault is considered to be Riedel Shear Zone which is associated with TML (McCarthy, 2011). Evidence of faults striking N-S is shown in Figures 3.2 & 3.3 in the southern portions of the study area. As indicated by Tooth et al. (2002), the juxtaposition of the Karoo Supergroup sedimentary rocks against the mafic rocks of the Bushveld Complex was influenced by the Zebediela Fault.

In the northern part of the study area, the preserved sediments of the Blouberg Formation are characterised by steeply dipping bedding planes (Bumby, 2007). The Blouberg Formation comprises northward-steeply dipping reverse faults with strata being overturned (Bumby et al., 2004). Hahn (2011) noted that the Blouberg Formation is preserved in an isolated small pull-apart basin above the Palala Shear Zone. The Waterberg Group is fault-controlled, bounded in the south and north by Melinda Fault and Thabazimbi-Murchison Lineament (TML), respectively (Eriksson et al., 2008). Melinda Fault zone is interpreted as a long-lived, fundamental, strike-slip fault system that is

responsible for the reactivation of the Palala Shear Zone. Thus, the Melinda Fault and Thabazimbi-Murchison Lineaments are striking ENE-WSW and have influenced the direction of most lineaments in the study area (Figure 3.3A).

The NW-SE striking Vaalwater Fault bisects the Waterberg Group rocks and bounds Makgabeng-Aasvoelkop Formation to the North (Erriksson et al., 2008). Makgabeng Formation of the Waterberg Group is preserved as an inclined foreset, few bedding faces exhibit inclination, indicating that the formation is tectonically undisturbed (Bumby, 2007). This formation is cut by several dykes with complex orientations (Hahn, 2011).

The intersection of lineaments in crystalline rocks is significant for the development of pathways for groundwater recharge to occur (Rao, 2006). The above summary of the tectonic history in the area suggests that cross-cutting of lineaments is significant to enhance the permeability of crystalline rocks. The rose diagram in Figure 3.3B summarises the general trends of lineaments resulting from tectonic events that occurred within and around the study area. The lineaments within the Mogalakwena Subcatchment are characterised by complex orientation with most of them striking ENE-WSW, E-W, and ESE-WNW though few lineaments show NNW-SSE and N-S. Lineaments with a crosscutting trend can increase the length of the fractures increasing the pathway for groundwater infiltration.

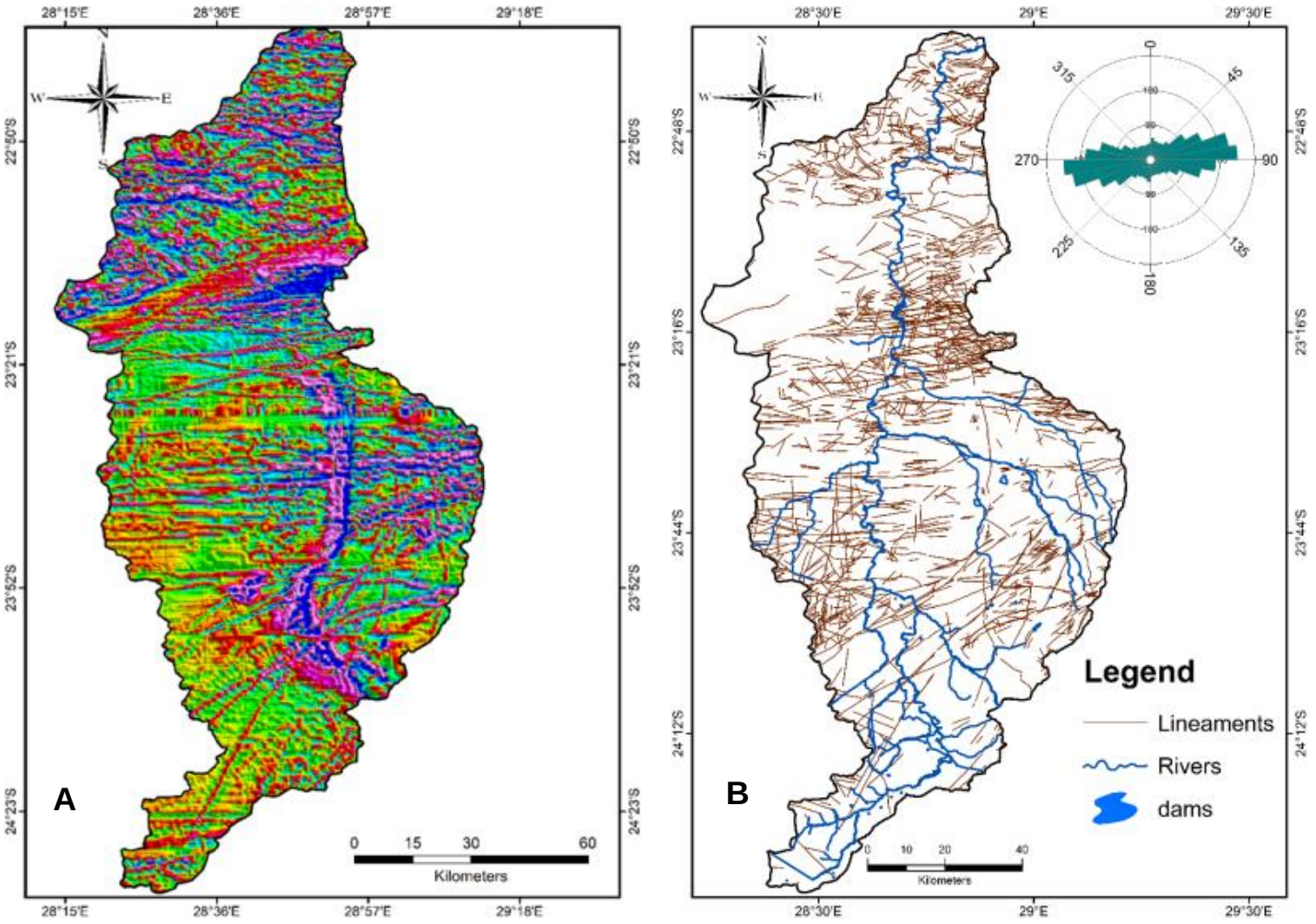

Figure 3.3: Vertical derivative magnetic (A) map of the area showing linear magnetic features that correspond to structures such as faults and dykes. (B) map of lineaments derived from interpretation of the three magnetic maps (cnf. Figures 3.2A, 3.2B and Figure 3.3A).

3.4 Hydrogeology

Considering the broad lithologic domains summarised in Section 3.2, the Mogalakwena Subcatchment can be categorised into two types of aquifers, *viz*., intergranular, and fractured or weathered basement aquifers. The intergranular aquifers are influenced by the sandstone of the Waterberg Group, the Quaternary Sediments and the alluvial deposits along the Mogalakwena River and low-lying areas that are situated in the central and southern parts of the area (Figure 3.4). The weathered and fractured aquifers are mainly associated with the mafic and ultramafic rocks of the Bushveld Complex and the Archaean granite gneisses that are in the southeastern and eastern parts of the area (Figure 3.4). In addition, the fractured and weathered aquifers are anticipated to occur within the high-grade metamorphic rocks of the Limpopo Belt in the northern part of the study area.

Intergranular aquifers are common within the Waterberg Group sedimentary rocks, where the rock formations are loose and unconsolidated, e.g., sand and gravel deposits (Lourens, 2013). However, borehole logging shows that the weathered aquifer is not well developed in the area. The fractured aquifer extends from the depth of 4 m to 50 m below the surface, while the depth of the intergranular aquifer extends from 4 m to 100 m, which is relatively thicker than the fractured aquifer system. According to Holland (2011), the borehole yield corresponding to the alluvium deposits ranges from 0.50 l/s to 9.00 l/s. The distribution and borehole yields of the boreholes in the Mogalakwena Subcatchment are shown by Figure 3.4. In general, the types of aquifers in the area are determined by the availability of primary and secondary porosities and greatly affect groundwater movement and storage.

The capacity of storage and borehole yield of fractured aquifers depends on the interconnection of structures such as joints, fissures, fractures, or any planes of weakness along with the contact between intrusive and country rocks (Vermeulen and Bester, 2009). Preeja et al. (2011), noted that the presence of groundwater in crystalline aquifers is associated with the fractured and weathered horizon. However, fractured aquifers are associated with groundwater contamination due to high salt concentration caused by

prolonged contact time between percolating water and the surrounding lithology (Vermeulen and Bester, 2009).

The northern part of the Subcatchment (Fractured aquifer1 as shown in Figure 3.4) is underlain by the Alldays Gneisses of the Limpopo Mobile Belt, whereas the south-east to eastern parts (Fractured aquifer2) is dominated by intrusive rocks of the Bushveld Complex and the Archean granite gneiss (Figure 3.4). According to Ahokpossi (2018), fractured aquifers are confined to semi-confined due to the absence of an impermeable layer between weathered material and aquifers. Groundwater infiltration in these lithologies depends on the availability of lineaments and increased lineament density, as well as fracture width-to-depth ratio (aperture of the fractures), which can enhance the hydraulic connectivity of the crystalline rocks.

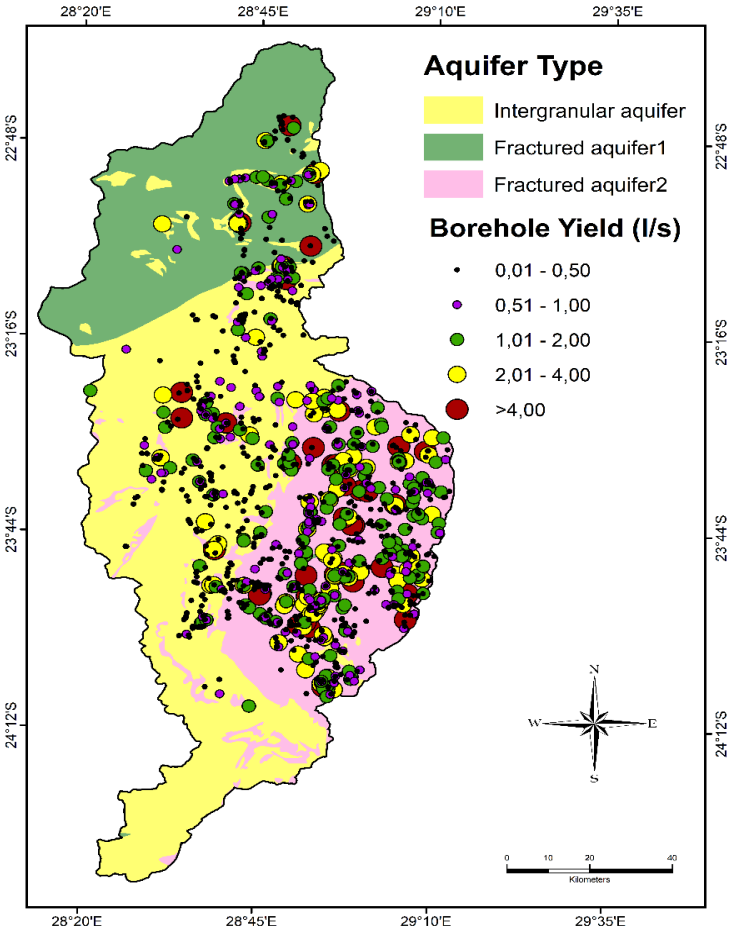

Figure 3.4: Simplified map of the aquifer types derived from the geological map of the area.

3.5 Drainage System

There is a limited number of rivers in the area due to the semi-arid climatic conditions and high evaporation rates. As a result, the amount of water supplied for domestic and agricultural uses from rivers or generally surface water is low. In the southern part of the study area, the Mogalakwena River rises as the Nyl River in the south of Mokopane and is joined by the Sterk River which rises from the Waterberg mountain ranges (Tooth, 2002). There are several ephemeral streams in the western and eastern parts of the Subcatchment, which drain into the Mogalakwena River. The tributaries that are in the western part of the area drain from the Waterberg sandstones, while the tributaries to the east, including Rooisloot, Pholotsi, and Dorpsriver emerge from the Maribashoek and Buffelshoek Mountains (McCathy et al., 2011).

The three tributaries that are situated in the eastern part of the area have moderate to low slopes and transport coarse sediments. The Mogalakwena River flows along a narrow river valley with a steep slope before it joins Limpopo River in the north (McCarthy et al., 2011; Tooth et al., 2002). The drainage patterns and density are important indicators of hydrological features (Sener et al., 2005). These parameters are important and determine the extent of interaction between rivers and aquifer systems. In general, increased evaporation rate has contributed significantly to the drying out of surface water bodies, making groundwater the only reliable water supply source for both domestic and agricultural use.

3.6 Topography

Topography is one of the factors that control the interaction between local and regional groundwater flow, and the exchange between surface water and groundwater (Harvey,1995). Preeja et al. (2011), indicated that the topographic relief determines groundwater flow in terms of partitioning rainwater into runoff and infiltration. Gentle slopes are associated with high groundwater recharge compared to steep slopes; this is due to sufficient time for water to slowly infiltrate and recharge groundwater.

Table 3.2: Summary of the topography within the Mogalakwena Subcatchment.

	Topography	**Quaternary Catchments**
Mogalakwena Subcatchment	Plain	A61G, A62B, A62C, A62D, A62G, A62J, A63A, A63B
	Slight undulating plains	A62E, A62F, A62G, A62H, A63A
	Slightly irregular plains	A63B
	Moderately undulating plains	A61H, A61J
	Strongly undulating plains	A62E
	Lowland with mountains	A61G, A62A, A62B, A62C, A62F, A63G, A62H, A62J, A63A, A63B
	Hills	A62E, A62F
	Low mountains	A61G, A61J, A61H

Mogalakwena Subcatchment is characterised by rugged topography and heterogeneous landscape, coupled with complex geology, as shown in Figure 3.5 and Table 3.2. Rankoana (2016), described the topography of the study area as irregular undulating lowland with hills and low-lying planes. The altitude ranges from low (667 metres above mean sea level) in the north to high (1886 mamsl) in the southern and southeastern parts of the area (Figure 3.5). Table 3.2 gives a detailed summary of the morphology for each Quaternary Catchment in the study area.

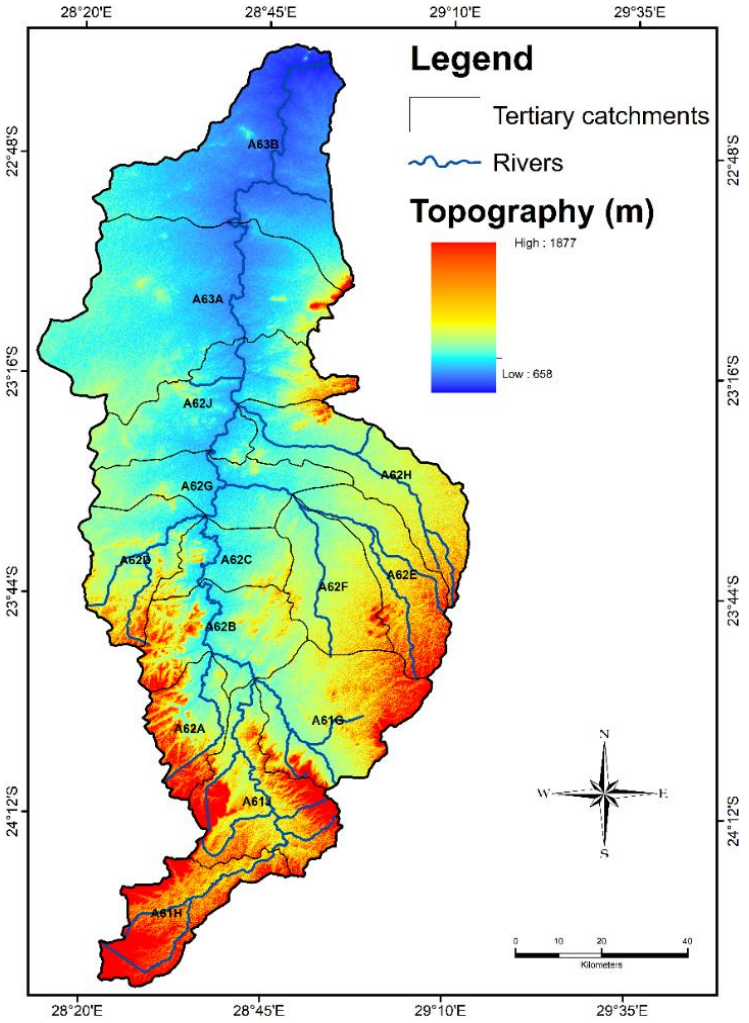

Figure 3.5: Topographic relief of Mogalakwena Subcatchment highlighting hilly and flat areas.

Figure 3.6 shows a few outcrops of the Bushveld granite intrusions and the resistant silica-rich sedimentary rocks of the Waterberg Group forming mountain ranges that are evident in the study area. The topography of the area is largely influenced by the presence of heterogeneous rocks that vary in resistance to the process of weathering and surficial processes such as erosion and deposition. The steep slopes that are situated in the southern part of the area are attributed to resistant rocks to erosion, which caps the Waterberg mountain ranges.

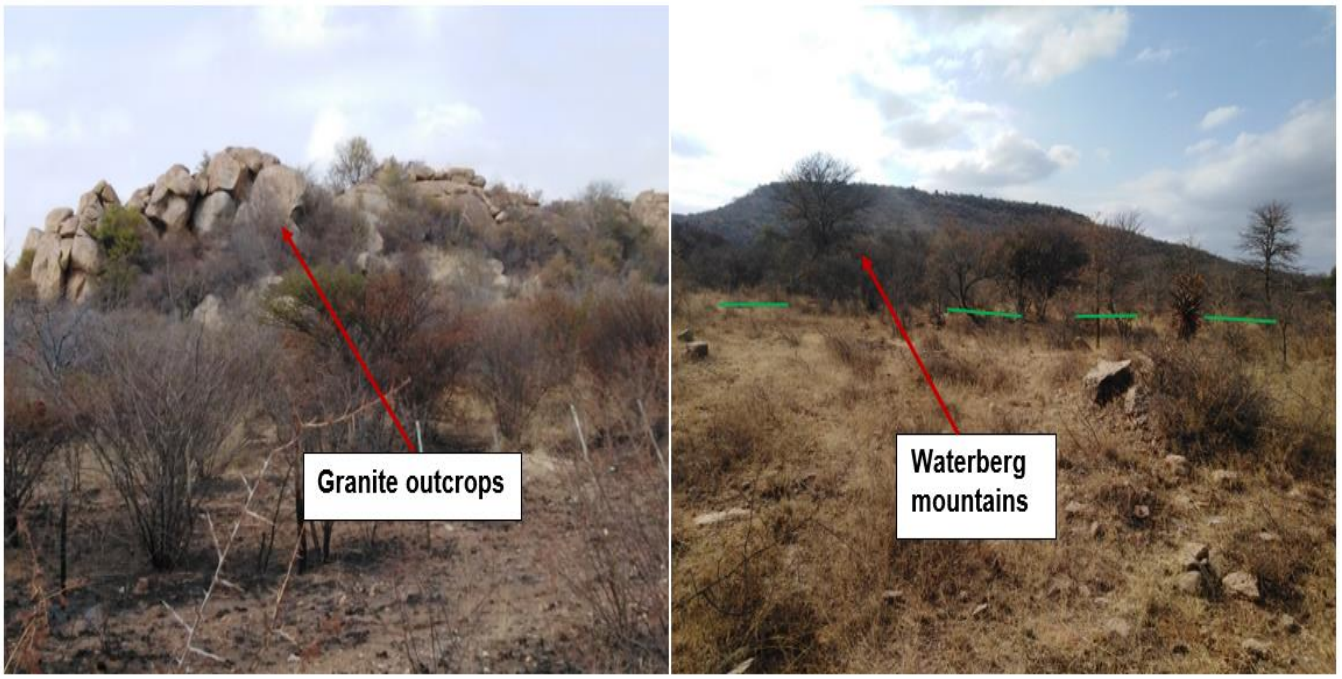

Figure 3.6: Photographs of granitic outcrops and Waterberg mountains that shape the landscape due to differential resistance to weathering process.

3.7 Soil Type

The infiltration of rainwater depends on the physical properties of the soil such as texture, grain distribution, sorting, water retention and yield capacity (De Giglio et al., 2015). De Giglio et al. (2015), further emphasised that a significant portion of rainwater infiltrates and is stored in the soil which can either be reduced by evapotranspiration, evaporation and/or groundwater recharge. Increased runoff is common in bare soil compared to cultivated land with vegetation cover, which enhances the low rate of groundwater recharge.

Ashton et al. (2001), classified the soils within Mogalakwena Subcatchment into four groups, namely sandy-clay loam soils covering the upper reaches of the Subcatchment, sandy loam soils occurring within the valley bottom in the central part of the area, sandy soils dominate the undulating terrain in the lower reaches of the Mogalakwena River and clay-rich, blocky vertisols associated with wetlands in the lower reaches of the Mogalakwena River. However, in this study, the soil types were classified into three based

on the hydraulic conductivity variations (Figure 3.7A). These include sandy soil, sandy loam, and clay soils, which cover 58%, 40% and 2%, respectively (Figure 3.7B). The sandy soil is the most hydraulically conductive, followed by sandy loam and clay soil. This implies that infiltration of rainwater increases in the area covered by sandy soil compared to clay depending on the availability of precipitation and topographic relief of the area.

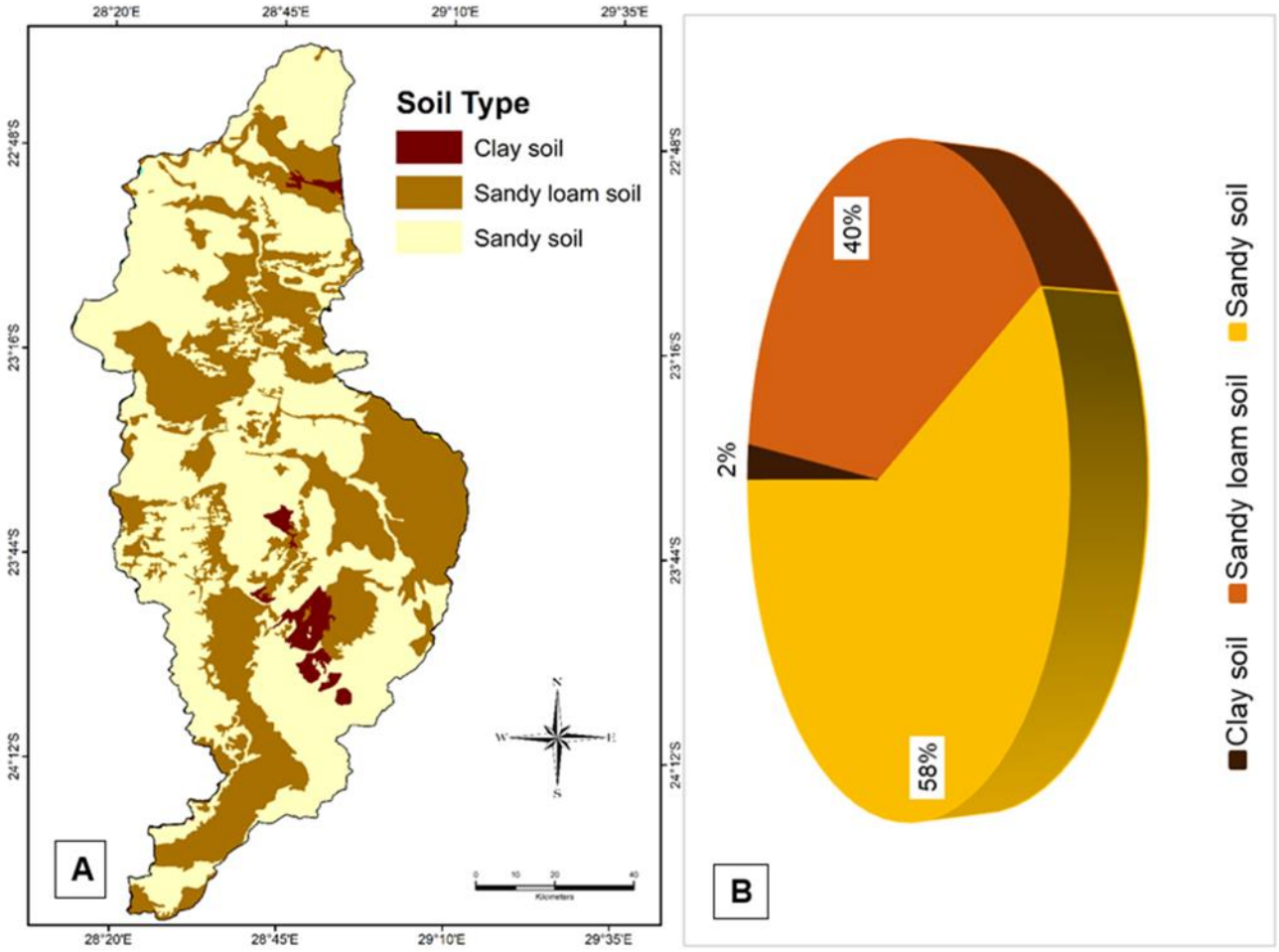

Figure 3.7: Soil coverage map (A) and pie chart(B) displaying the percentage of the distribution of the soils within Mogalakwena Subcatchment.

3.8 Land Cover

Land cover influences hydrological processes including soil moisture, evapotranspiration, and groundwater recharge (Zhang and Schilling, 2006). According to Shamuyarira (2017), vegetation cover reduces evaporation and runoff, while enhancing rainwater infiltration. Shamuyarira (2017), further highlighted that land covered by forests may represent groundwater potential zones as plants use large amounts of water through abstraction from the vadose zone and beneath the watertable. Change in topographic relief and vegetation cover coupled with land used for settlement can collectively reduce groundwater recharge (Sharp, 2010). Areas that are covered by settlements are usually associated with developments such as the construction of roads, buildings, and infrastructure, which can alter the topography and vegetation, making the land surface poor for groundwater recharge (Sharp, 2010).

The study area is dominantly covered by grassland and woodland bushes, with minor cultivated land (Figure 3.8). The most prominent land cover is woodland/bushes occupying 62% of the area (Figure 3.8B). The cultivated land and grassland are also predominant covering about 12% and 22%, respectively (Figure 3.8B). Approximately 2% of the land is utilised for rural settlement in the central to eastern parts of the Mogalakwena Subcatchment(Figure 3.8B). The remaining land is mainly used for mining activities, urban townships, and water bodies such as dams and wetlands.

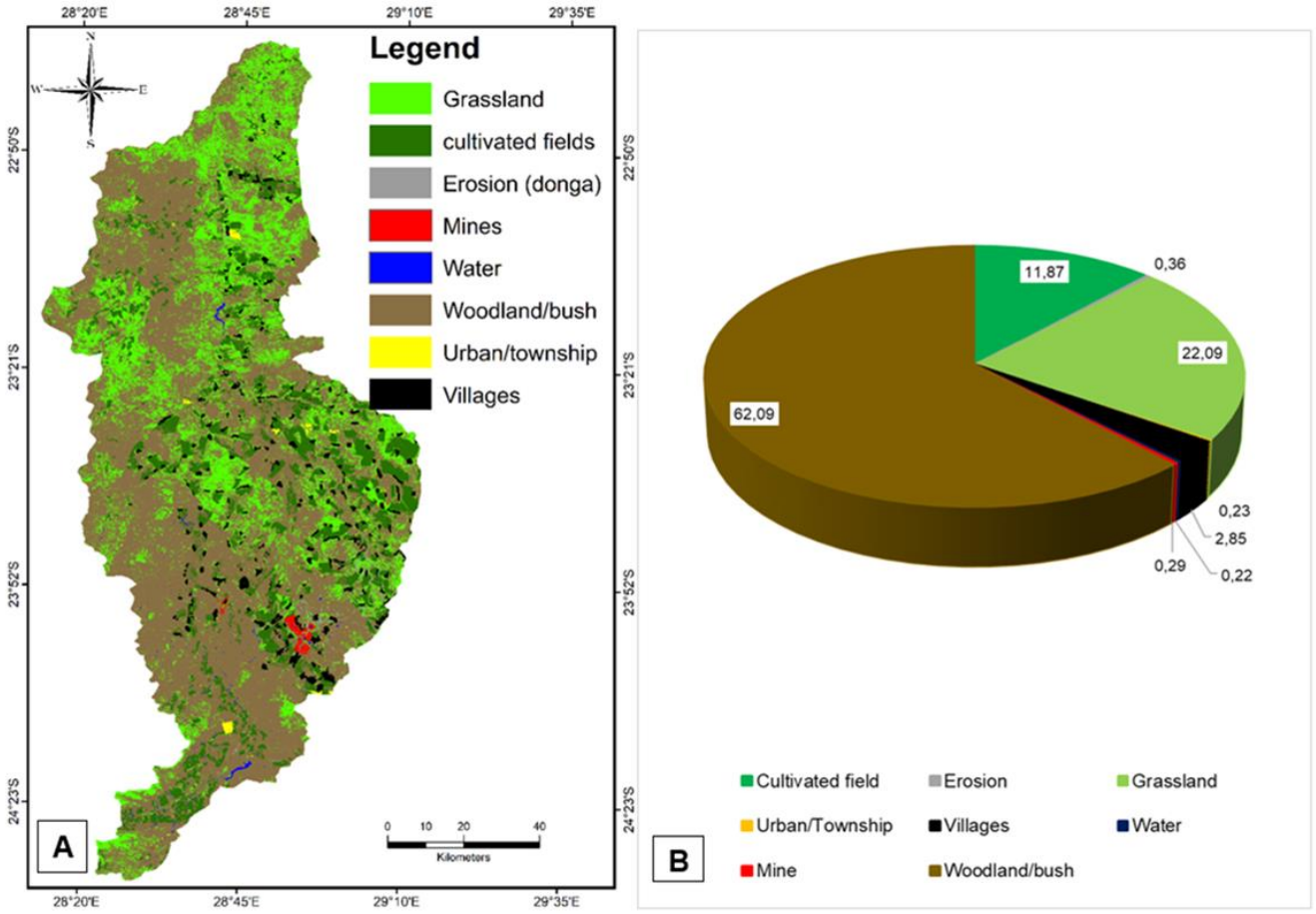

Figure 3.8: Map showing land cover/land uses (A) and a pie chart displaying the percentage of each land cover in the study area.

Besides settlement purposes, the main land use in the study area is subsistence livestock farming. The livestock depends on the available open fields for grazing and water for drinking from streams, dams, and drilled wells. Though agriculture is not an intensive activity, there are a few orange farms (Figure 3.9) that may have an impact on the groundwater in terms of large-scale demand for water use and the use of fertilizers such as nitrate and phosphorous. However, one of the common problems in the area is littering or lack of waste management close to boreholes and along the river courses (Figure 3.9). The lack of awareness about waste management has an adverse effect on the quality of the available freshwater for domestic use, and human health in general.

Figure 3.9: Photographs displaying land cover and land use within Mogalakwena Subcatchment.

3.9 Climate

Climate change has a significant influence on the hydrological cycle locally and regionally, it modifies the rainfall events, amount, groundwater recharge, streamflow, which consequently impact the availability of water resources (Zhu and Ringler 2012). The changing global climate has had a great impact on groundwater availability, low rainfall intensity, and rainfall distribution during the years, resulting in a substantial decrease in groundwater recharge (De Giglio et al., 2015). Groundwater recharge can be negatively impacted by climate change due to its dependence on recharge (Zhu and Ringler 2012).

The study area comprises seven climate monitoring stations, however only the central Waterberg Styloop Station was used to understand the rainfall, temperature, and evapotranspiration patterns between the years 2008 and 2020 as summarised in the following sections.

3.9.1 Temperature

South Africa is characterised by four seasons namely: Summer, Autumn, Winter, and Spring, however Summer and Winter are known as seasons affecting the groundwater system due to high rainfall and absence of rainfall, respectively. The summer season extends from October to April, and during this season large parts of the Limpopo Province receive a significant amount of rainfall. Mogalakwena Subcatchment is characterised by hot to warm summer temperatures and warm to cold winter temperatures. The maximum temperature in this area exceeds 30 ˚C, while the minimum ranges from 10 ˚C to 22 ˚C during the summer season (Figure 3.10). During the winter season, the maximum temperatures range from 23 ˚C to 30 ˚C, while the minimum temperatures vary from 10 ˚C to 3 ˚C (Figure 3.10).

3.9.2 Precipitation

Precipitation is the major source of groundwater recharge, and it has an indirect impact on groundwater discharge and withdrawal rates (Rwanga, 2018). The temporal and spatial changes in rainfall patterns are due to changes in temperatures and atmospheric circulation, which directly impact groundwater recharge (Nkhonjera and Dinka, 2017). Rainfall at Mogalakwena Subcatchment is seasonal with high precipitation being received during summer months (November to April) as shown in Figure 3.11. In addition, the area also receives low rainfall (< 100 mm per month) and no rainfall at all during certain months of the year (Figure 3.11). High rainfall greater than 100 mm is occasionally received during wet seasons (from October to February).

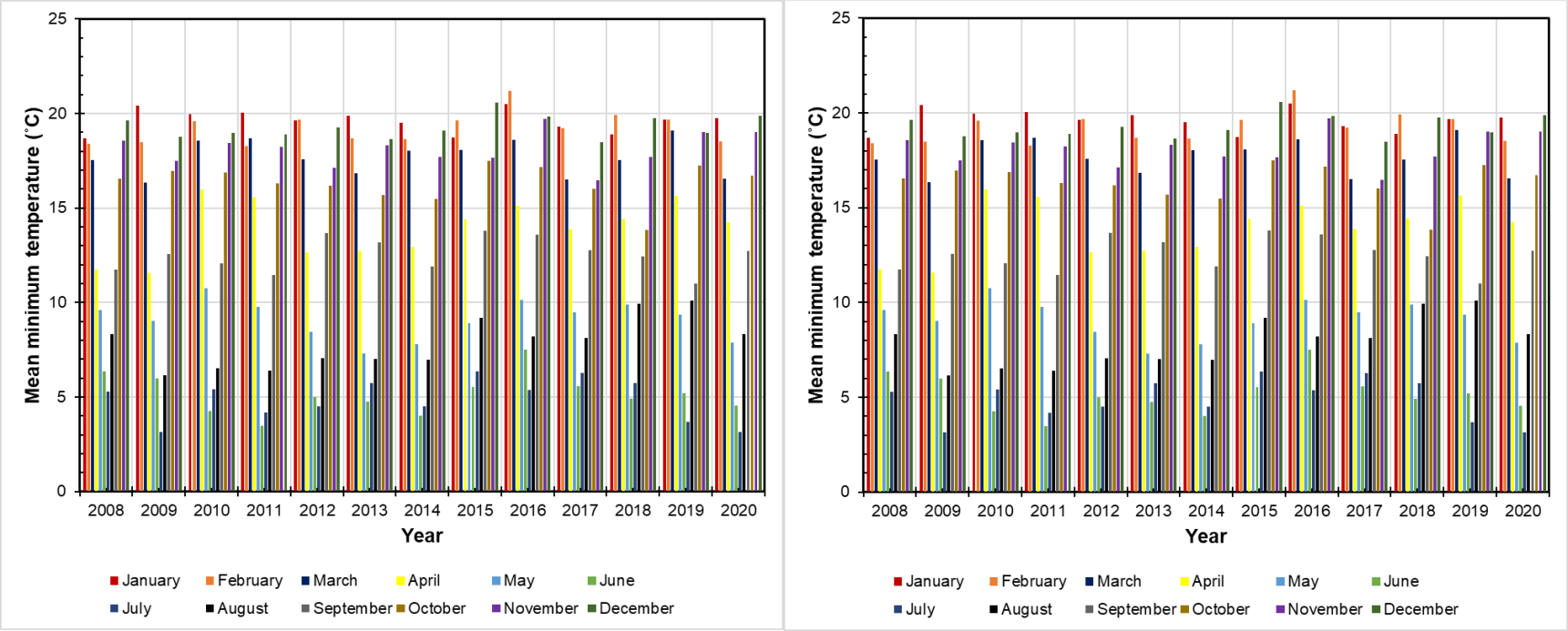

Figure 3.10: Bar graphs showing the mean of maximum temperature (A) and the mean of minimum temperature (B).

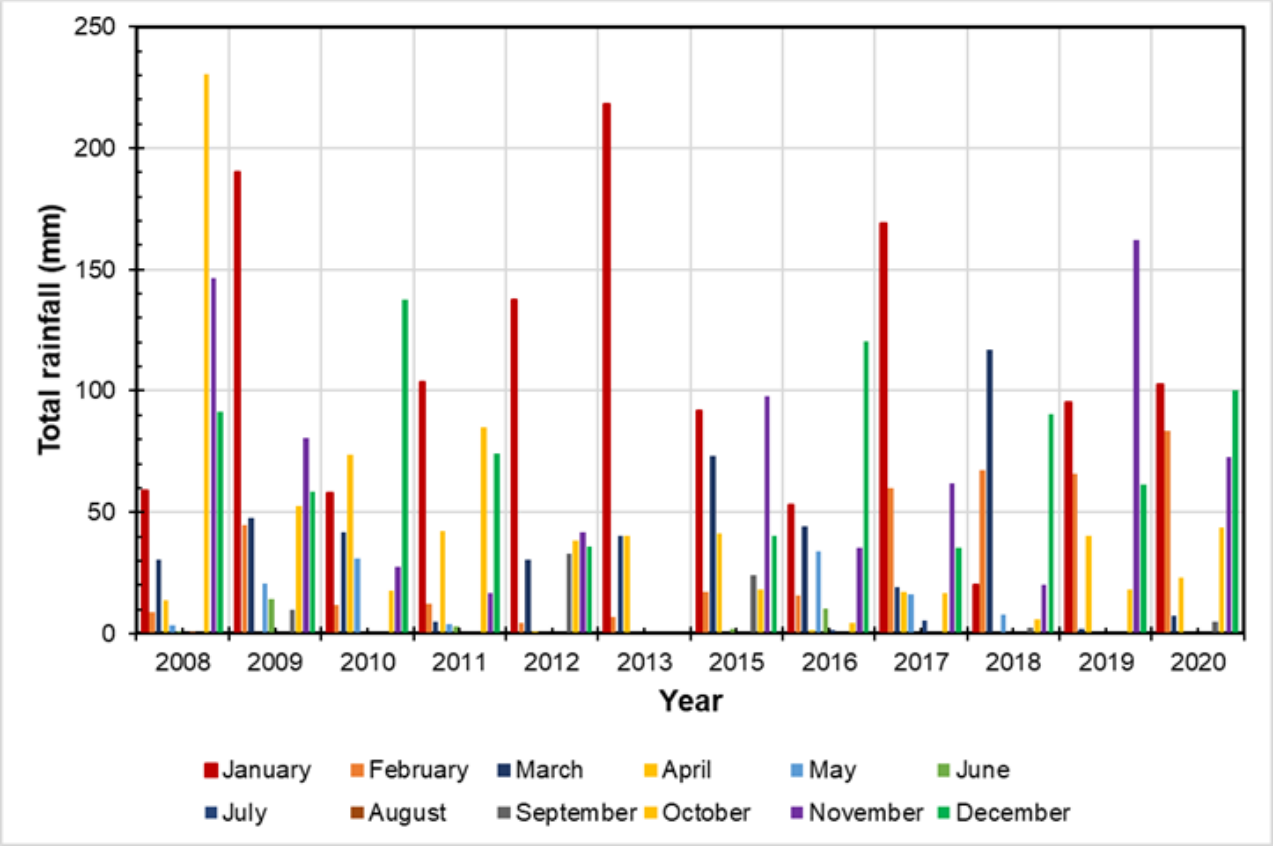

Figure 3.11: Bar graph showing rainfall patterns within Mogalakwena Subcatchment.

3.9.3 Evapotranspiration

Evapotranspiration is one of the important parameters that determine runoff, water balance, and water surplus (Nistor, 2019). The amount and types of vegetation cover in an area can be used to estimate evapotranspiration, which is one of the boundary conditions that are required for numerical modelling of groundwater flow. Generally, high evapotranspiration rates are expected in regions covered by forests compared to areas covered with grass (Barratt, 2018).

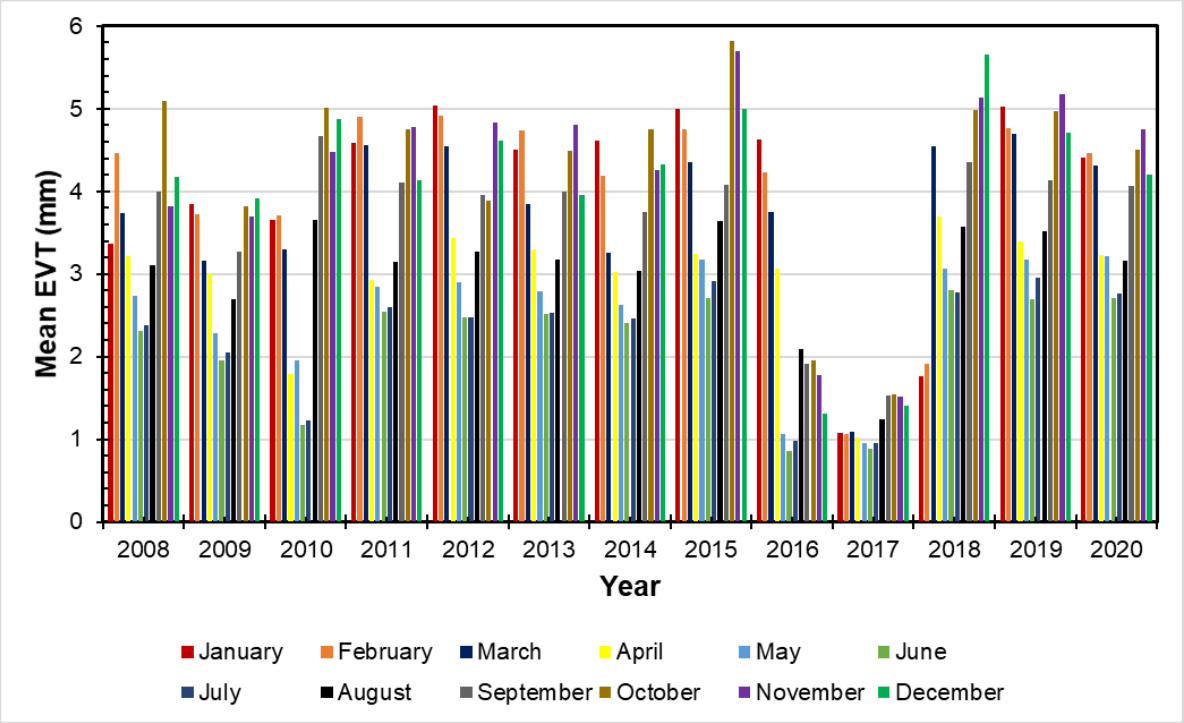

Figure 3.12: Graph showing the variation of evapotranspiration rates in Mogalakwena Subcatchment.

The evapotranspiration rates at Mogalakwena Subcatchment are high during summer and low in winter, which is consistent with the variability of temperatures. High evapotranspiration rates exceeding 3 mm are dominantly experienced between August and April, while the remaining dry months show low evapotranspiration rates, i.e., less than 3 mm (Figure 3.12). The high evapotranspiration rates are controlled by the land cover and high temperatures as discussed in sections 3.8 and 3.9.1, respectively. According to Healy and Cook (2002), evapotranspiration tends to rise during the day, causing a decline in water level in shallow watertable, thus making the watertable to rise during the night when evapotranspiration rates subside, provided that there is recharge from rain.

Chapter 4: Materials and Methods

4.1 Introduction

In this study, a steady-state model of groundwater flow was implemented using MODFLOW NWT and ModelMuse. ModelMuse is a graphic user interface for many versions of MODFLOW and it serves as a platform for importing the required input data to MODFLOW, and it enables post-processing the model results. ModelMuse allows to run steady-state or transient simulations using MODFLOW NWT and other modelling versions such as MODFLOW 2005, MODFLOW 6 and MODFLOW OWHM. In this study, MODFLOW NWT was used to simulate groundwater flow. Figure 4.1 summarises the methods implemented for steady-state numerical modeling of groundwater flow in this study.

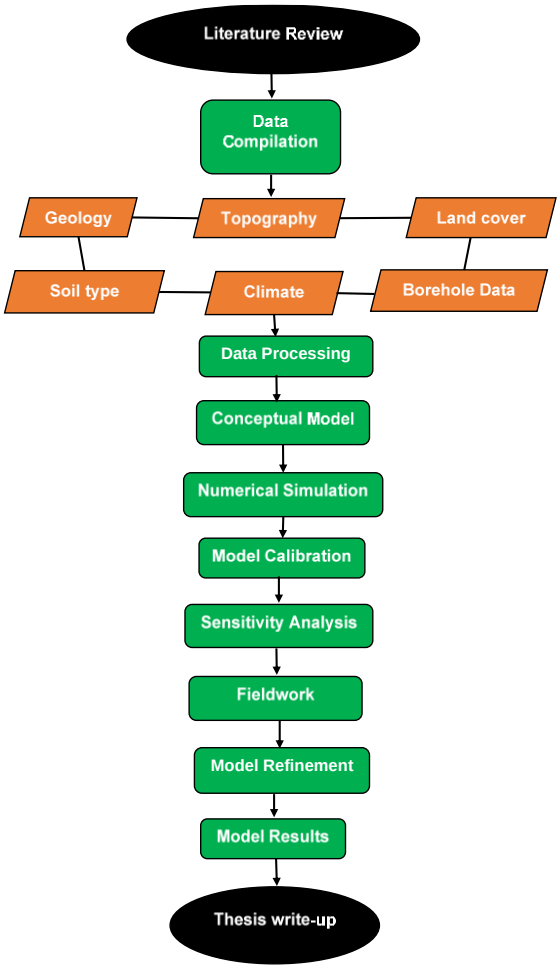

Figure 4.1: Simplified flowchart showing the present workflow used to implement numerical modelling of groundwater flow in the study area.

4.2 Data Compilation and Processing

To develop a conceptual model, first, appropriate spatial data, which comprise the boundary of the model domain, borehole depth and position, and digital elevation data (DEM), etc., are necessary. All the spatial data, including polygons, lines and points were prepared with the same projection and datum (UTM Zone 35S and WGS84 datum) in the ArcGIS environment, as these spatial data will be imported and recognised by MODFLOW via ModelMuse. Different data sets relevant for achieving the aims of the project were compiled from various sources. The climate data (rainfall, temperature, and evapotranspiration) were obtained from the Agricultural Research Council (ARC) and South African Weather Services (SAWS), respectively. The soil data were also obtained from the ARC, while the Department of Water and Sanitation provided the water level, borehole yield and hydrochemical data. The geological and lineament data were accessed from the Department of Geology and Mining of the University of Limpopo. The data sets were pre-processed to establish a conceptual model of groundwater flow using softwares including ArcGIS, LogPlot and QGIS, among many others.

4.3 Hydrogeological Model Description

MODFLOW uses algebraic finite difference equations to numerically solve three-dimensional partial differential equations that define groundwater flow in porous medium (Harbaugh et al., 2000). MODFLOW is utilised worldwide for groundwater modelling due to its simplicity, flexible modular structures, comprehensive coverage of hydrogeological processes and free accessibility (Schwartz, 2006). Additionally, the model runs using ModelMuse as a graphical user interface and it provides 3D-visualisation, which includes side, front and top views. MODFLOW is capable of simulating flow and contaminant transport in both steady-state and transient-state flow in different environmental conditions and shapes of the flow system.

In this study, MODFLOW-NWT was selected based on its capability to solve complex and heterogeneous hydrological systems. MODFLOW-NWT is a standalone Newton formulation of MODFLOW-2005 designed to solve problems concerned with nonlinearities of unconfined groundwater flow equations (Niswonger et al., 2011). In this study, MODFLOW-NWT is the preferred program relative to other MODFLOW

versions due to the following improved functionalities that make it different from that one of MODFLOW-2005 (Niswonger et al., 2011; Ely and Kahle, 2012):

I. MODFLOW-NWT uses an upstream weighting package (UPW) for calculating horizontal flow between cells of unconfined aquifers. In addition, it improves model stability and convergence as compared to the LPF package of MODFLOW 2005,
II. all active variable-heads at the beginning of the simulation remain active throughout the simulation, i.e., it minimizes dry cells during the simulation process. In addition, the Newton solver is very important in solving problems representing an unconfined aquifer,
III. MODFLOW-NWT enables modified horizontal conductance for unconfined conditions to smooth discontinuities during the drying and rewetting of cells,
IV. modified storage formulation to smooth storage changes during cell drying/wetting and transition between unconfined and confined conditions,
V. modified storage formulation for unconfined conditions to prevent variations in storage for head changes occurring beneath the cell bottom,
VI. groundwater heads are calculated for dry cells, even if they are below the cell's bottom, unlike MODFLOW 2005, which excludes when heads tend to be below the elevation of the cell's bottom.

The flow of groundwater is explained by Darcy's law which is defined by an equation for computing the amount of water flowing through an aquifer (Futornick, 2015). Darcy's law also obeys the continuity equation for groundwater flow stating that water is neither created nor destroyed in a hydrological cycle, and water budget, i.e., the difference between the total inflow and the total outflow is, therefore, equal to zero (Futornick, 2015). The following equation represents Darcy's law (Kumar, 2013):

$$Q = -KAdh/dl$$

Where Q is discharge, K is permeability or hydraulic conductivity of the porous medium (L/T), A is the cross-sectional area of the porous medium along which groundwater flows and dh/dl is the change in hydraulic head per unit distance along the flow path.

The continuity equation can be expressed as (Kumar, 2013):

$$\sum input = \sum output + \triangle storage$$

The above equations of conservation mass and continuity are the cornerstone of the groundwater flow equation in a porous medium.

4.4 Conceptual Model

As defined in chapter two, the conceptualisation of groundwater flow is the initial step essential for simplification of the hydrological system for modelling purposes. The data set required to develop a conceptual model includes geology, topography, groundwater abstraction, piezometric heads, groundwater recharge, the permeability of different rock types, soil types, and evapotranspiration. Figure 4.2 provides the distribution and summary of all the elements/features used to construct the conceptual model of groundwater flow in this study.

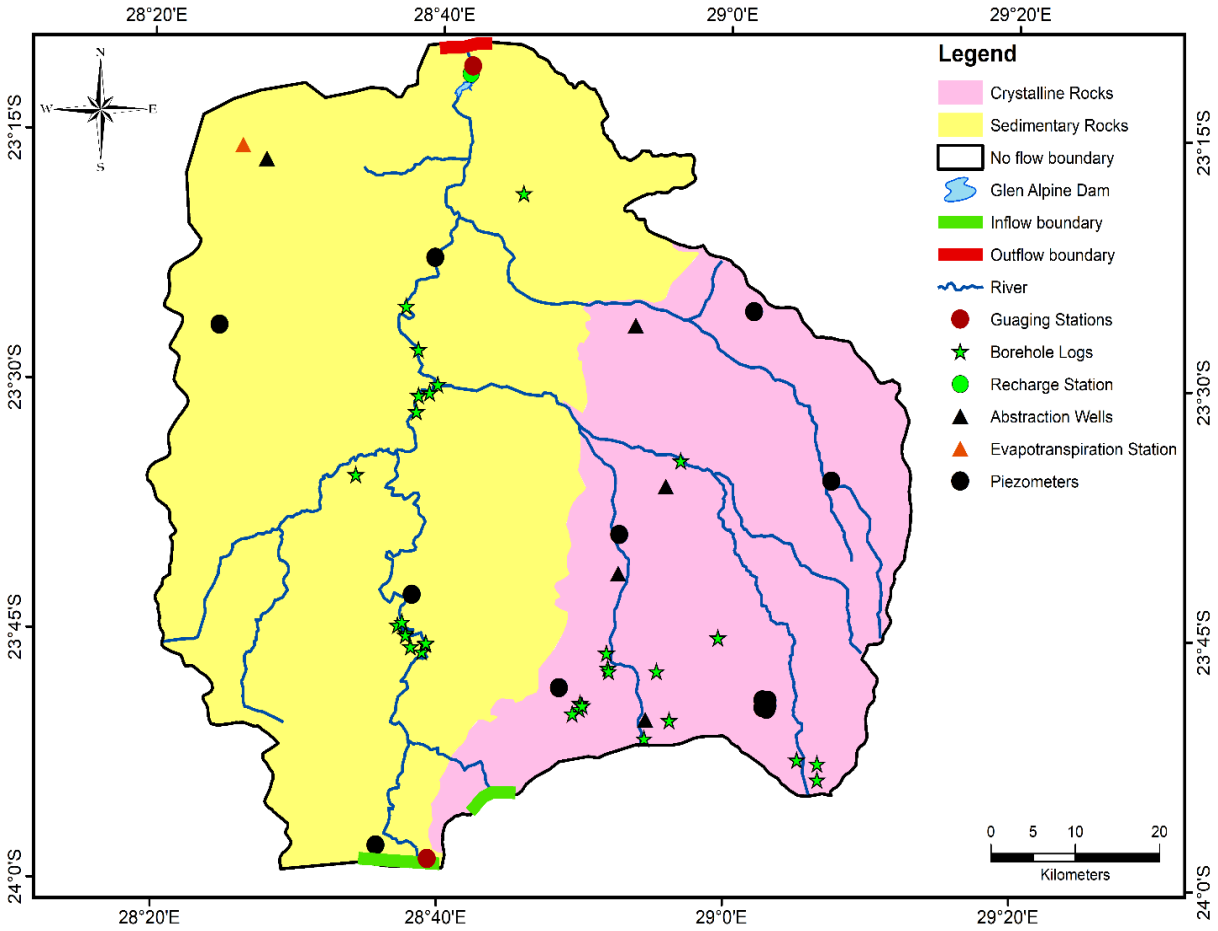

Figure 4.2: Map showing the location of data used to develop the conceptual model of groundwater flow.

4.4.1 Model Domain

A detailed conceptual model was developed using spatial data relevant for the construction of MODFLOW features such as rivers, dams, wells, and spatial features that represent general head boundary conditions (El Alfy, 2014). The model boundary covers an areal extent of 5896 km^2. The area of modelling interest is geologically underlain by the sedimentary rocks of the Waterberg Group and Quaternary sediments that cover the western parts of the model domain, while the eastern sector is underlain by the crystalline rocks of the Bushveld Complex and Hout River Gneisses (Figure 4.3A). Furthermore, the upper part of the model domain is dominantly covered by sandy and sandy loam soils with subordinate clay soils cover (Figure 4.3B).

Flat topography dominates the model domain except for the southwestern and south-eastern regions which are covered by the Waterberg and Bushveld Mountains, respectively (Figure 4.3C). A piezometric surface is important for defining hydraulic gradient, flow direction, groundwater discharge and recharge zones (Hentati et al., 2016). In this study, the piezometric surface was calculated by subtracting static water level from the elevation of the borehole collar above the mean sea level.

The kriging interpolation technique was implemented to convert the discrete piezometric data in excel dataset format into raster data format using ArcGIS. Lag size, range (search radius), partial sill, and nugget were defined as 1000, 500 and 250 for kriging purposes, respectively. Contour lines were constructed to enhance the visual understanding of the piezometric surface (Figure 4.3D). The topography and piezometric surface show a strong correlation, indicating that the groundwater flow mimics surface water flow (Figure 4.3D). The digital elevation and piezometric surface indicate that the river flows from the south to the north, and no flow boundaries along the east and western parts of the model were defined (Figure 4.3C&D).

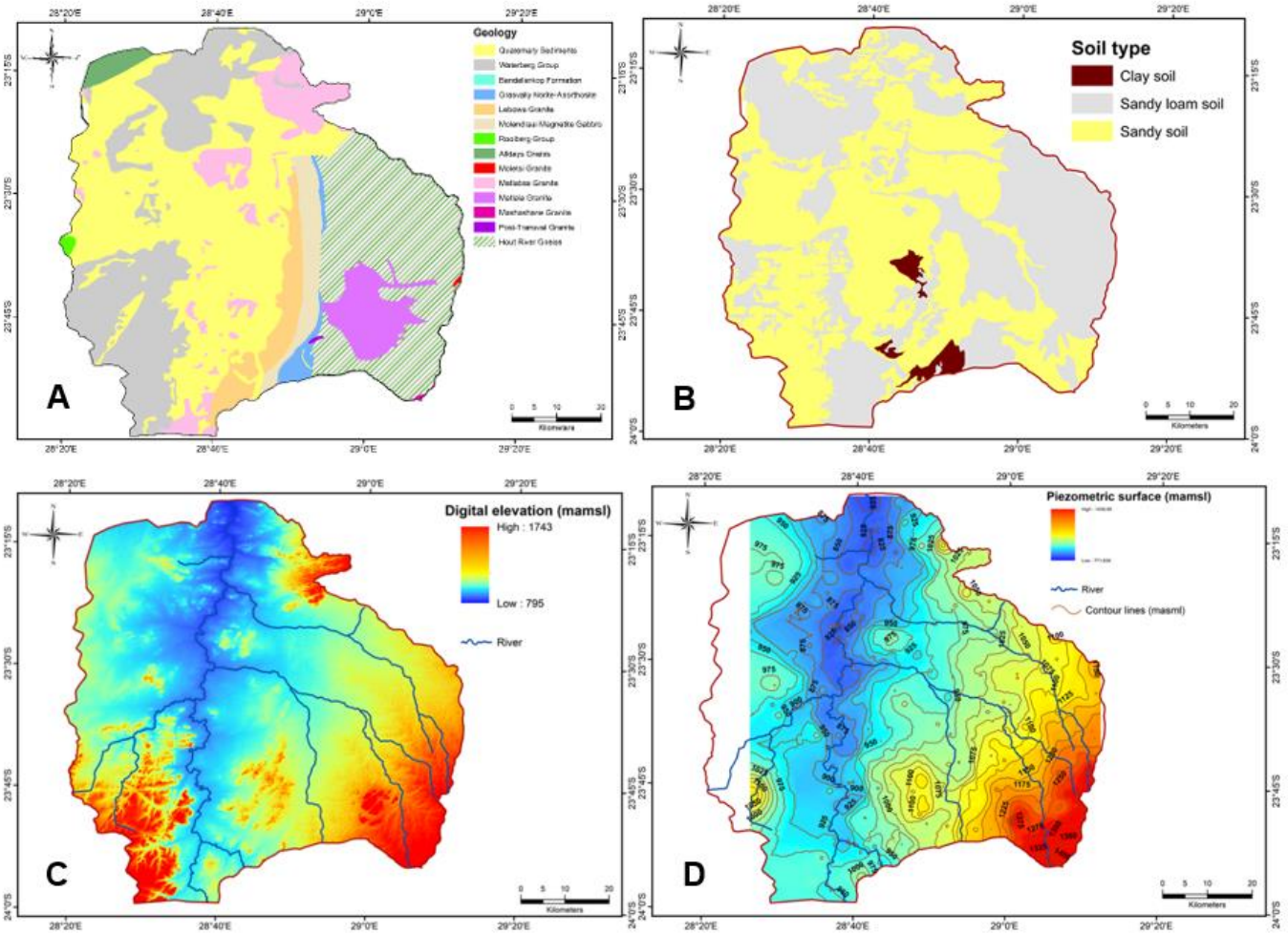

Figure 4.3: Maps showing hydraulic conductivity zones (A), soil types defining hydraulic conductivity of the upper layer of the model (B), digital elevation defining model top (C), and piezometric surface (D) of the model domain used for the conceptualisation of the initial head.

4.4.2 Hydrostratigraphy

The hydrostratigraphy in the study area was thoroughly assessed using 31 lithologic logs ranging from 28 to 119 m in depth below the surface (Figure 4.2). Sixteen of the total number of boreholes were drilled within the sedimentary rocks Waterberg Group in the central-western part of the area, while 15 boreholes penetrated through the crystalline rocks that comprised of the Bushveld Igneous Complex and the Archaean granites situated in the eastern and south eastern parts of the model area (Figure 4.2). The interpretation of the borehole log data suggests that there are two hydrostratigraphic units within the model domain, namely, the upper and lower layers. The upper layer of the model is represented by thin soil (~4m thick, but varies laterally), dominantly consisting of sandy soil, sandy loam soil, and clay soil, with decreasing order of aerial coverage as summarised in Section 3.7.

The drillhole log data suggest that the second layer is an aquifer, which varies in thickness from 4 to 50 m in the east to 4 to 100 m in the western part of the model domain. Thus, the depth of the bottom of the aquifer varies from west to east. In addition, the hydraulic conductivity of the aquifer varies from west to east in accordance with rock types that lie below the model domain. To overcome the complexity and irregular depth of the bottom of the aquifer, a shapefile with attributes X, Y, Z, corresponding to easting, northing, and the depth of the bottom of the aquifer, respectively was imported as an object using ModelMuse. The Z value of the imported point object was interpolated at each grid cell, and this enabled the generation of a continuous bottom of the aquifer that varies from west to east.

The eastern part of the area is underlain by crystalline rocks that are relatively old. The high permeability within these rocks is associated with the weathered and fractured sections of the hard rocks. The western part of the model domain is underlain by Waterberg arenites, and the intergranular aquifer system in the west is twice as thick as the weathered and fractured aquifer system in the east. The bottom and top of the upper layer of the model were defined using digital elevation data, which was obtained from the USGS global data archive (https://www.usgs.gov). The spatial resolution of the DEM is 30 m by 30 m, which is adequate to provide the necessary details required for the present modelling purpose.

Figure 4.4 illustrates the selected borehole logs from the study area showing the location of the water-strike, type of lithology, and the borehole yield. The aquifers were determined based on the presence of the water-strike within the vertical stratigraphic succession of rocks. Furthermore, the aquifers are located at different morphology with intergranular at approximately 796 m above mean sea level (a.m.s.l.), while the fractured aquifers are situated at about 1093 m a.m.s.l. The borehole logs in the sedimentary region depict multiple water strikes at a depth varying from 45 m to 100 m (Figure 4.4 A, B & C), whereas water strikes in the crystalline rocks are situated at shallow depths varying from 20 m to 30 m (Figure 4.4D & E). Both aquifers are overlain by a thin layer of sandy loam and sandy soils with minor clay soil which vary in thickness from 2 to 4 m (Figure 4.4). Figure 4.6 portrays a cross-section from A to B depicting the variability of the topography of model top, aquifer thickness and rock types from west to east. In addition, the figure shows the approximate width of the rock types that lie below the model domain in the eastern part of the area.

4.4.3 Hydraulic Conductivity Zones

The determination of the aquifers' hydraulic properties is essential for numerical modelling of groundwater flow. The borehole logs shown in Figure 4.4 suggest the presence of a single aquifer in both the eastern and western parts of the area. However, the thickness of the aquifer laterally varies from west to east, in that in the western part of the area its thickness increases to 100 m, while in the eastern part it is as thick as 50 m. In addition, the permeability coefficient of the aquifer varies from west to east depending on rock types, which lie below the model domain. Thus, while developing the conceptual model, hydrogeologic parameters were spatially differentiated by creating hydraulic conductivity zones to deal with the west-to-east variation of the hydraulic conductivity of the aquifer. This was implemented by creating spatial data in an ArcGIS environment that represent hydraulic conductivity zones. Based on the simplification of the geological map, five hydraulic conductivity zones were created as shown in Figure 4.5 below.

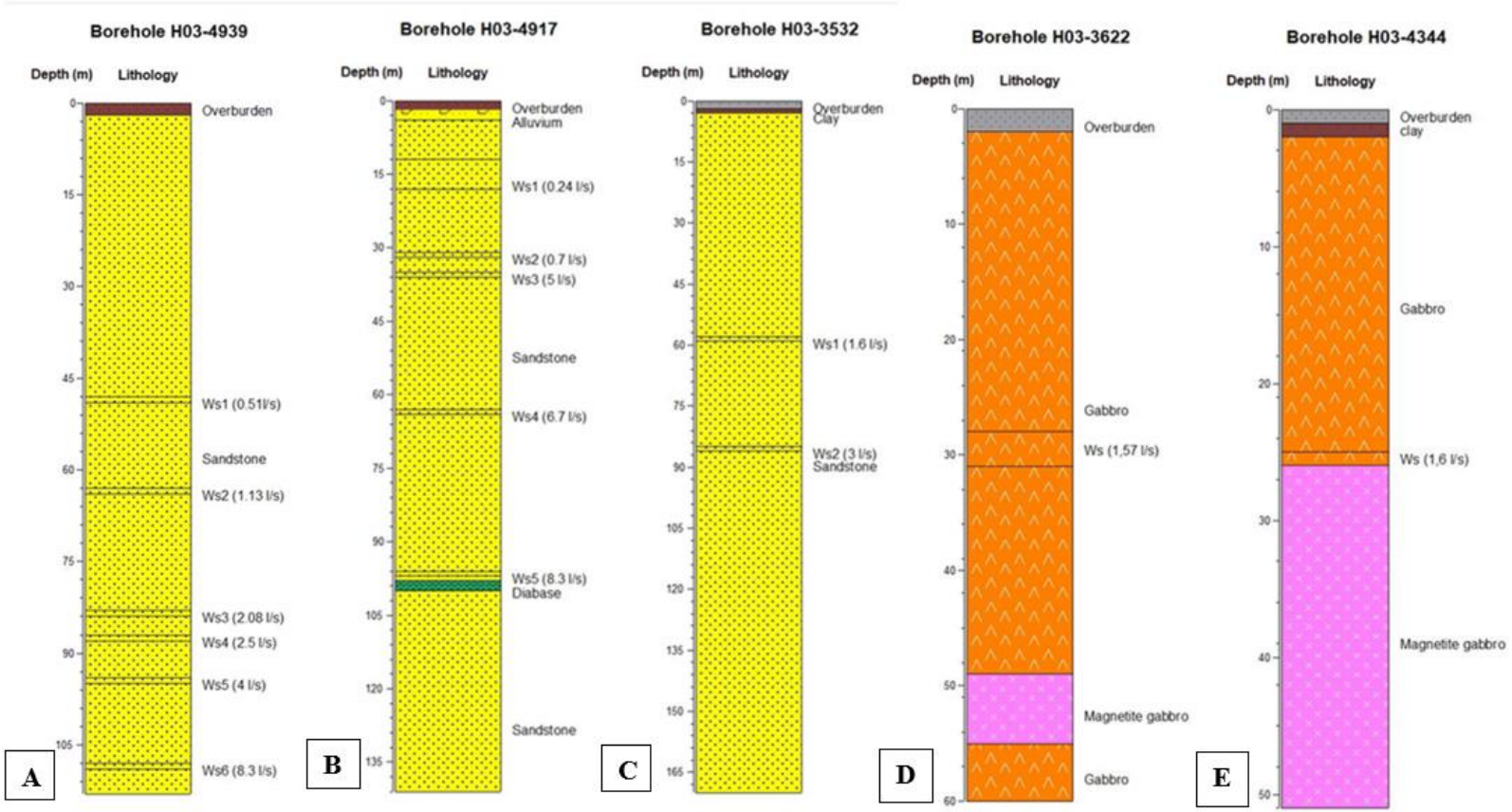

Figure 4.4: Borehole logs used to construct the conceptual model of hydrostratigraphy of the model area.

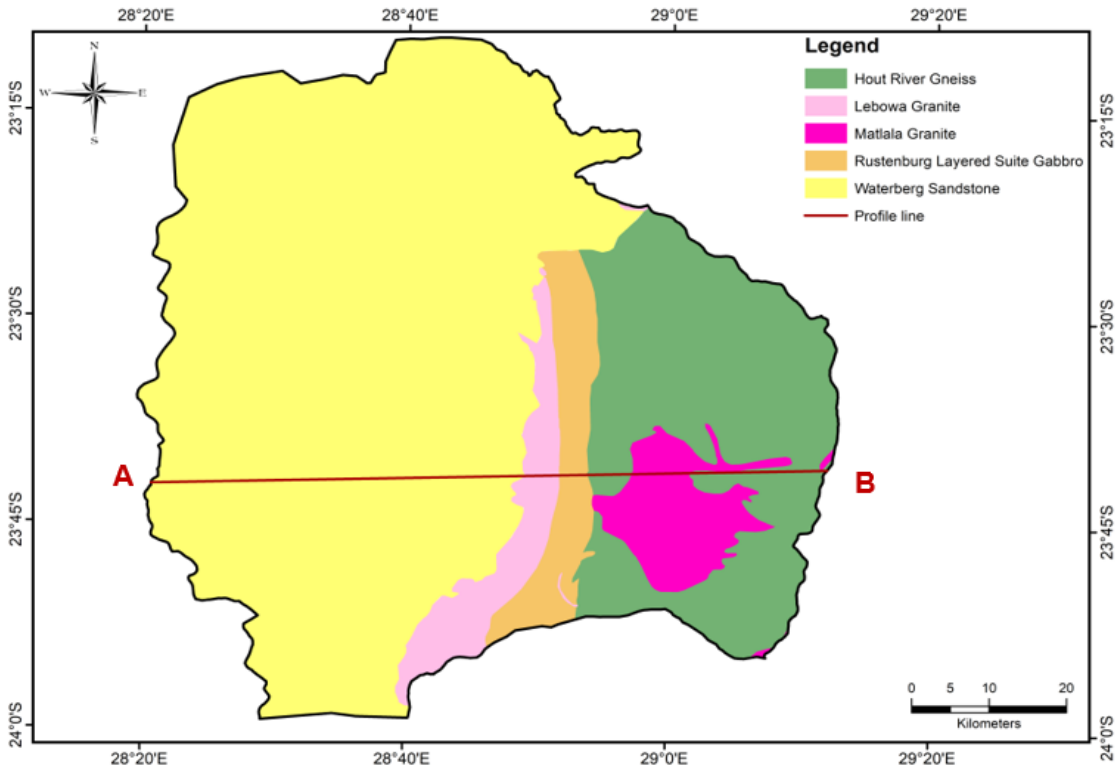

Figure 4.5: Map showing hydraulic conductivity zones defining the layer properties. A cross-section was constructed from the western to the eastern part of the model domain (line A-B).

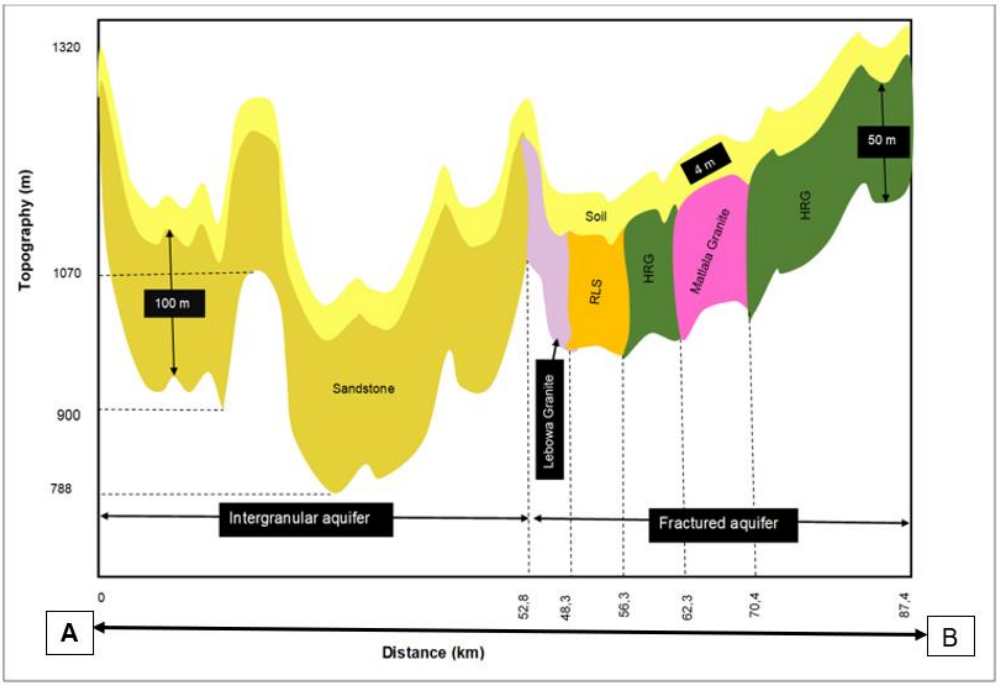

Figure 4.6: West-to-east cross-section showing the variation of the topography of model top, aquifer thickness and rock types that lie below the model domain.

The factors controlling hydraulic conductivity (K) such as lithology, age of rocks, the extent of weathering, and geological structures were considered in the selection of hydraulic conductivity zones (K-zones). The primary aquifer situated in the western part of the model area exhibits high borehole yield ranging from 2 to 10 l/s, while the fractured and weathered aquifer located in the eastern part of the model domain varies in yield from 0,5 l/s to 5 l/s (Figure 4.4). The range of hydraulic conductivities corresponding to the three soil types and five K-zones covering the upper and second layer, respectively were compiled from published and unpublished data (Table 4.1).

Table 4.1: The hydraulic conductivity of rocks that cover the model area (Holland, 2011; Ahokpossi, 2017).

Lithology	**Hydraulic Conductivity (m/s)**
Hout River gneiss	9E-06
Lebowa granite	1E-06
Matlala granite	7E-06
Rustenburg Layered Suite gabbro	6E-06
Waterberg sandstone	2E-05
Clay soil	9E-07
Sandy soil	8E-05
Sandy loam soil	1E-06

4.4.4 Boundary Conditions

In this study, a variety of GIS data were compiled and used as boundary conditions. Digital elevation model (DEM), water level, geologic map, and the outline of rivers were used to outline the boundary conditions. The western and eastern boundaries of the model domain are represented as a no-flow boundary based on the observations of the surface water divide, river flow patterns and the contrast in the topographic relief along the model boundary. Along the two boundaries, topography sharply decreases away from the model area, making clear demarcation of the no-flow boundary. Below is the summary of the boundary conditions that were implemented.

I. Surface Water: River and Dam

It is assumed that rivers exchange water with the underlying groundwater aquifer system, implying that the river can either supply or gain water to/from the aquifer. In this study, Mogalakwena River and Glen Alpine Dam were considered as internal boundaries which can influence the groundwater system. The hydraulic conductance of the interface that defines the property of the materials between the aquifer and the bottom of the river and dam was calculated using the formula (Oladeii, 2000):

$$Cb = KLW/M$$

Where Cb is the conductance of the interface, K is hydraulic conductivity, L and W are the length and width, respectively, while M is the thickness of the riverbed or the interface, which is assumed to be made up of fine sediments.

The riverbed was traced on Google Earth-pro to estimate the length and width of the river. The estimated conductance of the river and dam was about 0,0008 and 0,0001 m^2/s, respectively. These assumptions were also compared with values obtained from the literature review and were adjusted during the model calibration.

II. General head boundary

Two general head boundaries (GHB) were defined in the northern and southern parts of the model domain. These boundaries were chosen based on piezometric contour lines, river patterns, and topographic relief. The Mogalakwena River flows from the south to the north following the morphology of the model domain. Based on this analogy, the south GHB was defined as an inflow boundary whereby water enters the aquifer along with low topographic relief, while the northern GHB is assumed to be an outflow or groundwater discharge boundary, i.e., water exists in the model area along this boundary.

To evaluate the validity of the inflow and outflow boundaries, hydrochemical data were used. This was achieved by considering Na/HCO_3, Ca/Ma, (Ca+Mg)/(Na+K) ratios, and electrical conductivity (EC) (Figure 4.7). Along the inflow boundary, or

groundwater recharge zone is assumed to be characterised by a high Ca/Mg ratio, which is consistent with the inflow situated in the southern part of the model domain (Figure 4.7A). In addition, Na/HCO_3 ratio is relatively low along the inflow boundary and gradually increases towards the outflow boundary in the northern part of the area (Figure 4.7C). Similarly, (Ca + Mg)/ (Na +K) ratio is high along the inflow boundary and decreases northward as we approach the groundwater discharge zone (Figure 4.7C), which is consistent with the electrical conductivity which shows an increasing trend from the south (inflow) to the north (outflow) boundaries (Figure 4.7B).

The general head boundaries were constructed using polylines with consideration of both topography and river flow. The flux across the boundaries was calculated using the below equation (Oladeii, 2000):

$$Q_b = c_b(h_{source}(h_{source} - h)$$

Where Q_b is discharge rate, C_b is the conductance of the interface, which corresponds to the property of the materials between GHB and the aquifer, while h is piezometric surface along the boundary, and h_{source} is head or topographic height.

The discharge rates recorded at the two river gauging stations along the Mogalakwena River were used to calculate the conductance of the GHB (Figure 4.2). The calculated C_b was higher in the north, i.e., at the lower reach compared to the south (at the upper reach of the river) due to a high discharge rate in the northern boundary. The high discharge rates can be due to increased tributaries flowing into the Mogalakwena River, causing overflow/floods along the Glen Alpine Dam.

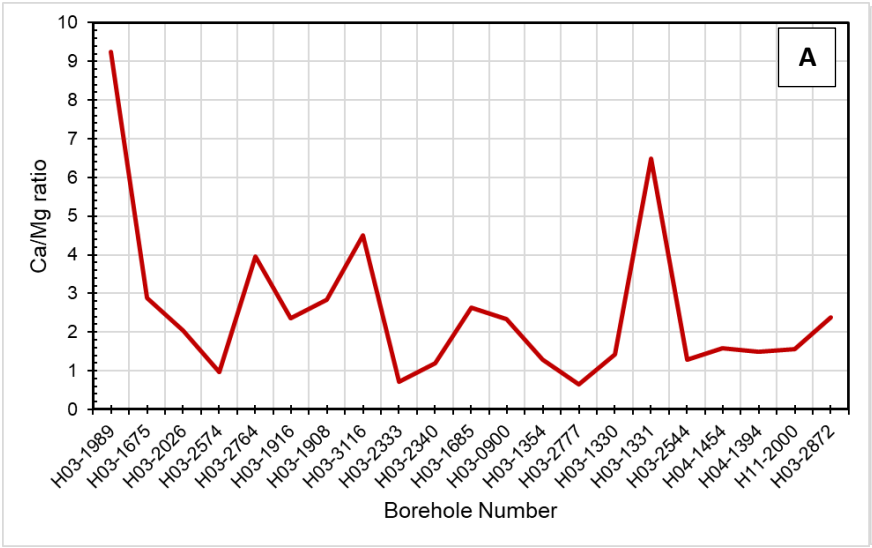

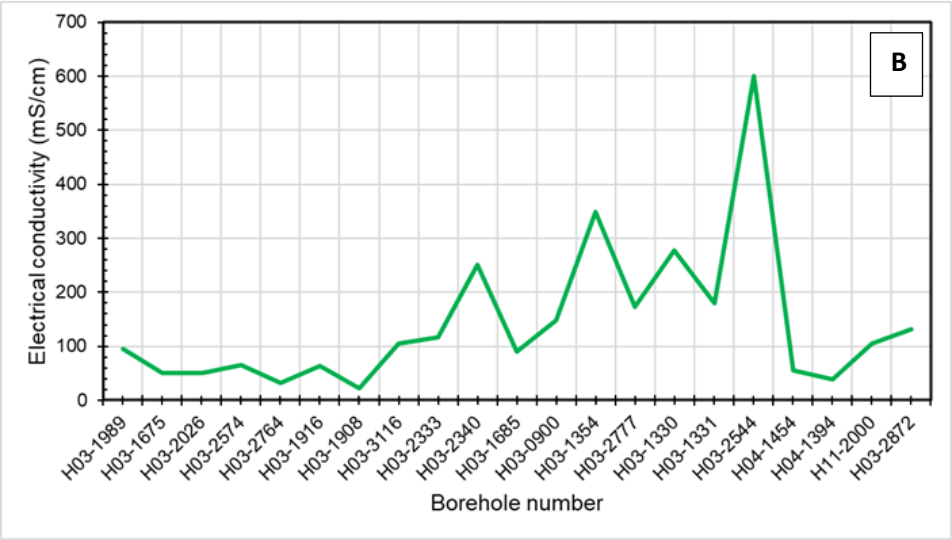

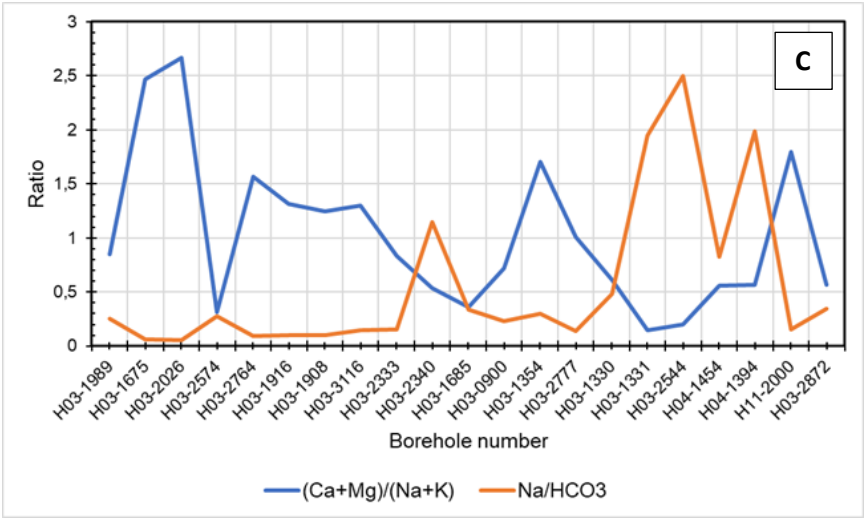

Figure 4.7: Graphs showing the Ca/Mg ratio (A), electrical conductivity (B) and (Ca+Mg)/(Na+K), and Na/HCO_3 (C) at the inflow and outflow boundaries.

4.4.5 Groundwater Recharge: Chloride Mass Balance

Groundwater recharge is defined as the percentage of precipitation that ultimately reaches the watertable (Freeze and Cherry, 1979). Estimation of recharge is essential in groundwater modelling to investigate water balance. Chloride Mass Balance (CMB) is one of the most reliable techniques used for recharge estimations (Cook, 2003). The basic assumption is that chloride can neither be absorbed nor desorbed during the flow of water through aquifers and is assumed to be a conservative tracer and can be used to estimate the amount of groundwater recharge (Cook, 2003). However, the CMB can negatively be affected by the incorporation of additional chloride from other sources for instance weathering of rocks and soil, hence the obtained recharge should be considered as the lower limit of groundwater recharge (Banks et al., 2009).

The major limitation of CMB in the study area was the poor dataset as chloride was not consistently monitored in groundwater hence the data was incomplete for the time series. The following equation was used to estimate groundwater recharge (Kinzelbach and Aeschbach, 2002):

$$Rt = \frac{PCl_p}{Cl_{gw}}$$

Where Rt is total recharge, P is precipitation, Cl_P is chloride concentration in precipitation and Cl_{gw} is chloride concentration in groundwater. Using the above equation, groundwater recharge was estimated and implemented as one of the stresses applied to the aquifer.

4.4.6 Evapotranspiration

Evapotranspiration describes water loss either from the land surface to the atmosphere or evaporation and transpiration (Zotarelli et al., 2010). Evaporation and transpiration may occur simultaneously preventing the water from reaching the groundwater aquifer. The evapotranspiration data was collected using the Campbell Scientific Africa by the Agricultural Research Council (ARC). ARC used the Pennmann Monteith (FAO-56) approach to estimate the evapotranspiration rate. The Pennmann Monteith (FAO-56) equation is shown below (Zotarelli et al., 2010):

$$ET_o = \frac{0.408\Delta(R_n - G) + \gamma \frac{900}{T + 273} \mu_2 (e_s + e_a)}{\Delta + \gamma(1 + 0.34\mu_2)}$$

Where:

ET_o is the reference evapotranspiration (mm/day),

Δ is the slope of the vapour pressure curve (kPa °C^{-1}),

R_n is the net radiation at the crop surface (MJ m^{-2} day^{-1}),

G is the soil heat-flux density (MJ m^{-2} day^{-1}),

γ is the psychrometric constant (kPa °C^{-1}),

T is the mean daily air temperature (°C),

u_2 is the wind speed at a height of 2 m (m s^{-1}),

e_s is the saturation vapour pressure (kPa),

e_a is the actual vapour pressure (kPa) and

(e_s − e_a) is the saturation vapour pressure deficit (VPD) (kPa).

The daily total relative evapotranspiration data (ETo) for the study area was obtained from data recorded at four monitoring stations within the model domain. However, only the Waterberg Styloop Station showed consistency in the evapotranspiration rate recordings, hence was selected as a representative for the entire model area. The potential evapotranspiration was estimated using the single crop coefficient method. Approximately 54% of the model domain is covered by the shallow root depth of woodland/bushland trees/plants. The potential evapotranspiration rate was estimated by multiplying the plant coefficient of 0.8 by the recorded ETo as indicated by the equation below (Kinoti, 2018):

$$PET = ET_O \times K_c$$

Where:

PET-Potential evapotranspiration rate

ETo-Relative evapotranspiration rate

K_c-Crop coefficient or the trees that largely cover the area

4.4.7 Groundwater budget

The estimation of the groundwater budget is important, and it enables quantifying the amount of outflows and inflows (Anderson et al., 2015). Construction of groundwater budget during conceptualisation assists in evaluating whether all essential parameters and processes interacting with the groundwater system were considered (Anderson et al., 2015). As stated by Anderson et al. (2015), the groundwater budget can be expressed in terms of the following equation:

$$Inflow = outflow \pm \Delta storage$$

The important parameters for groundwater balance include precipitation, evapotranspiration, evaporation, baseflow, and surface water flows. The inflows include groundwater recharge from rainfall or the contribution of other sources such as seepage from surface water bodies such as rivers, dams or wetlands (Anderson et al., 2015). Flows from bedrock or hydrologic units near the model boundary, injection of water from wells, infiltration from irrigation, etc (Anderson et al., 2015).

The total water balance for the model domain was estimated using the following equation:

$$RCH + RIV_{in} = EVT + Wells + RIV_{out} + Surface\ runoff$$

Where RCH stands for recharge, RIV_{in} is river inflow, EVT is evapotranspiration, wells are abstraction wells and RIV_{out} is river outflow (baseflow). The area of the model domain was used to calculate the volume of the total recharge and evapotranspiration. The river inflow and outflow were calculated from the two gauging stations in Figure 4.1. Furthermore, the estimated surface runoff was adopted from previous studies (Tshikolomo et al., 2013). Table 4.2 summarises the approximate water balance for the area of interest.

Table 4.2: Estimations of groundwater budget at Mogalakwena Subcatchment.

Component	***Inflow*** *(m^3/d)*	***Outflow*** *(m^3/d)*
Recharge	58582656	
River	404684	809368
Evapotranspiration		16810675
Pumping wells		216438
Surface runoff		736838,5
Total	58987340	18573320

4.5. Numerical model

The conceptual model presented in sections 4.1 to 4.4 was translated into a numerical MODFLOW model. MODFLOW is a finite-difference groundwater flow modeling program and consists of many packages whereby each package performs a specific feature on the simulated hydrologic system (Harbaugh et al., 2000). In this study, the hydrologic systems of the model were represented by layers, rows, and columns, thus enabling the creation of blocks or grid cells. The input to each package was carried out using ModelMuse graphical user interface that translates spatial data created in ArcGIS environment to objects, which MODFLOW can read. The packages that were implemented in this study are presented below:

4.5.1 Required MODFLOW Packages

I. Upstream Weighting Package (UPW)

The UPW package is the internal flow package for MODFLOW-NWT that allows the calculation of inter-cell conductance in the absence of rewetting data (Futornick, 2015). Additionally, the package specifies properties influencing the flow between cells (Futornick, 2015). The package allows the application of a Newton solver for problems related to unconfined groundwater flow due to conductance derivatives required by the Newton method (Ely and Kahle, 2012). The UPW package smoothes the horizontal-conductance and storage-change

functions during the drying and wetting of cells to provide a continuous derivatives solution by the Newton method (Niswonger et al., 2011).

II. Unsaturated Zone Flow (UZF)

The UZF package was established to simulate the flow and storage of water in the unsaturated zone, and it partitions flow into recharge and evapotranspiration as well as overland surface runoff into streams, lakes, rivers, dams, etc (Niswonger et al., 2006; Ely and Kahle, 2012). The UZF package is one of the MODFLOW 2005 and MODFLOW NWT packages that substitutes recharge and evapotranspiration by providing improved recharge estimations with consideration of effects of flow, evapotranspiration, and storage in unsaturated zones (Kinoti, 2018). According to Niswonger et al. (2006), the UZF package assumes that the occurrence of unsaturated flow is a response to gravitational potential gradient and excludes the negative potential gradient. Furthermore, the method assumes that the hydraulic properties of the unsaturated zone are the same for every vertical column of the mode cells (Niswonger et al., 2006).

The UZF package was considered as an alternative method for recharge and evapotranspiration. The package internally calculates the residual water content based on the difference between the specified yield and the saturated water contents (Niswonger et al., 2006). Contrary to the recharge package, the infiltration rate is applied to the land surface rather than the specified recharge rate directly to groundwater (Niswonger et al., 2006). Additionally, the applied infiltration rate is limited by the saturated vertical conductivity (Niswonger et al., 2006).

In contrast to the Evapotranspiration package, evapotranspiration losses in UZF initially occur in the unsaturated zone above the evapotranspiration extinction depth, and water extraction from groundwater only occurs if the target is not met (Niswonger et al., 2006). Furthermore, the UZF package allows direct water discharge to the land surface whenever the water table's depth altitude exceeds the land surface (Niswonger et al., 2006).

In this study, the following UZF required parameters: infiltration rate, evapotranspiration, ET extinction depth, ET extinction water content, Brooks-Corey

epsilon (exponent), and saturated water content were assigned as 5e-8, 2e-8, 2, 0,044, 3,8, 0,0412 and model top, respectively. The ET extinction depth and the ET extinction water content are essential for the simulation of evapotranspiration. The extinction water content is the water content in an unsaturated zone flow below which evaporation can be neglected. As outlined in Section 3.8 and shown in Figure 3.7, the dominant type plants that cover the area are woodland bush and grass. The ET extinction depth was assumed based on the root depth of the woodland bush.

III. Head Dependent Flux

- General head boundary

The general head boundary package (GHB) or Cauchy boundary (2nd kind boundary condition) was implemented to simulate head-dependent flux or the exchange between the source and the groundwater aquifer. In this study, the GHB package was activated to simulate the inflow in the south and the outflow in the northern part of the model domain (Figure 4.2). The general head boundaries included the inflow, outflow, and Glen Alpine Dam with the conductance 0, 0001, 0,0001 and 0,001 m/s, respectively. The boundary head was assigned to model top and direct interpretation was applied.

- RIV package

The river package enables the model to calculate the amount of streambed percolation and groundwater inflow to each river reach (Oladeii, 2000). The process uses the riverbed conductance and the difference between the calculated model cell hydraulic head and the river stage (Oladeii, 2000). The river package allows the simulation of the river/aquifer interaction depending on the pressure gradient between the river and groundwater system. The riverbed conductance controls the flow rate from or to the river based on the difference between river stage and modelled groundwater head in the uppermost active cell (Oladeii, 2000). Furthermore, the riverbed conductance determines the maximum leakage rate to the aquifer when heads fall below the riverbed (Oladeii, 2000).

The river package enabled the inclusion of the Mogalakwena River and its tributaries into the boundary conditions. The river stage and thickness of the riverbed were assigned as model top and 2 m, respectively. The riverbed conductance for this model was assigned to 0,0008 m/s and direct conductance interpretation was implemented.

- WEL Package

The WEL package is a 1st type boundary condition (Dirichlet boundary), and it is a specified flux that enables the assessment of the stress applied to groundwater aquifer during withdrawal of water or injection of water into the groundwater aquifer. The rate of abstraction is considered as one of the stresses that were applied to the hydrological system. Five abstraction wells were selected for numerical simulation based on water use, i.e., the wells that supply water for irrigation purposes. The pumping wells were imported from the ESRI shapefile as separate objects and assigned to the respective grid cell according to the geographic coordinates of each well. Table 4.3 shows the abstraction rate of each pumping well used for this model.

Table 4.3: Location of abstraction wells and pumping rate

Borehole ID	**X**	**Y**	**Pumping rate** (m^3/day)
BH1	696801	7388458	380,16
BH2	694355	7362593	1486,08
BH3	691157	7378806	95,04
BH4	649530	7424840	371,52
BH5	693248	7406299	8,64

IV. MODFLOW Solver Package

The solvers package determines the method of solution of the general algebraic equation of groundwater flow expressed as a matrix of ‘n’ by ‘m’ dimension, where ‘n’ is the number of rows and ‘m’ is the number of columns. In this study, the Newton solver was chosen to determine the solution of the matrix equation. This solver uses the newton linearisation method to solve non-linear differential equations including

representation of unconfined aquifers (Futornick, 2015). The newton solver is responsible for solving the finite difference equation at each step of the stress period (Futornick, 2015). In this study, the model complexity was defined as simple with head tolerance, flux tolerance, and the number of outer iterations set to 0.0001, 0.06, and 250, respectively.

V. Post Processor: Zone budget

Zone budget (ZONEBDGT) is a computer program that computes subregional water budgets utilising the MODFLOW groundwater flow model results. While using the zone budget, the user assigns the subregions by specifying the zone number for each boundary condition and hydrologic system. A separate budget is computed for each zone. The budget for a zone includes the exchange of water between zones (e.g., river and groundwater aquifer). The first step while activating the zone budget is to identify a zone (e.g., boundary conditions such as wells and rivers, etc.). Then to assign zone ID to the identified zone. In this study, the zone budget was implemented to assess the flux between the dam and the aquifer. In addition, the zone budget was used to understand the exchange of water between surface water source such as rivers and the aquifer. The aquifer, river and dam were assigned zones 1, 2 and 3, respectively. The resulting zones were assessed in terms of flux between pairs of zone, inflows, and outflows. The results allowed to understand the interaction between surface water and groundwater thereby enabling to perceive the impact on groundwater aquifers.

4.5.2 Hydraulic Head Observation Package

A head observation package (HOB) was activated to enable the comparison of the observed head with the simulated head. Twelve monitoring wells with groundwater levels monitored for a period of 10 years were used as observation wells. Only four observation wells are drilled in the western part of the area, which is underlain by the primary aquifer system, while eight monitoring wells are situated in the eastern part of the model domain, which is underlain by a fractured aquifer system. The water level in the wells ranges from as shallow as 8 m depth to 30 m below the ground. Prior to simulation, the depth of each water level was converted into elevation above mean sea level by subtracting the depth from the elevation of each borehole collar.

4.5.3 Steady-State Model

The model was initiated with a steady-state flow to simulate groundwater flow with constant parameters, assuming that the parameters remain constant throughout the specified time of the model. The results of the steady-state model are important and used as initial heads for the transient state model. The steady-state flow of groundwater equation is shown below (Futornick, 2015):

$$\frac{\partial}{\partial_x}\left(K_{xx}\frac{\partial}{\partial}\right)(+\left(K_{yy}\frac{\partial}{\partial y}\right)+\left(K_{zz}\frac{\partial}{\partial z}\right)-Q=S_S\frac{\partial h}{\partial t}$$

Where:

K_{xx}, K_{yy}, and K_{zz}- are hydraulic conductivities along x, y, and z coordinate axes

h- piezometric surface or water level in the borehole

Q- volumetric flux per unit volume and it represents sources and/or sinks. Q is negative for outflow and negative for inflow.

S_s- specific storage of the porous material

t-time

However, in a steady-state model, the parameters are invariant of time and the right side of the partial differential equation reduces to zero.

I. Spatial Discretisation

Any aquifer system modelled using MODFLOW requires discretisation of the model domain into several rows and columns forming discrete blocks whereby the governing equation of groundwater flow is solved for hydraulic head and flow rate (Futornick, 2015). The blocks are commonly known as cells and satisfy Darcy's law, which is written differently to accommodate simplification and notation of the equation (Futornick, 2015):

$$q_x = -k_x \boldsymbol{\partial h/\partial x}$$

q_x is volumetric flow rate, $-k_x$ is hydraulic conductivity and $\boldsymbol{\partial}$h is the change in hydraulic head across a given length x.

The model domain was discretised into rectangular grids of 200 m by 200 to provide a reasonable resolution that can be representative of the spatial features or objects that were used as input data into MODFLOW (Figure 4.8). In addition, the grid cell size fairly accounts for contrast in hydraulic heads corresponding to various boundary conditions and stresses that were implemented to the model. Furthermore, the grid cell size accounts for the large area of the model domain, the complexity of the model, and the availability of data. The distribution of important data set was also prioritised in the selection of the grid cell size (e.g., Glen Alpine Dam). A vertical discretisation of 2 was also applied to improve the quality of results for the thick primary aquifer. Furthermore, the Glen Alpine Dam was refined using a grid refinement size of 25 m by 25 m to improve the resolution of the groundwater head corresponding to the dam.

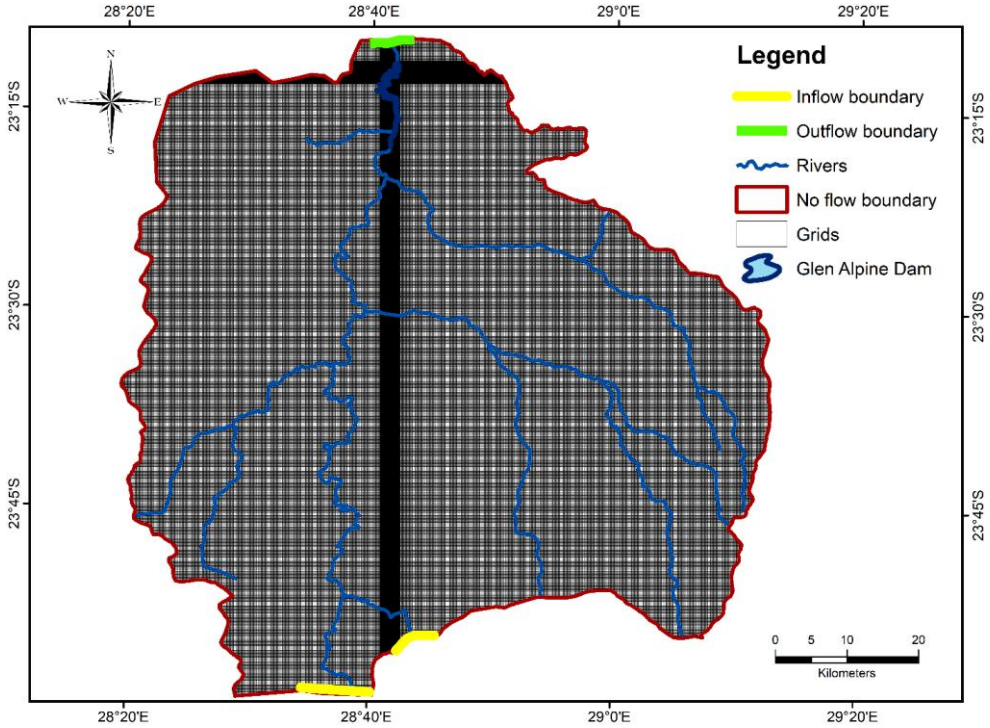

Figure 4.8: Map showing the grid cells and the boundary conditions of the model.

II. Sensitivity Analysis

The sensitivity analysis of the steady-state model focussed on the variation of the model input parameters to assess the model's response. The model was run multiple

times while varying the model parameter at a percentage rate of +/-20% from the original estimated model parameter value. The corresponding RMS for every simulation was recorded.

III. Steady-State Model Calibration and Error Estimation

Model calibration is the process of adjusting the model's input parameters (e.g., hydraulic conductivity) and boundary conditions (head or flux) to accurately match observation data (e.g., hydraulic head, flow rate, etc.) in a real hydrological system (Anderson et al., 2015). The model calibration enables to fit of the observed heads with the simulated heads (Reilly and Harbaugh, 2004). Manual or trial and error methods can be used during the calibration process to have a clear understanding of the model's behaviour. Calibration parameters are done to simulate a reasonable water budget and find the best fit between observed and simulated heads.

In this study, three error matrices were adopted to evaluate the level of calibration of the model. These include the root mean square error (RMS), the mean absolute error (MAE) and the mean error (ME). The RMS is the root of the average difference between observed and simulated heads (Kinoti, 2018).

$$RMS = \frac{1}{n}\sum_{n=1}^{n}(Obsi - Simi)^{0,5}$$

The MAE is the average of the absolute, non-squared error of the difference between observed and simulated heads (Kinoti, 2018).

$$MAE = \frac{1}{n}\sum_{n=1}^{n}|Obsi - Simi|$$

ME measures the average difference between observed and simulated heads (Kinoti, 2018).

$$ME = \frac{1}{n}\sum_{n=1}^{n}(Obsi - Simi)$$

The RMS and MAE are important in measuring the average magnitude of errors, and they indicate whether the calibration criteria set before or during calibration was met

(Kinoti, 2018). The ME indicates the skewness of the overall bias on the calibrated model between simulated and observed heads (Kinoti, 2018).

4.6 Fieldwork

Fieldwork was undertaken in August 2021; the fieldwork was intended for sampling water and analysis of the stable isotopes of the water molecule. The boreholes which are currently supplying water for the various communities which are located within the model domain were selected for sampling. A total of eighteen water samples were collected from boreholes, rivers, and Glen Alpine Dam using 1L sampling bottles (Figure 4.9). The samples were stored in a cooler box to avoid sunlight exposure which may modify the original water chemistry. The coordinates of each sampling point were recorded using a portable handheld GPS.

In addition, the Thermo Orion Star A329 Multiparameter meter for measurement of the physical parameters of water was used to measure pH, EC, temperature, and the amount of dissolved oxygen in the water. The water samples were submitted to iThemba Labs Environmental Isotope Laboratory (EIL), in Johannesburg for analysis of stable isotopes of oxygen (^{18}O) and deuterium (^{2}H). The equipment used for the analysis of stable isotope consists of Los Gates Research (LGR) liquid water isotope analyser. The laboratory standards were used to calibrate against international reference materials for each analysed batch of samples. The analytical precision was estimated to be 0.5‰ for $\delta^{18}O$ and 1.5‰ for $\delta^{2}H$.

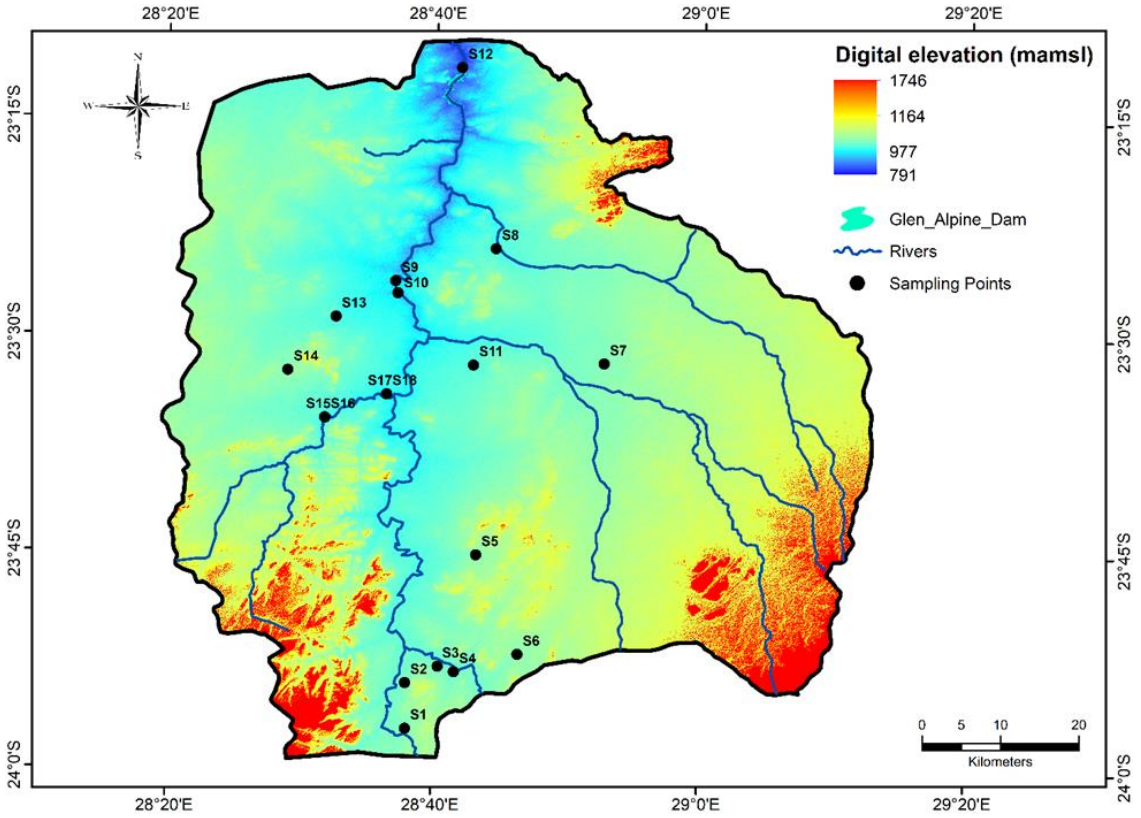

Figure 4.9: Map showing the location of the water sampling points.

4.6.1 Sampling Sites

As indicated in section 4.4, the model domain covers a large areal extent which required more time for the fieldwork. Thirteen groundwater samples were collected from different villages within the model domain based on the distribution and functionality of the boreholes. The fieldwork was intended to sample water at widely distributed points throughout the model domain so that the results allow us to understand the variation in the stable isotope composition of water in the study area. Most of the boreholes are secured in brick/zinc pump houses and use a submersible pump for water abstraction. The boreholes supply water via two pipes, one for supplying the community, while the second pipe enables regular monitoring of water quality and collection of water samples. Figure 4.10 below shows a typical example of the borehole that was sampled during the fieldwork.

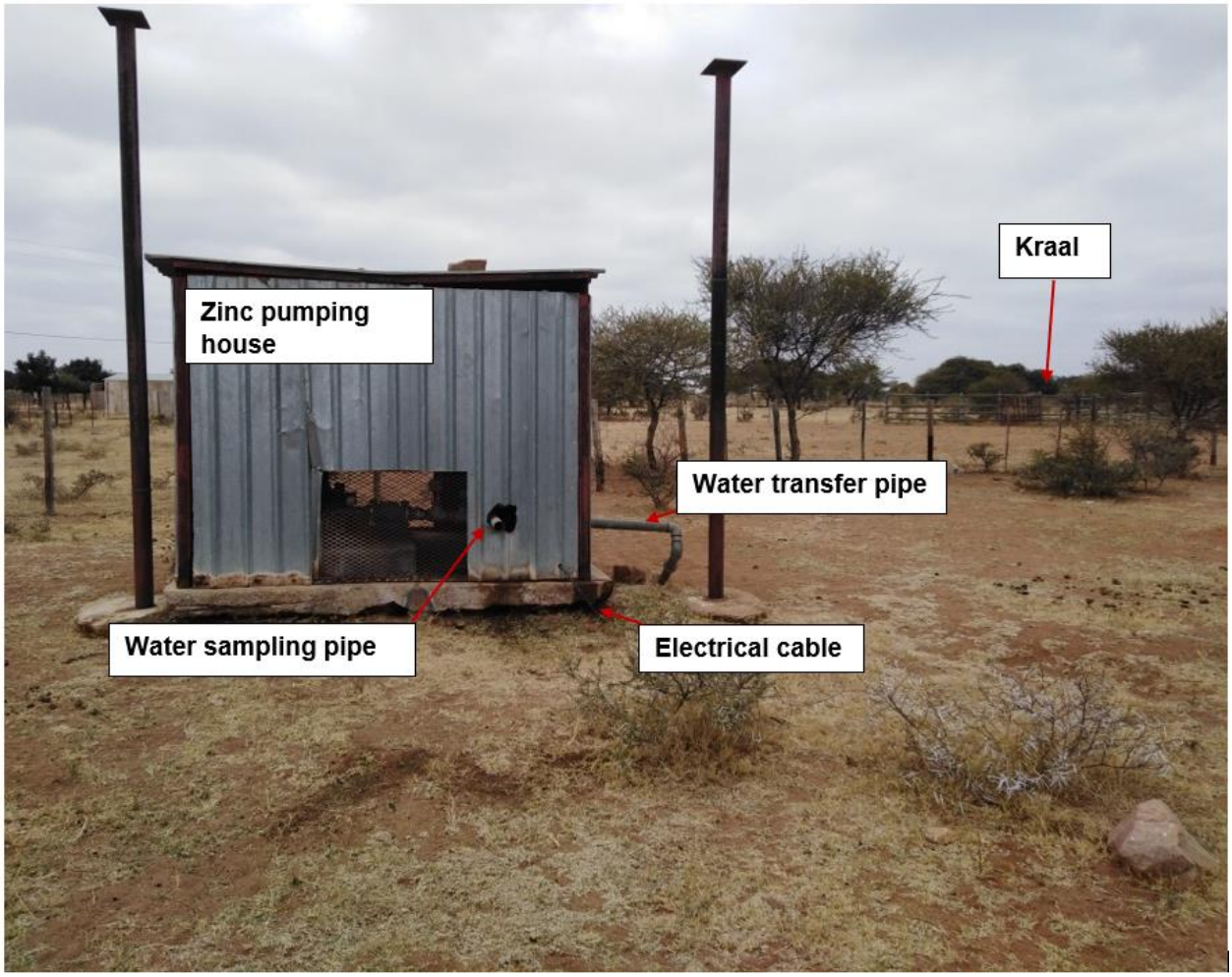

Figure 4.10: A photograph of the borehole setting within Mogalakwena Municipality.

For surface water, five sites were sampled from Mogalakwena River, its tributary (Motse River) and Glen Alpine Dam. The surface water samples are important to investigate the extent of interaction between surface water and groundwater in terms of depletion and enrichments of $\delta^{18}O$ and $\delta^{2}H$ ratios. Figure 4.11 shows the typical surface water sampling sites, the surrounding geology or soil type and any anthropogenic activities that can contaminate the water resource in the area.

Figure 4.11: Photographs of the sites that were visited during the fieldwork.

In general, the water levels in both Mogalakwena River and Glen Alpine Dam were very low. The eastern tributaries were dry, whereas the western tributaries had water. This may imply that the western tributaries had more influence on the groundwater system as compared to those situated in the eastern part of the model domain. This may be attributed to the variation in the geology of the area.

Chapter 5: Hydrochemistry and Environment Isotopes

Hydrochemistry and environmental isotopes are important for understanding the origin or source of water, the processes that occur in the hydrologic cycle, and the dynamics of surface and groundwater interactions (Zhou and Lu, 2017). In addition, hydrochemical and isotope data are important to conceptualise the hydrological system of an area, and they enable the establishment of the connection between surface water and groundwater. In this study, both hydrochemical and isotope data were processed and used to constrain the boundary conditions (e.g., inflow and outflow). In the following sections, the water quality in the Mogalakwena Subcatchment is summarised. The results of the hydrochemical and isotope data are also presented in this section.

5.1 Water Quality

The quality of surface water and groundwater in the Mogalakwena Subcatchment was evaluated based on the South African standards for domestic and industrial use (SANS241, 2015). Below is the summary of selected chemical specious emphasised in terms of the standard limits that guide safe consumption of water in the study area.

5.1.1 Nitrate

Nitrate contamination in groundwater can result from nitrogenous compounds that originate from anthropogenic sources, which include domestic and industrial waste, intensive use of fertilisers for improvement of agricultural production, and sewage (Tessema et al., 2014). Nitrate is present in inorganic fertilisers used in farming, in canned meat where nitrate is being used as a preservative (DWAF, 1996). Vinger et al. (2012), discovered that nitrate pollutes groundwater when boreholes are drilled at distances between 13 m to 18 m from the pit latrines, and the use of fertilisers for improvement of crop production.

According to SANS241 (2015), groundwater with a nitrate concentration above 20 mg/L is not recommended for consumption. Although nitrate is non-toxic, its

conversion to nitrite can be a threat to human health. Vegol et al. (2004), indicated that oxidisation of iron by nitrite in the haemoglobin of the red blood cells forms methaemoglobin, which causes deficiencies in the oxygen-carrying ability of the blood that is controlled by haemoglobin.

Figure 5.1A shows the distribution of boreholes with elevated nitrate as defined by the SANS241 (2015). About 45% of the boreholes are contaminated by nitrate leaving only 55% of boreholes with acceptable nitrate concentration in groundwater. In this Subcatchment, animal manure and sewage from cattle kraals and residential areas are identified as the main sources of nitrate (Netshiendeulu and Motebe, 2012).

5.1.2 Electrical Conductivity (EC) and Total Dissolved Solids (TDS)

Electrical conductivity is defined as the water's capability to conduct electricity (Siosemarde et al., 2010). The electrical conductivity of water is due to the presence of ionic species that include sodium, nitrate, chloride, potassium, and calcium, among others (Siosemarde et al., 2010). EC is a function of incorporated solids dissolved in water; hence it is considered as the alternative way of measuring TDS in water. TDS in groundwater naturally occurs due to mineral dissolution, decomposition of plants, and soil (DWAF, 1996). Dahaan et al. (2016), described the relationship between TDS and EC using the following equation:

$$TDS = KeEC$$

Where TDS is in mg/L, EC is in µS/cm and Ke is a proportionality constant, and it ranges between 0.55 and 0.8.

TDS is the measure of the amounts of solid residues attributed to water evaporation during high temperatures (Dahaam et al., 2016). High TDS due to the dissolution of minerals negatively affects the taste and colour of the groundwater (Mohsin et al. 2013). According to SANS241 (2015), the standard limit of EC approved for the consumption of water is ≤ 170 mS/m. In the study area, about 30% of the boreholes are characterised by high EC exceeding the standard limit (Figure 5.1B). According to DWAF (1996), there is an ongoing process of increase in salinity of groundwater due to natural and manmade processes which occur in water flowing downstream contributing to high TDS content.

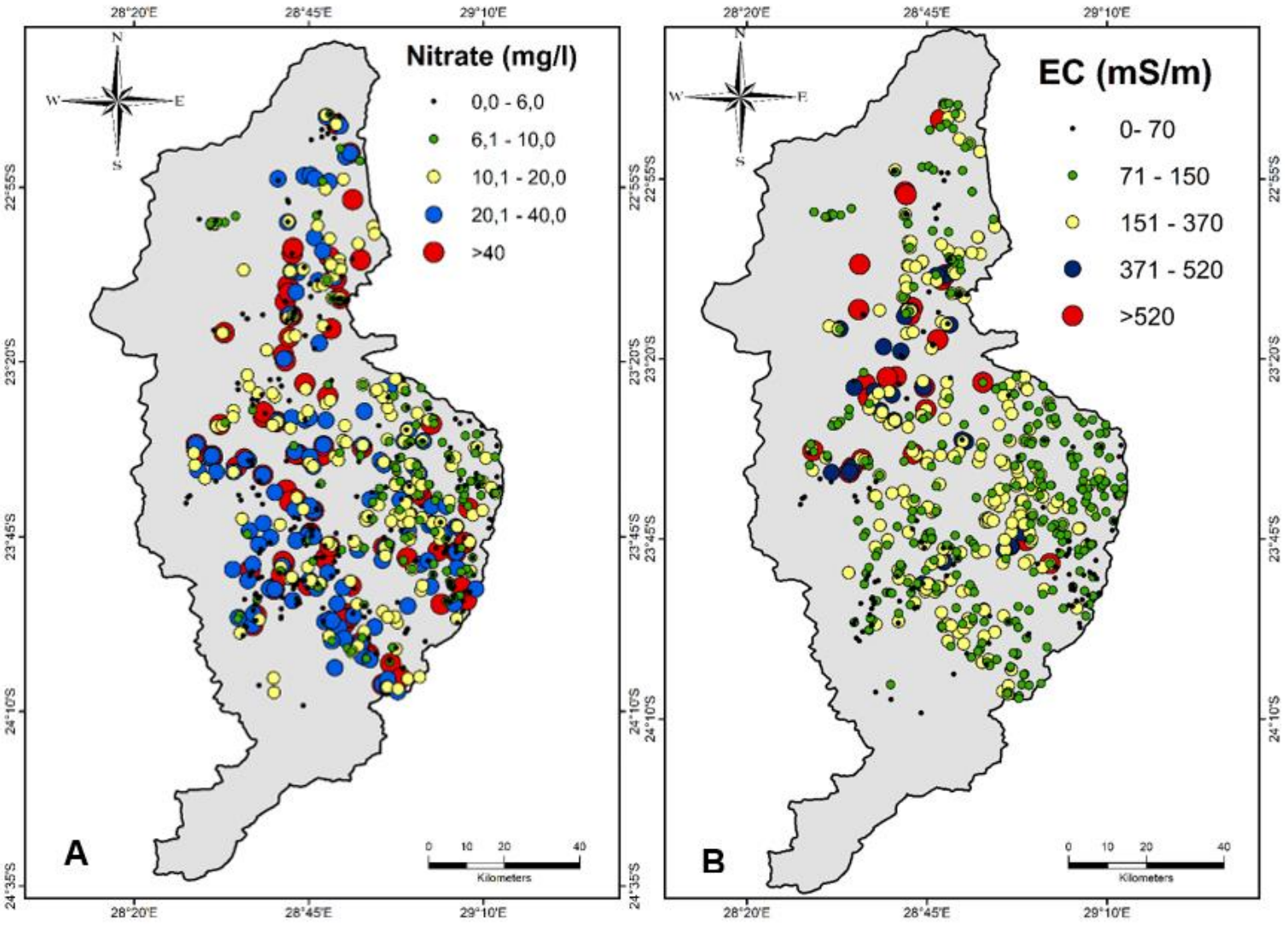

Figure 5.1: Map showing the concentration of nitrate (A) and electrical conductivity (B) within the study area.

5.1.3 Fluoride

The source of fluoride in groundwater can be due to fluoride minerals (fluorspar (CaF_2) and fluor-apatite), phosphate-containing fertilisers, and weathering of mica-rich rocks such as gneisses and felsic rocks (Tessema et al., 2014). Fluoride concentration in groundwater is also controlled by the solubility of fluoride-bearing minerals, the ability of the aquifer to exchange anions, the pH value, the temperature and type of geological formation, and the contact time between water and formation (Dar et al., 2011). According to Molekoa et al. (2019), fluoride minerals such as CaF_2 are non-reactive in groundwater at a pH of 7 due to their low solubility and are absorbed in clay or interchangeable materials. An increment in pH involves the substitution of the interchangeable fluoride by the hydroxyl group from silicate minerals causing fluoride enrichment. Molekoa et al. (2019), used the below muscovite equation to explain the mechanism of release of fluoride from felsic rocks to groundwater:

$$KAl_2\,[AlSiO_3\,O_{10}]\,F_2 + 2OH^- \rightarrow KAl[AlSiO_{10}][OH] + 2F^-$$

The intake of extended fluoride concentrations exceeding 1.5 mg/L can cause teeth mottling, skeletal fluorosis, dental fluorosis, and deformation of bones (DWAF, 1996). High fluoride concentrations are observed in the southern parts of the Mogalakwena Subcatchment as shown in Figure 5.2. The main source of fluoride in groundwater in the southern parts of the area is the Lebowa Granite of the Bushveld Complex. According to Hartzer (1995), the largest fluorite deposit is in the northwestern parts of Mookgopong (Naboomspruit) in the middle of Mokopane (Potgietersrus) and Bela-Bela (Warmbath). This deposit occurs as a replacement layer within the relict bedding of a coarse-grained leptite (Hartzer, 1995). Approximately 88 % of the boreholes in the area contain fluoride concentration within the acceptable range, while 12 % of the boreholes show elevated fluoride content.

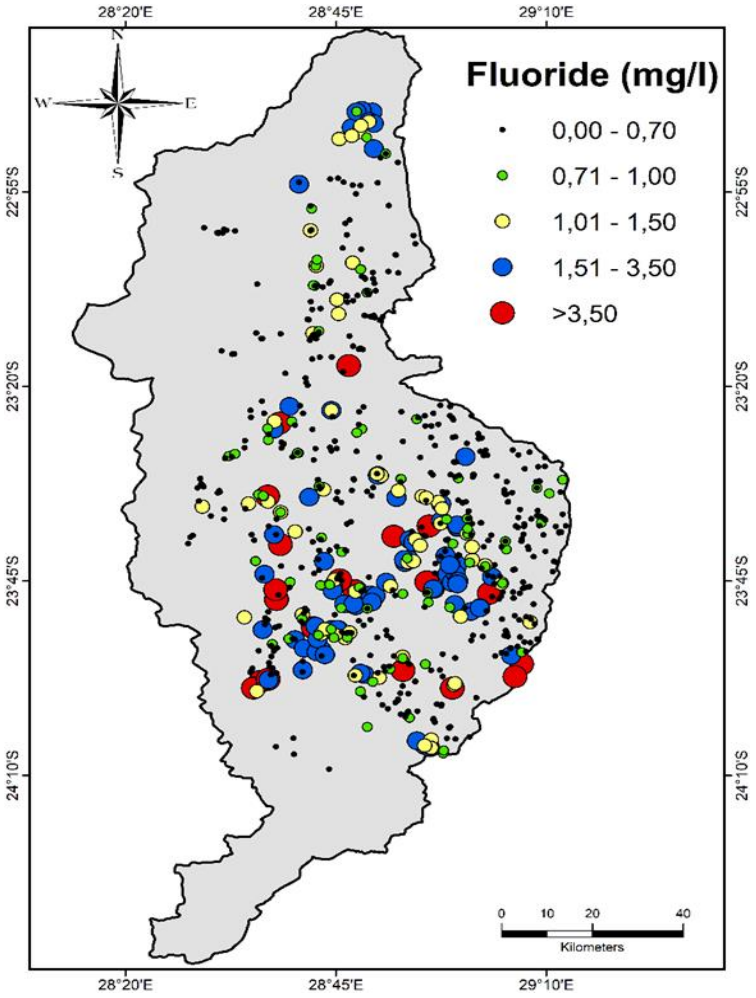

Figure 5.2: Map showing the distribution of fluoride concentrations within the study area.

5.1.4 Water Hardness

Water hardness measures the reaction between water and soap, and it defines the ability of water to bind with soap to form lather (Wimalawansa, 2016). Water hardness is a result of a variation of dissolved polyvalent metallic ions, predominately magnesium and calcium originating from soil and weathering of carbonate-rich minerals or rocks including limestones and magnesium-rich dolomites (Wimalawansa, 2016). Water hardness can be classified into four categories based on the magnesium (mg) concentrations namely very hard (>180 mg/L), hard (121-180 mg/L), moderately hard (61-120 mg/L) and soft water (0-60 mg/L).

Figure 5.3 shows the distribution of boreholes with different concentrations of magnesium (Mg) and calcium (Ca). Approximately 28% of the boreholes have high Mg content exceeding the standard limits within the study area (Figure 5.3A). Similarly, Figure 5.3B shows the distribution of calcium concentrations in the subcatchment with 9% of the boreholes having high concentrations greater than 150 mg/L. High calcium content causes lathering of soap by producing insoluble calcium salts resulting in scum precipitation (DWAF, 1996). Hard water consequently forms scales on heat exchange surfaces including hot water pipes, kettles, geysers, and cooking utensils (DWAF, 1996). Extensive consumption of hard water can however cause renal/kidney stones and produces a noticeable deposit of precipitates in containers (Wimalawansa, 2016). Soft water tends to corrode metal surfaces and pipes resulting in the incorporation of metals in drinking water (DWAF, 1996).

5.1.5 Salinity

Nasr and Zahran (2014), defined salinity as being equivalent to sodium chloride (NaCl) salt percentage which can be dissolved in soils from pollutants in rainwater. According to Krishan (2019), high groundwater salinity is common in arid and semi-arid regions affected by water scarcity. The breaking down of salt-rich minerals due to weathering is the major source of salt in groundwater (Nasr and Zahran, 2014). The weathering of minerals with low solubility and abundance occurs at greater depth due to the longer residence time of the percolating water causing a change in water type as sodium, chloride and sulphate (SO_4) increases (Stober and Bucher, 1999).

The sources of chloride (Cl) in groundwater are weathering of amphibole or biotite/ release of Cl from crystal-lattice and halite solution of fractured fluid inclusions and of current halite between mineral grains (Stober and Bucher, 1999). The salt concentration in water tends to accumulate in the distribution networks leading to blockage of pipes (Nthunya et al., 2018). The main sources of chloride in surface water and groundwater are sewage effluent discharge, irrigation return flows and various industrial processes (Naidoo, 2015).

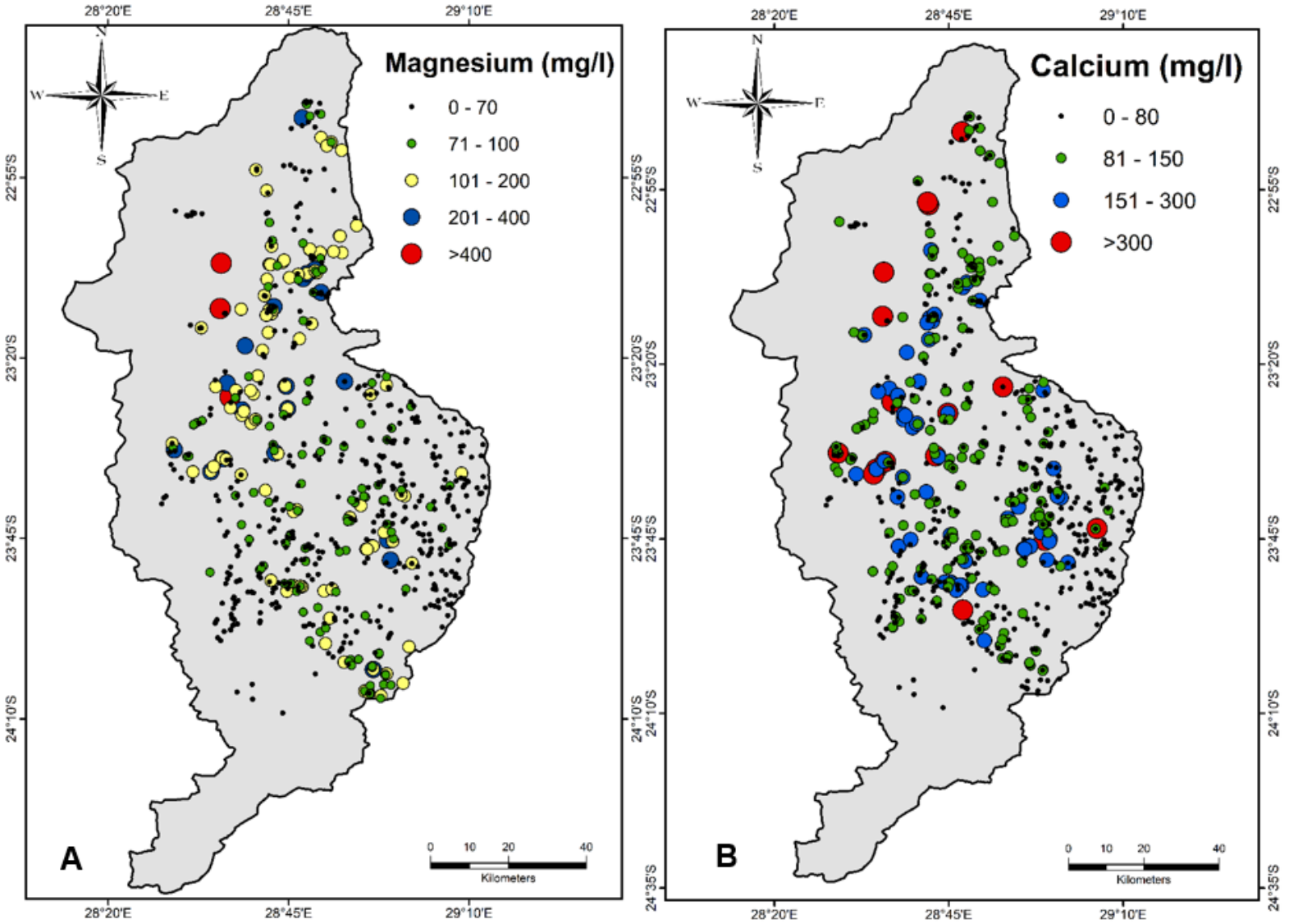

Figure 5.3: Maps showing the distribution of the borehole with magnesium (A) and calcium (B) in the study area.

Groundwater with sodium concentrations greater than 200 mg/L is not recommended for consumption and can produce a noticeable taste in drinking water (DWAF, 1996). Sodium may cause a reduction in permeability, drainage and increase erosion in soil, cause plant toxicity and induce deficiency of other elements (Vogel et al., 2004). Figure 5.4A indicates that high concentrations of sodium exceeding 500 mg/L are found in the northern part of the Mogalakwena Subcatchment.

Groundwater with high chloride concentrations usually contains high Na content (Vogel et al., 2004). Chloride originates from the dissolution of salts such as calcium chloride or sodium chloride (halite) as shown by the formulas below (Vogel et al., 2004):

$$NaCl_{(s)} \rightarrow Na^{+}_{(aq)} + Cl^{-}_{(aq)}$$

$$CaCl_{2(s)} \rightarrow Ca^{+}_{(aq)} + 2Cl^{-}_{(aq)}$$

Elevated concentrations of chloride greater than 300 mg/L are undesirable for consumption and impart a salty taste in the water while accelerating the corrosion rates of metals (Naidoo, 2015). Magnesium chloride in water generates hydrochloric acid after heating which is corrosive and creates problems in the boiler (Alkhateeb, 2014). In dense settlement areas, high Cl content in groundwater can be due to anthropogenic contamination such as animal, human and/or industrial waste. Figure 5.4B indicates that approximately 23% of the boreholes have Cl concentration exceeding the standard limits in the northern part of the study area.

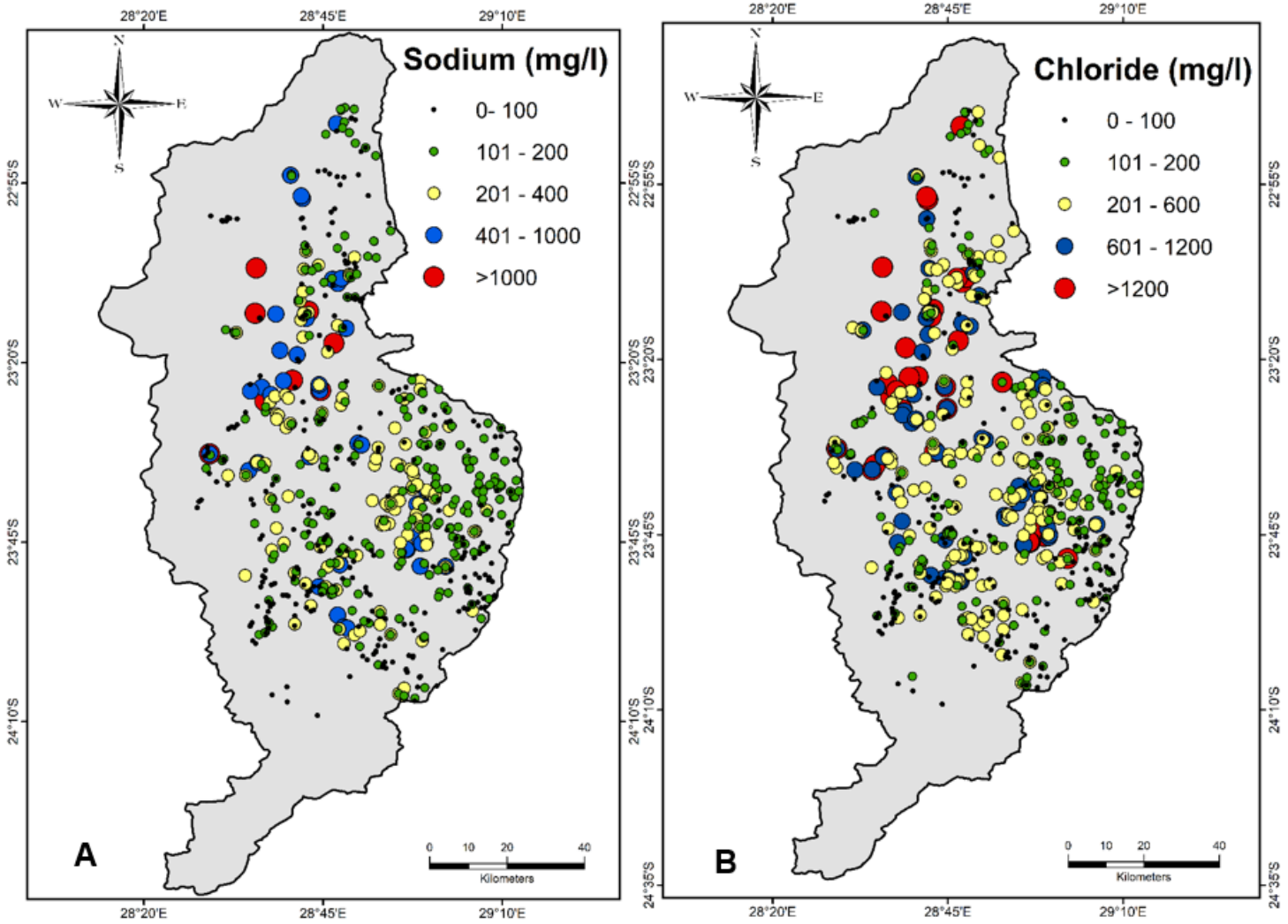

Figure 5.4: Map showing the distribution of borehole with sodium (A) and chloride (B) concentrations at Mogalakwena Subcatchment.

5.2 Hydrochemistry of the Study area

The hydrochemical facies provides information about the complex processes of the chemical reaction between water and the rocks that lie below the surface (Kumar, 2013). Hydrochemical data are usually presented using piper diagrams and related graphic displays. The piper diagram comprises two triangles on the baseline with milliequivalents of major cations (Mg, Ca, and Na+K) and anions (Cl, SO_4 and HCO_3+CO_3) plotted separately. The points plotted in the triangular fields are then projected onto the central diamond-shaped field, which represents the chemistry of water (Kumar, 2013). The location of the water sample on the diamond polygon of the Piper diagram helps to determine the type and quality of the water (Singh and Kumar, 2015). The piper diagram can be used to understand the processes that are taking place in the subsurface formation, such as mixing of groundwater with different compositions, ion exchange and rock-water interactions (Singh and Kumar, 2015).

In this study, groundwater chemistry was further analysed using piper diagrams to understand the chemical evolution of water. Groundwater in the Mogalakwena Subcatchment is heterogeneous in composition showing variance between weak and strong acids. There is a range of variations in composition from alkaline to alkalis. The groundwater shows four water types Mg-Ca-HCO_3, Ca-Mg-Cl, NaCl and mixed type (Figure 5.5 & 5.6). The dominant ionic composition found in groundwater within the study area are Na, K, Mg, Ca, CO_3, HCO_3 and Cl. According to Kumar (2013), the dominance of Mg, Na and Ca in groundwater indicates ion exchange. However, these ions may also originate from the dissolution of minerals such as feldspar and mica due to rock-water interactions with the surrounding granites and gneisses.

Mogalakwena Subcatchment is characterised by a semi-arid climate with high temperatures and evaporation rates. The elevated evaporation rates increase the salt concentration (NaCl) in shallow aquifers and on the soil as a residue. The salt residue left in the soil is later dissolved by the percolating rainwater during precipitation. The presence of Cl can further be attributed to anthropogenic sources or human excretions. The high CO_3 and HCO_3 concentrations originate from atmospheric carbon

dioxide but may also result from organic material found from the humic soils in the northern to eastern parts of the Subcatchment.

Figure 5.5 shows a progressive change in the groundwater composition from Ca-Mg-HCO_3 towards the Ca-Mg-Cl water type. The Ca-Mg-HCO_3 water type indicates recently recharged and shallow water attributed to the weathering of silicate minerals in crystalline rocks (Titus et al., 2009). According to Holland (2011), $MgHCO_3$ originates from the ferromagnesian minerals, calcite precipitation and process of ion exchange. Mg and Ca originate from the Alldays Gneisses and lime soils in the northern part of the study area. However, ion exchange from Mg to Ca may have also contributed. The progressive modification of groundwater indicates freshly recharged water which was altered during rock-water interactions as water percolates downward into deeper formation.

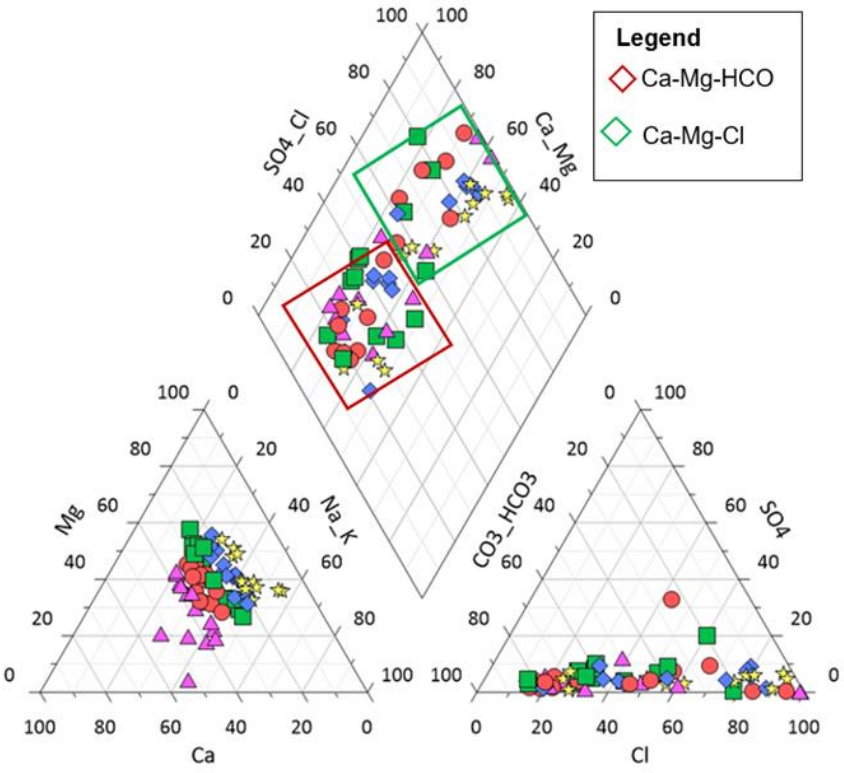

Figure 5.5: Piper diagrams showing the hydrochemistry of groundwater in the northern part of the study area that is underlain by the Alldays Gneissic of the high-grade metamorphic rocks of the Limpopo Mobile Belt.

Figure 5.6A shows the Na-Cl water type which is common in deep aquifers with ancient groundwater associated with ion exchange. Na probably originates from the cation exchange of Ca for Na hence few boreholes in Figure 5.6A fall under Ca-Cl water type. Sodium and chloride enrichment may also result from high evaporation that occurs in the western sector of the study area. According to Kumar (2013), Na-Cl water type is common in lower topographic relief (observed in the western part of Mogalakwena Subcatchment) due to a prolonged residence time and rock-water interactions. Na-Cl water type is salty and undesirable for consumption and irrigation because high Na content deteriorates soil texture and affect plant growth (Singh and Kumar, 2015).

Ca-Mg- HCO_3, Na-HCO_3 and mixed water type (Ca-Mg-Cl) are shown in Figures 5.6B, which represents the south and the eastern parts of the study area, which are geologically underlain by the crystalline and sedimentary rocks of the Bushveld Complex and Waterberg Group. The evolving groundwater chemistry from Ca-Mg-HCO_3 towards the mixed water type (Ca-Mg-Cl) and Na-HCO_3 suggests the processes of ion exchange between Ca and Na. The Mashashane Granite is enriched in Na than Ca hence dissolution or weathering of plagioclase can be the source of Na, while chloride may originate from rainwater or dissolution of halite. Additionally, sodium and bicarbonate can be released from the weathering of albite mineral to kaolinite in the crystalline rocks of the Bushveld Complex (Holland, 2011). The evolving water types may also be influenced by anthropogenic sources associated with settlements and platinum and chrome mining in the eastern parts of the study area.

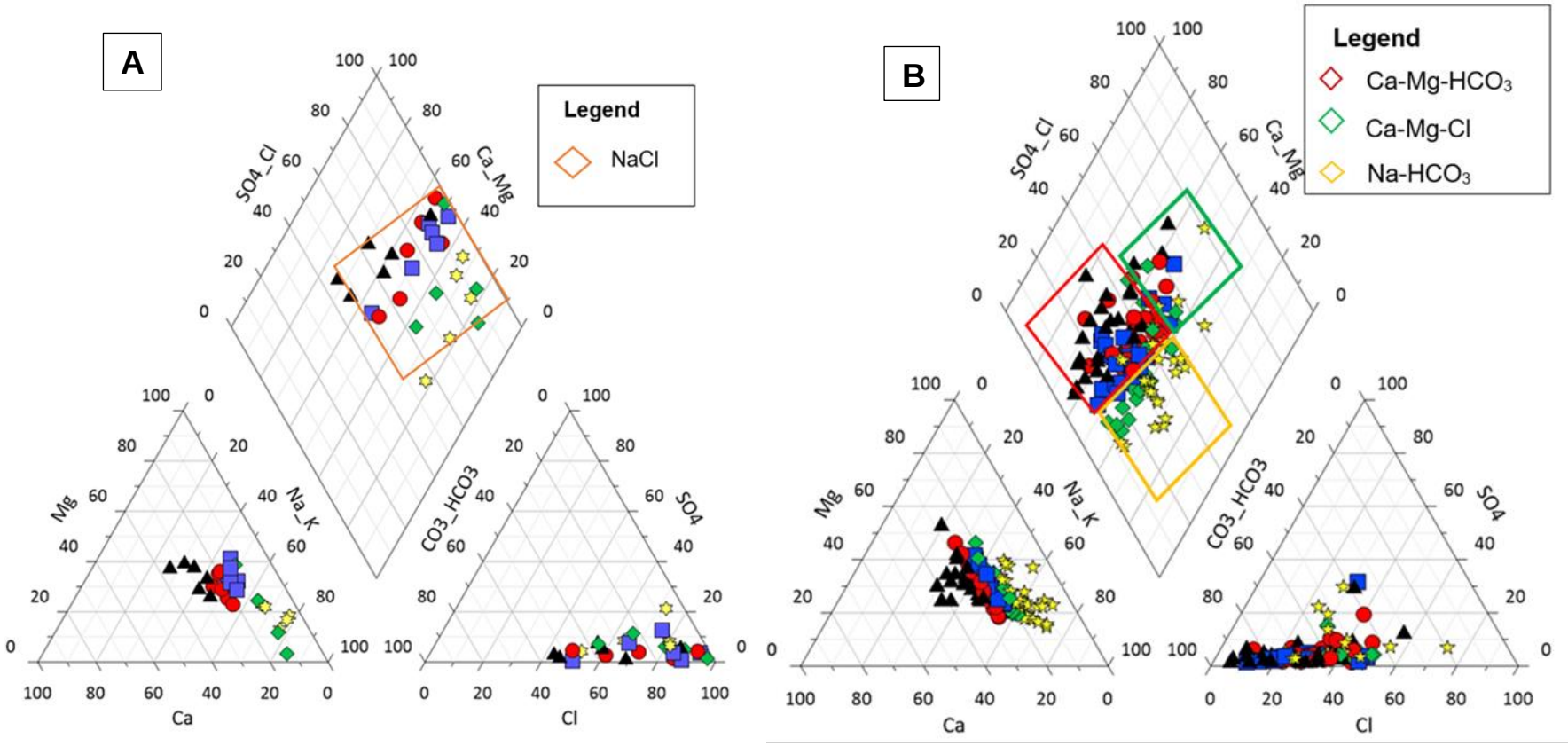

Figure 5.6: Piper diagrams showing the hydrochemistry of groundwater that occur in various types of rocks. (A) shows the hydrochemistry of groundwater that occur in sedimentary rocks located in the western and southern parts of the area, while (B) shows hydrochemistry of groundwater in the Bushveld Complex, which is in the eastern part of the study area.

5.3 Environmental Isotopes

Isotopes are naturally occurring atoms of the same element but different in mass due to the difference in the number of neutrons in the nucleus (Clark and Fritz, 1997). The stable isotopes of hydrogen and oxygen are widely used to investigate the provenance of groundwater, flow direction, groundwater/surface water interaction and identification of the processes altering the isotopic composition of precipitation including evaporation or rainfall water mixing (Clark and Fritz, 1997; Tessema et al., 2014; Oljira 2006). The use of oxygen and hydrogen isotopes is recommended over chemistry because the isotopes provide information about the water molecule itself rather than the solutes in the water which originate from external forces (Oljira, 2006).

The stable isotope compositions are expressed in parts per thousand (or expressed in permils) as delta (δ) values. The delta notation defines the following ratios (Clark and Fritz, 1997):

$$\delta = \left({}^{Rsample}/_{Rstandard} - 1\right) \times 1000$$

Where R is the ratio of the heavy to light isotopes ($^{2}H/^{1}H$ and $^{18}O/^{16}O$), and δ provides information concerning the extent the sample deviates from the isotopic composition of the standard sample. A negative delta indicates a depletion in heavy isotopes relative to the standard samples, implying that the sample is isotopically light compared to the standard and vice versa (Cook and Herczeg, 2012). The isotopic content of water is controlled by the process of fractionation, either equilibrium or kinetic fractionation. According to Tessema et al. (2014), the kinetic fractionation is mostly dependent on humidity, whereas equilibrium fractionation depends on temperature. Yang et al. (2019), highlighted that $\delta^{18}O$ is considered the best indicator of kinetic fractionation as compared to deuterium, hence during the evaporation process, $\delta^{18}O$ is more enriched in the reactant phase or water.

The composition of isotopes $\delta^{2}H$ and $\delta^{18}O$ values in precipitation are represented relative to the international reference standard, the standard mean ocean water (SMOW) or the equivalent of Vienna SMOW (Cook and Herczeg, 2012). The following equation may be used to express the relationship between $\delta^{18}O$ and $\delta^{2}H$ in precipitation as outlined by Cook and Herczeg (2012):

$$\delta^2 H = s\delta^{18} O + d$$

In the above equation, d is the deuterium excess, and it indicates the extent of kinetic isotope fraction and the distance over which moist air travelled away from its source (Craig, 1961), while s denotes the proportionality constant that defines the relationship between δ ^{2}H and δ ^{18}O.

According to Craig (1961), the relationship between δ ^{2}H and δ ^{18}O of the global meteoric water relative to the SMOW can be expressed in terms of the following linear equation:

$$\delta^2 H = 8\delta^{18} O + 10$$

However, due to the variation in deuterium excess from one area to the other because of different geological times, a local meteoric water line must be developed (Clark and Fritz, 1997). In this study, the Pretoria local meteoric water line is expressed by the following equation (Tessema et al., 2014):

$$\delta^2 H = 6.7\delta^{18} O + 7.2$$

The stable isotopes are used to distinguish the historical rainfall from different climates compared to the present. A strong correlation between isotope content of precipitation and groundwater suggests direct local recharge to the groundwater aquifers (Cook, and Herczeg, 2012). However, the following factors may cause the isotope signatures of water to deviate from the global meteoric water line (Clark and Fritz, 1997):

I. effects of the altitude-the windward side of the mountain show decrease in δ ^{2}H and δ ^{18}O as altitude increases,
II. effects of latitude- δ ^{2}H and δ ^{18}O decreases with increasing latitude,
III. Continental effects- the δ ^{2}H and δ ^{18}O contents decrease inland compared to the coast, because of the removal of moisture from air masses as moisture-laden air travel far away from its source,
IV. seasonal variation- in mid and high latitudes, the winter rainfall is usually depleted in δ ^{2}H and δ ^{18}O,
V. effects of rainfall amount- Increased precipitation rates are associated with lower δ ^{2}H and δ ^{18}O values.

The isotopic composition of oxygen and hydrogen are dominantly affected by evaporation and rainfall as compared to the other factors (Yang et al., 2019). Yang et al. (2019), further highlighted that there is a positive correlation between temperature and stable isotope composition in water. Increased temperatures are associated with high evaporation rates which influence the accumulation of heavier isotopes in the residual water or liquid phase. Analysis of $\delta\ ^{2}H$ and $\delta\ ^{18}O$ in both precipitation, surface water and groundwater are important indicators of recharge processes. Using isotopes, one can establish if recharge was immediate or delayed (Clark and Fritz, 1997).

Table 5.1 summarises the results of the stable isotope ratios of the 18 samples collected in the model domain. The results show that $\delta^{18}O$ varies from the most enriched ratio of -0,96 ‰ to the relatively depleted value of -5,42 ‰, whereas $\delta^{2}H$ ranges from -15,3 ‰ to -31,5 ‰ (Table 5.1). Surface water samples (S4, S9, S12, S16 and S17) and shallow aquifers (S8 and S15) are characterised by enrichment in heavy isotopes of water molecules, which is consistent with extensive evaporation of surface water and unconfined aquifers, respectively. However, the water sampled at the Glen Alpine dam shows different isotope signatures, which may be attributed to the mixing of water with different isotope compositions.

Alternatively, the low isotope signature of the dam can be attributed to the distance over which the source of rain (moisture) has travelled away from its source, which is consistent with the low d-excess of 1,27 ‰ relative to other samples (Table 5.1). In general, the average d-excess of water samples collected from the boreholes that are located upstream of the Mogalakwena River (S1, S2, S3, S5 and S6) labelled as A in Figure 5.7 is greater than the d-excess of samples collected towards the lower reaches of the stream (S8 and S10). This may be attributed to the distance over which moisture-laden air mass has travelled away from its source, i.e., the downstream samples are far away from the primary source of moisture.

Table 5.1: Results of stable isotopes within the Model area.

Sample No	**Surface water or groundwater**	**$\delta^{2}H$** (‰)	**$\delta^{18}O$** (‰)	**D-excess**	**Water level** (m)	**Elevation** (masl)	**Piezometric surface** (masl)
S1	Groundwater	-25,6	-4,94	13,91	13,8	992	978,2
S2	Groundwater	-27,8	-5,24	14,06	13,28	955	941,72
S3	Groundwater	-29,0	-5,39	14,07	10,3	960	949,7
S4	River	-15,3	-0,96	-7,56	-	955	-
S5	Groundwater	-27,8	-5,12	13,13	13,2	998	984,8
S6	Groundwater	-22,7	-4,26	11,39	13,2	999	985,8
S7	Groundwater	-26,4	-4,63	10,56	12,5	984	971,5
S8	Groundwater	-22,0	-3,76	8,08	8	905	897
S9	River	-22,6	-2,99	1,30	-	845	-
S10	Groundwater	-24,5	-4,23	9,39	20,4	852	831,6
S11	Groundwater	-26,8	-4,61	10,03	14,9	920	905,1
S12	Dam	-31,5	-4,10	1,27	-	820	-
S13	Groundwater	-31,0	-4,90	8,23	9,5	903	893,5
S14	Groundwater	-30,8	-4,98	9,06	7,8	991	983,2
S15	Groundwater	-28,6	-4,86	10,27	3,05	900	896,95
S16	River	-28,9	-4,48	6,99	-	899	-
S17	River	-27,9	-4,19	5,70	-	876	-
S18	Groundwater	-31,3	-5,42	12,09	13,4	876	862,6

The isotopic signature of the samples in the area is scattered along the Pretoria Local Meteoric Water Level (PLMWL) and global meteoric water level (GMWL) (Figure 6.6). However, the four samples (S1, S2, S3 and S5) collected in the southern part of the model domain plot on the PLMWL, which suggest that direct recharge from the local rainfall, which is consistent with the high d-excess (Figure 5.7).

The isotope signatures of S13, S14, S15 and S18 labelled as B in Figure 5.7 are highly depleted in both $\delta\ ^{2}H$ and $\delta\ ^{18}O$ values, which suggests that extensive evaporation of precipitation might have taken place prior to infiltration. In addition, the relatively low

d-excess values corresponding to these samples except for sample S18, suggests a regional source of moisture that has undergone extensive air circulated over a long distance. However, the surface water bodies (represented in red colour) dominantly plot below both the PLMWL and GMWL (Figure 5.7).

The surface water sample S4 is located upstream of Mogalakwena River and it shows a distinctive isotopic ratio enriched in both δ ^{2}H and δ ^{18}O values, but depleted in d-excess, which suggest that the sample has undergone evaporation to a different extent resulting in an enrichment of heavy isotopes. The sample S9 is located downstream of Mogalakwena River, and it similarly shows an enriched in δ ^{2}H and δ ^{18}O contents, but relatively low compared to sample S4. This suggests that extensive evaporation rates are accompanied by kinetic fractionation of isotopes, leaving the heavy isotopes in the residual water.

The evaporation line of the water samples is characterised by a gentle slope (see the solid green line in Figure 5.7), and significantly deviates away from both PLMWL and GMWL. The deviation of the evaporation line from the reference lines may be attributed to different geographic locations with contrasting climatic conditions. According to Gupta and Deshpande (2005), the lowering of the slope of the evaporation line can be attributed to extensive evaporation rate under high temperature and low humidity conditions. The evaporation line in the study area is represented by the equation:

$$\delta^{2}H = 3.2\delta^{18}O + 12.4$$

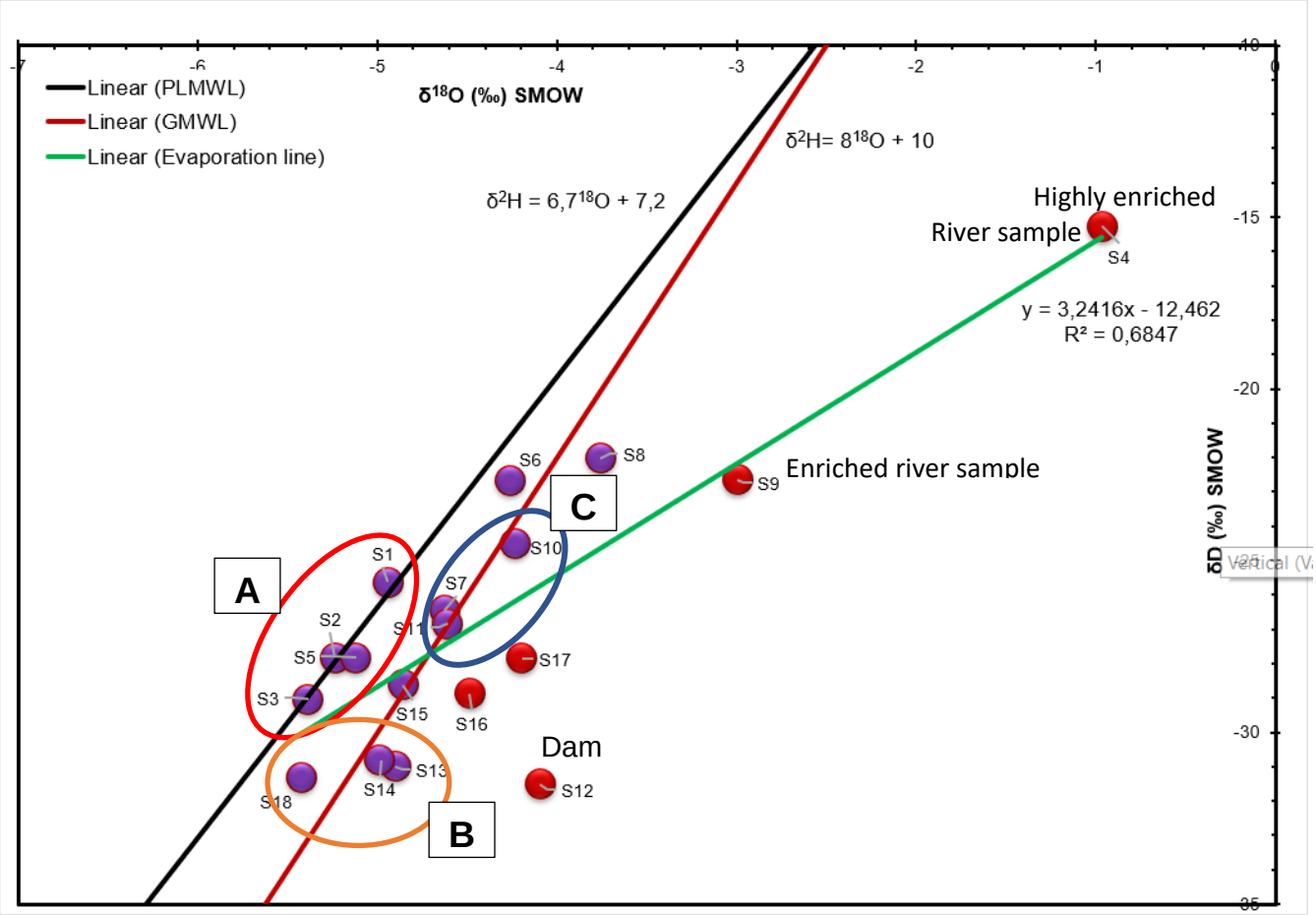

Figure 5.7: δ^2H versus $\delta^{18}O$ showing the isotopic compositional variation of groundwater and surface water samples with respect to PLMWL and GMWL. Labels A, B and C are described in the text.

The deuterium excess is defined by the following equation (Feng et al., 2009):

$$d = \delta^2H - 8\delta^{18}O$$

It enables to understand the degree of kinetic fractionation. The d-excess determines the deviation of the stable isotope content from the GMWL. In addition, the d-excess provides information related to the source of precipitation and the evolution of moisture during transport (Tessema et al., 2014; Machavaram and Krishnamurthy, 1995). The d-excess for the collected samples in the study area is shown in Figure 5.8 and Table 5.1. The groundwater samples depict a mean d-excess of 11.10‰, while the surface water samples mean is -2.7‰ (Figure 5.8 and Table 5.1).

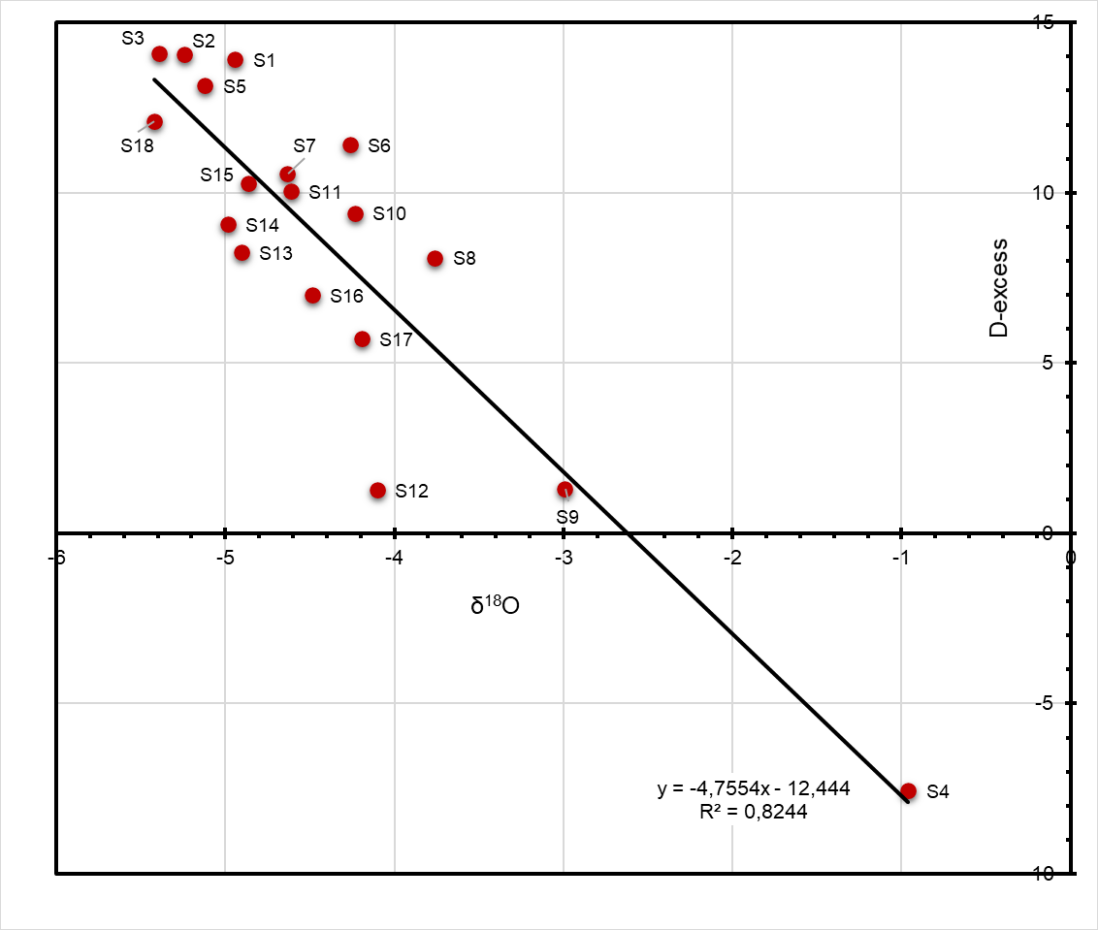

Figure 5.8: Correlation between d-excess and oxygen 18.

According to Yang et al. (2019), a high d-excess value indicates that the relative humidity of the air is low compared to the evaporation rate throughout the precipitation process. A low d-excess is associated with enrichment of heavier isotopes δ ^{2}H and δ ^{18}O influenced by high evaporation rates (Gupta and Deshpande 2005), which is consistent with the high δ ^{2}H and δ^{18}O values of surface water compared to the borehole samples. This explains the low d-excess observed at the surface water bodies, i.e., the high daily temperatures of Mogalakwena Subcatchment increase the evaporation rate making surface water such as rivers and dams enriched with heavy isotopes. Thus, the increased evaporation rates in the study area are therefore accounted for the enrichment of δ^{2}H and δ^{18}O in surface water relative to groundwater. Furthermore, Figure 5.8 shows that surface water samples (S4, S9, S12, S16 and S17) are characterised by contrasting d-excess relative to borehole samples, evaporation plays a vital role in the determination of the isotope signature in the study area.

Chapter 6: Groundwater Potential Zones

The delineation of groundwater potential zones is a very challenging task considering the semi-arid climatic conditions and heterogeneous geology of the Mogalakwena Subcatchment. However, multi-criteria decision analysis using Geographic Information System (GIS) and Analytical Hierarchical Process (AHP) has been widely applied worldwide to delineate groundwater potential zones (Arulbalaji et al., 2019). In this study, a multi-criteria approach was applied to integrate six parameters that include lineament density, geology, land use, slope, drainage density, and soil. Based on this approach, a map of the groundwater potential of the study area was created.

6.1 Thematic Layers

6.1.1 Geology

The complex geology of the Mogalakwena Subcatchment was discussed in detail in section 3.2 (Figure 3.1). In this section, a knowledge-based method was used, and the rock types in the study area were categorised into two types, *viz.* sedimentary and crystalline rocks. The sedimentary rocks were assigned a high rank as compared to the crystalline rocks owing to increased permeability. The high ranking of the sedimentary rocks is due to their primary porosity, which makes them more permeable as compared to the crystalline rocks that only possess secondary porosity.

6.1.2 Soil

The study area is covered by three soil types, namely sandy, sandy loam, and clay soils, as shown in Figure 3.7. The texture and hydraulic conductivity of the soil are the main parameters considered for the estimation of infiltration rate. Based on this, the sandy soil was assigned a high rank, followed by the sandy loam then the clay soil was given the least rank.

6.1.3 Land Cover/ Land Use

Land use is the classification of both natural features and human activities occurring on the land surface at a particular period (Vatsala and Ramakrishnaiah, 2021). The dominant land cover at Mogalakwena Subcatchment is forest, agriculture, and grassland as shown in Figure 3.8 in Chapter 3. The different land cover greatly influences the groundwater infiltration. In this study, the land cover was ranked according to its influence on the infiltration of rainfall and the development of groundwater in the underlying rocks (Table 6.2).

6.1.4 Lineament Density

According to Roy et al. (2020), regions with high lineament density are characterised by good groundwater potential assuming that lineaments increase the permeability of rocks. The lineament density map of the Mogalakwena Subcatchment was created from the lineament map in Figure 3.3B. The density was subdivided into 5 classes, namely: very low (0-0,5), low (0,5-1), medium (1-1,5), high (1,5-2) and very high (>2) (Table 6.2). The high rank was assigned to the very high class owing to an increase in lineament density increases the permeability of rocks. Figure 6.1A shows the variability in lineament density in the study area. Higher lineament densities are observed in the southeastern and far northern parts of the study area dominantly underlain by crystalline rocks of the Bushveld Complex and the Limpopo High-Grade Metamorphic Belt, respectively.

6.1.5 Slope

The slope was created using digital elevation data in an ArcGIS environment. A gentle slope allows infiltration of rainwater and development of groundwater aquifer, whereas a steep slope enhances surface runoff which reduces the chances of groundwater recharge. Mogalakwena Subcatchment is characterised by a gentle slope with the exception of the southern parts of the study area (Figure 6.1B). The slope of the study area was subdivided into 5 categories, namely: very low (0-2), low (2-8), medium (8-15), high (15-30), and very high (>30). The highest grade was allocated to the gentle slope considering that it allows high infiltration rates.

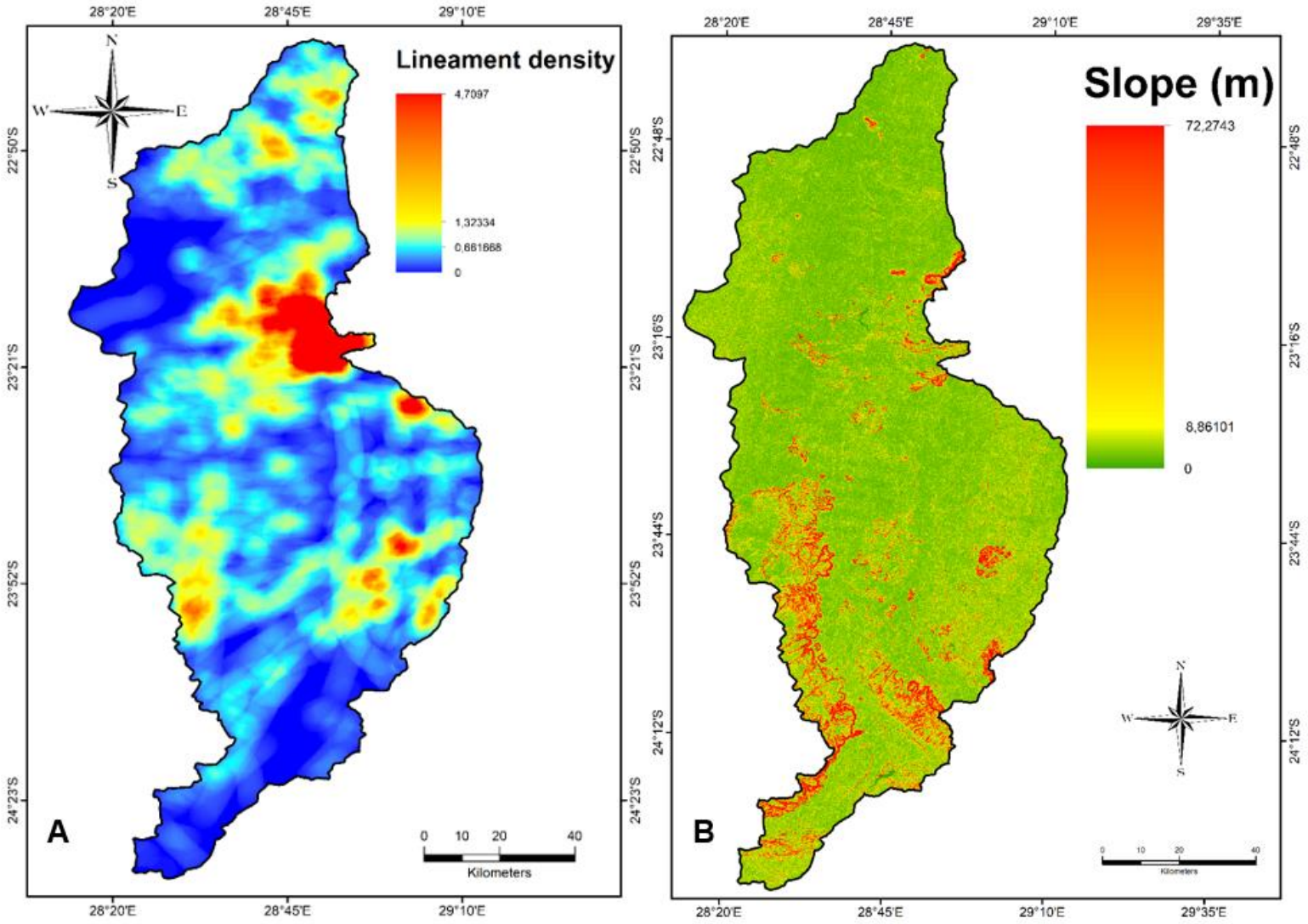

Figure 6.1: Lineament density map (A) and slope map (B) of Mogalakwena Subcatchment.

6.1.6 Drainage Density

Drainage density can be described as the total length of stream segments per unit area (Magesh et al., 2012). The drainage network is dependent on the lithological units and provides essential information related to the index of infiltration rate (Arulbalaji et al., 2019). High drainage densities are associated with low infiltration rates, whereas low drainage densities are characterised by high infiltration rates (Arulbalaji et al., 2019). Roy et al. (2020), emphasised that low drainage densities are associated with gentle slopes along with permeable subsoil with dense vegetation. High drainage densities are common in mountainous regions that are characterised by sparse vegetation and impermeable subsurface rocks (Roy et al., 2020). The drainage density map of the study area was created using the digital elevation data and ArcGIS (Figure 6.2). The drainage density was divided into five categories: very low, low, medium, high, and very high. The highest rank was assigned to the very low drainage system due to the inverse relationship between drainage density and permeability.

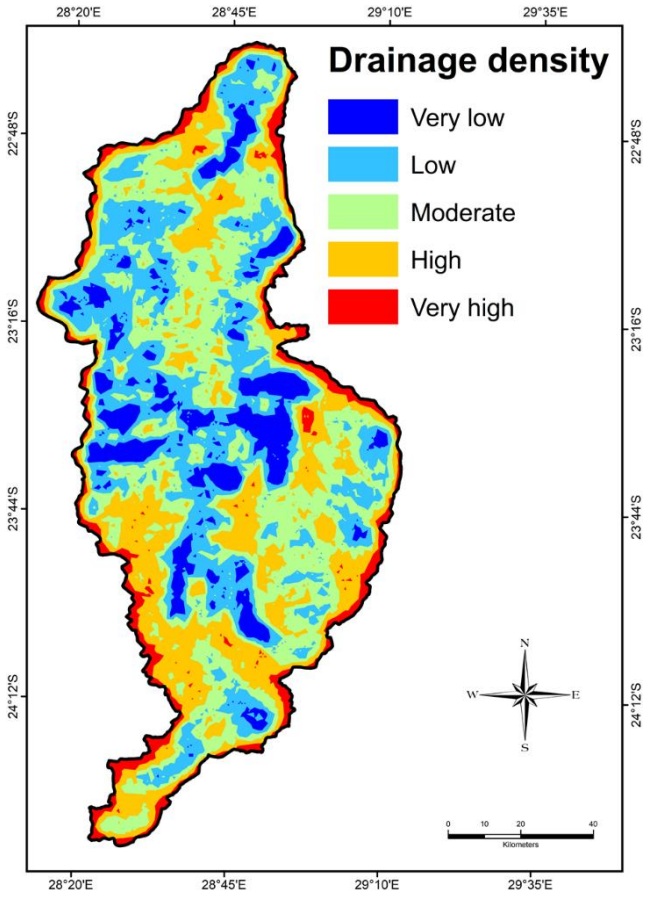

Figure 6.2: Drainage density map of the study area.

6.2 Analytical Hierarchy Process (AHP)

The AHP involves the evaluation of thematic layers and assigning a number based on the layer's significance to the development of groundwater occurrence compared to the other layers (Vatsala and Ramakrishnaiah, 2021). The assigned numbers are used as the weight of each layer. The parameter with high weightage represents the layer that has a significant influence on the groundwater potential, e.g., geology in Table 6.1 (Arulbalaji et al., 2019). Each layer was subdivided into classes and the classes were ranked from 1 to 5, where 1 represents low groundwater potential, while 5 represents high groundwater potential. The overall weight for each class was calculated by multiplying the rank with the weight percentage for the corresponding layer (Table 6.2).

Table 6.1: Normalised pairwise comparison matrix table of the six thematic layers selected for this study

Factor	Geology	Lineament density	Slope	Soil	Land use	Drainage density	Weight
Geology	6	5	4	3	2	1	0,408
Lineament density	6/2	5/2	4/2	3/2	2/2	1/2	0,204
Slope	6/3	5/3	4/3	3/3	2/3	1/3	0,136
Soil	6/4	5/4	4/4	3/4	2/4	1/4	0,102
Land use	6/5	5/5	4/5	3/5	2/5	1/5	0,082
Drainage density	6/6	5/6	4/6	3/6	2/6	1/6	0,068

6.3 Weight Overlay Analysis

The six thematic layers (lineaments, geology, slope, land use/cover, drainage and soil) were integrated with the ArcGIS environment to produce a single map showing the groundwater potential of the Mogalakwena Subcatchment. The union analysis tool was applied to the six thematic layers to calculate the overall weightage at different locations in the study area. The overall weightage (ranging from 6,8 to 492) of the six layers was used to produce the groundwater potential zones. The groundwater potential zones were grouped into five classes, namely very low (6,8-150), low (150-260), moderately high (260-360), high (360-420), and very high (420-490) groundwater potential as shown in Figure 6.3.

Table 6.2: Weight categorisation of parameter controlling groundwater potential zones

Factor	Weight percentage	Rank	Overall weight
Geology			
Sedimentary rocks		5	204
Crystalline rocks	40,8	3	122,4
Lineament density			
Very low		1	20,4
Low		2	40,8
Medium		3	61,2
High		4	81,6
Very high	20,4	5	102
Slope			
0-2		5	68
2-8		4	54,4
8-15		3	40,8
15-30		2	27,2
>30	13,6	1	13,6
Land use			
Grassland		3	24,6
Cultivated land		3	24,6
Mining		2	16,4
Woodland		4	32,8
Township		2	16,4
Water		5	41
Villages		2	16,4
Erosion	8,2	1	8,2
Soil			
Sandy		5	51
Sandy loam		3	30,6
Clay	10,2	1	10,2
Drainage density			
Very low		5	34
Low		4	27,2
Medium		3	20,4
High		2	13,6
Very high	6,8	1	6,8

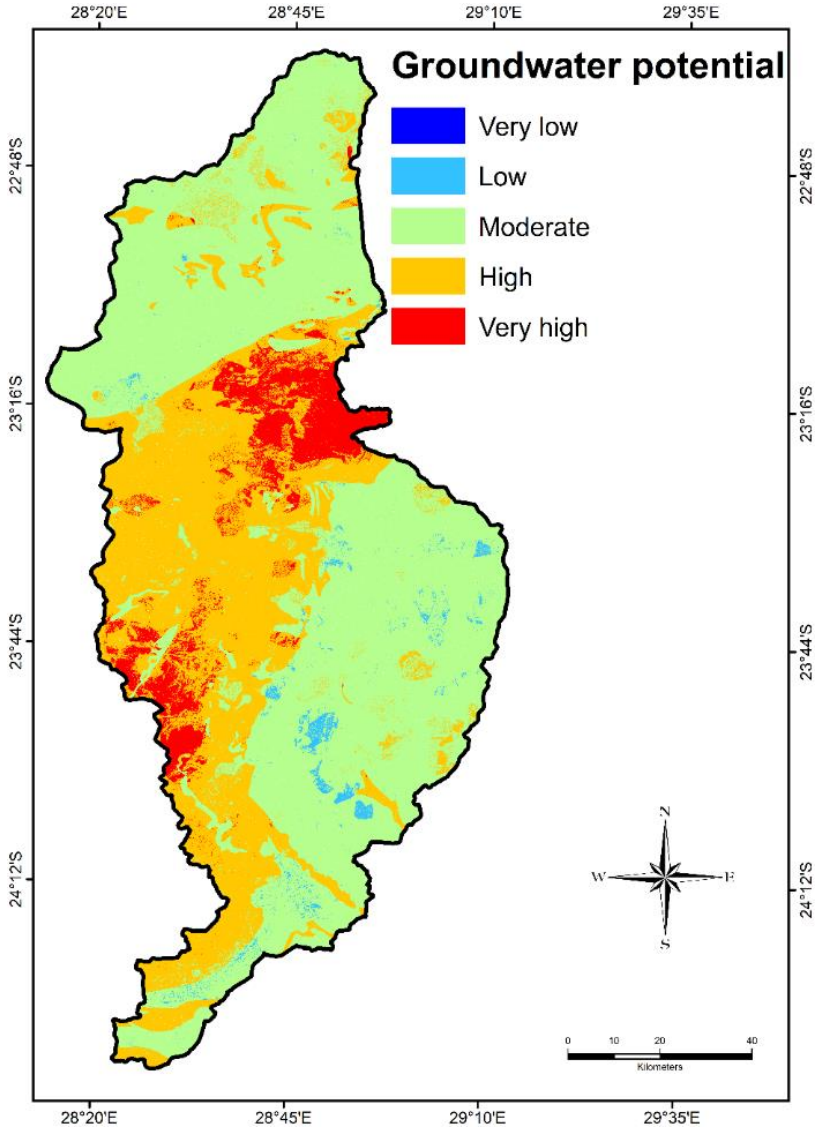

Figure 6.3: Groundwater potential map of the study area.

The groundwater potential zone labelled very high is attributed to the underlying sedimentary rocks that are relatively permeable and the presence of dense lineaments. The moderate groundwater potential zone is dominant in the southeastern and northern parts of the study area that are underlain by the crystalline rocks which appear to be due to structural features such as joints, faults and related weak zones that enhance the permeability and groundwater infiltration.

6.4 Validation of groundwater potential zones

The depth of the groundwater level was utilised to verify/validate the reliability of the selected groundwater potential zones in Figure 6.3. This was achieved by comparing the groundwater potential zones with the groundwater levels. Fifteen boreholes with groundwater level monitored between 2008 and 2019 were used for this study.

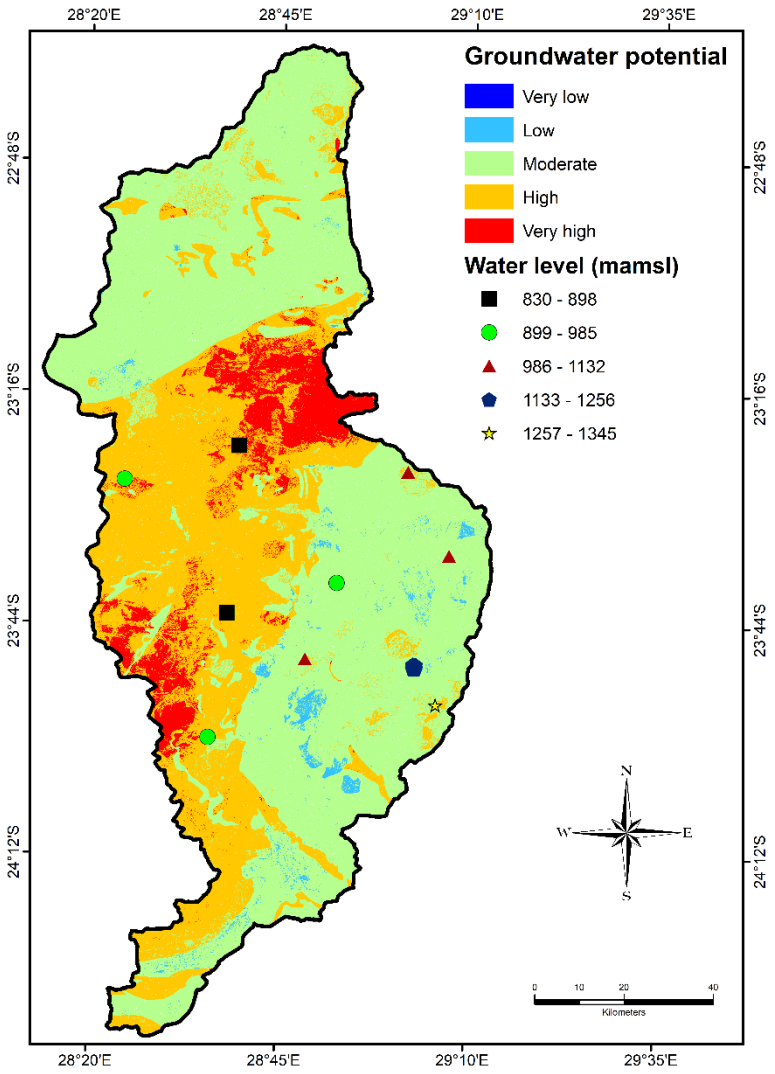

Figure 6.4: Validation of groundwater potential zones using groundwater level.

Figure 6.4 shows the variability in groundwater level between the very low to very high groundwater potential zones. The very high to high, moderate and low to very low groundwater potential zones are characterised by shallow (830 to 985 mamsl), intermediate (986 mamsl) and deep (1133-1345 mamsl) groundwater levels, respectively (Figure 6.4).

Chapter 7: Groundwater Flow Model Results and Discussion

7.1 Introduction

A steady-state numerical model of groundwater flow was applied to investigate the aquifers' response to the various hydrological stresses that were implemented in the numerical simulation of groundwater flow. This chapter presents a discussion of the model results.

7.2 Steady-state model results

7.2.1 Sensitivity analysis

The results of the sensitivity analysis are significant for understanding the uncertainties during the model calibration. Table 7.1 shows variability in RMS as the model input parameters fluctuates. The percentages with no recorded RMS indicate that the model could not run (Table 7.1).

Table 7.1: RMS results as the model parameters are varied.

				Hydraulic conductivity			
Percentage	***River Conductance***	***RCH***	***EVT***	***HRG***	***Matlala granite***	***RLS***	***Sandstone***
-80	*18,44*	*-*	*-*	*18,28*	*18,61*		*18,5*
-60	*18,44*	*-*	*-*	*18,4*	*18,56*	*18,46*	*18,49*
-40	*18,44*	*-*	*18,54*	*18,44*	*18,52*	*18,45*	*18,47*
-20	*18,45*	*-*	*18,54*	*18,45*	*18,48*	*18,45*	*18,46*
0	*18,45*	*18,45*	*18,45*	*18,45*	*18,45*	*18,45*	*18,45*
20	*18,45*	*18,55*	*18,42*	*18,42*	*18,42*	*18,45*	*18,43*
40	*18,45*	*18,62*	*18,4*	*18,4*	*18,4*	*18,45*	*18,42*
60	*18,45*	*18,67*	*18,38*	*18,34*	*18,37*	*18,44*	*18,41*
80	*18,45*	*18,72*	*-*	*-*	*18,35*	*18,44*	*18,4*

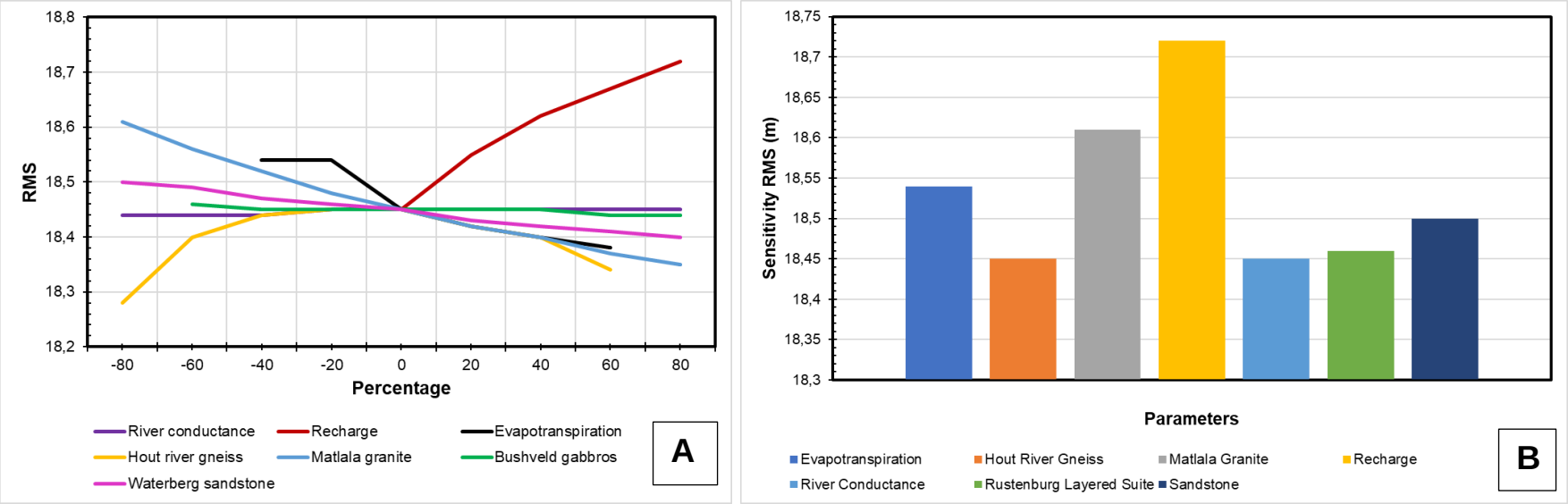

Figure 7.1: Graphical display of the results of sensitive analysis of the model (A) and maximum sensitivity of the model to various parameters and hydrological stresses (B).

Figure 7.1A demonstrates the change in RMS as a function of change in model parameters. The results indicate that the model is sensitive to the recharge rate, hydraulic conductivity of the rocks, river conductance and evapotranspiration rate (Figure 7.1). The model is most sensitive to recharge rate, followed by the hydraulic conductivity of the Matlala granite, evapotranspiration rate, the hydraulic conductivity of sandstone (Figure 7.1B).

7.2.2 Model Calibration

The success of the model calibration was evaluated by comparing the simulated and observed heads. This was achieved by correlating the piezometric values of the observed and simulated heads as shown in Figure 7.2. The points plotting on the straight line show the best fit between the observed and the simulated heads, while the ones that plot on the left side of the best fitting line suggest higher simulated heads than the observed heads and vice versa. The coefficient of determination R^2 defines how close the simulated hydraulic heads approach the observed heads, and it is found to be 0,9984, which indicates that there is a strong correlation between the simulated and observed heads.

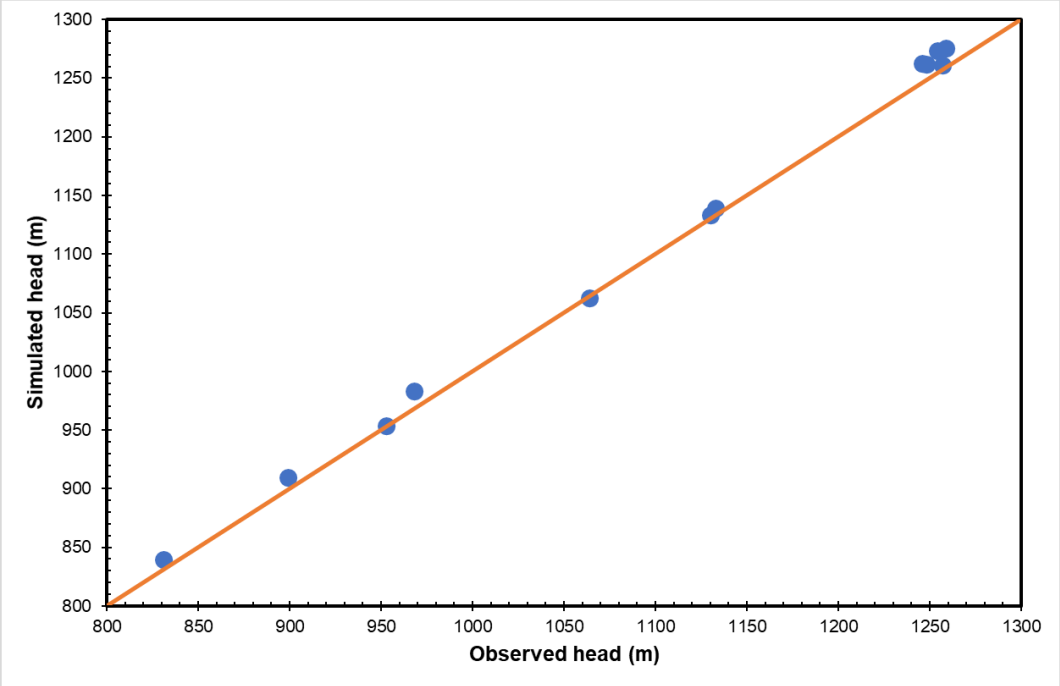

Figure 7.2: Simulated versus observed heads showing the degree of correlation.

An alternative method of assessing the model calibration is through the comparison of the piezometric surface contours of the simulated and observed heads. However, the

water level measured at the observation wells were not sufficient to create a contour map for the observed heads. The contour map of the simulated heads is shown in Figure 7.3. High piezometric levels are mainly observed in the southeastern parts of the model domain, while they are low along the Mogalakwena River (Figure 7.3). The low piezometric surface along the streams suggest that there is a strong interaction between the aquifer and the river. The low contour values along the main river (Mogalakwena River) indicates that the river is taking water from the aquifer making the piezometric surface low along its flow path. If the amount of rainfall decreases from time to time, the river stage becomes lower than the groundwater level, and this consequently results in loss of water from the aquifer to the river, i.e., the river gains water from the aquifer, while the water level in the aquifer drops as the amount of rainfall that recharges both groundwater and surface diminish due to climate change, and man-made induced hydrological stresses. Thus, the sustainability of the aquifer as the main source of water supply in the area depends on the fluctuation of climate, i.e., the amount of rainfall and temperature.

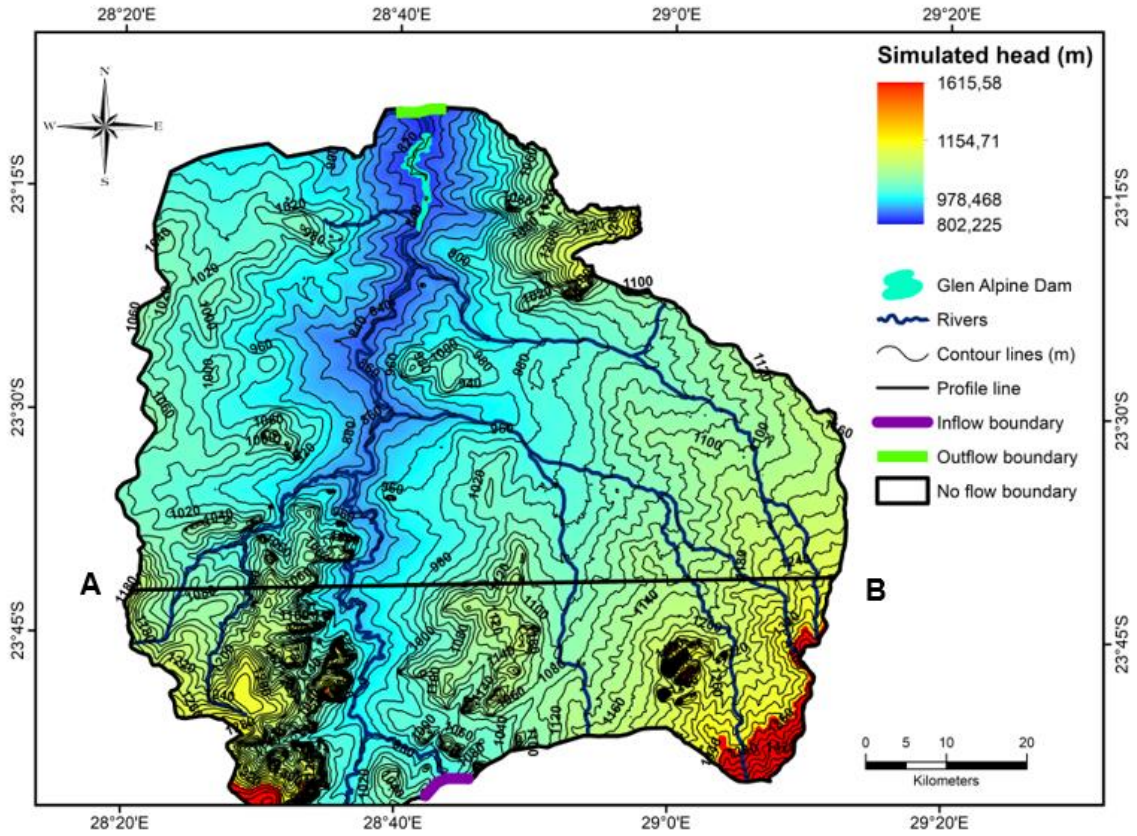

Figure 7.3: A contour map of the simulated piezometric surface.

Figure 7.4 shows a cross-section of the simulated head along the line AB as outlined in Figure 7.3. The simulated head mimics topographic elevation, i.e., the southern part of the area is characterised by a high piezometer, while the discharge zones in the northern part of the area are shown by low water levels. The cross-section further shows that the water level is very low corresponding to the river channel attesting to the interaction between the aquifer and the river.

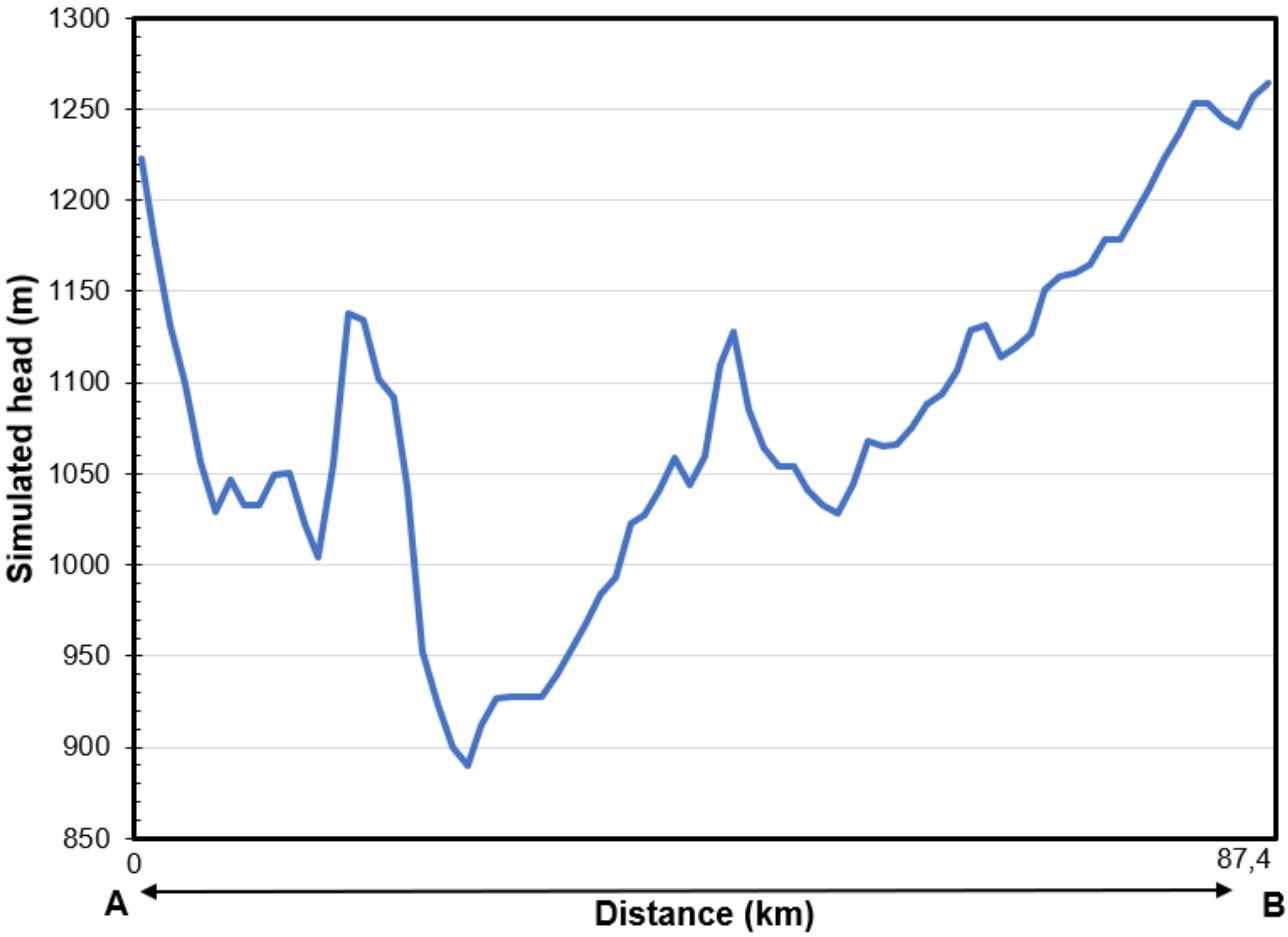

Figure 7.4: A cross-section of the simulated head from point A to B.

The overall error estimations between the observed and simulated heads were determined using three error metrics that are RMS, ME, and MAE (Table 7.2). The results suggest that the model overestimated groundwater level compared to observed hydraulic heads.

Table 7.2: The results of the three error matrices corresponding to each observation wells.

Borehole ID	**X**	**Y**	**Screen elevation**	**Observed head**	**Simulated head**	**RMS**	**ME**	**MAE**
			(m)	(m)	(m)	$(Obs-sim)^2$	Obs-Sim	|Obs-Sim|
M03-2545	669492	7413856	798	831	839,56	73,27	-8,56	8,56
M04-2554	707284	7407838	1046	1064	1062,83	1,37	1,17	1,17
M03-3767	643910	7406451	946	968	983,2	231,04	-15,2	15,2
M04-2261	716430	7389053	1109	1133	1138,96	35,52	-5,96	5,96
M03-3855	666697	7376508	889	899	909,73	115,13	-10,73	10,73
M04-2280	708516	7364386	1224	1246	1262,81	282,58	-16,81	16,81
M04-2277	708279	7364789	1235	1257	1261,18	17,47	-4,18	4,18
M03-3770	684147	7366147	1119	1130	1133,71	13,76	-3,71	3,71
M04-1457	708870	7364758	1223	1248	1261,64	186,05	-13,64	13,64
M04-2265	708879	7364140	1234	1254	1273,44	377,91	-19,44	19,44
M04-2268	708739	7363769	1250	1259	1275,62	276,22	-16,62	16,62
M03-3672	662400	7348728	943	953	953,86	0,74	-0,86	0,86
Sum						1611,08	-114,54	116,88
Maximum						377,91	1,17	19,44
Minimum						0,74	-19,44	0,86
Mean						134,26	-9,55	9,74
Standard deviation						131,79	6,86	6,56
Estimated error						**11,59**	**-9,55**	**9,74**

The following factors may have attributed to the discrepancy between the simulated and observed heads (Kinoti, 2018):

I. the complexity and heterogeneity of the hydraulic conductivities of the geology of the model area. The scale of the hydraulic conductivity zones is broad (1:250,000), and this may have contributed to the discrepancy between the simulated and observed heads,
II. unaccounted groundwater inflows and outflows. This refers to unforeseen inflows and outflows, which may not have been incorporated into the boundary conditions or hydrological stresses,
III. uncertainties in the observed water levels,
IV. a limited number of observed heads,
V. the grid size could be coarse and may not provide adequate spatial resolution corresponding to certain boundary conditions (e.g., abstraction wells and river).

7.2.3 Water Budget Analysis

One of the most imperative aspects of numerical modeling of groundwater flow is to establish a reasonably meaningful groundwater balance which enables the successful implementation of sustainable water use measures. The model results include the simulated water budget consisting of the components of inflows and outflows. The inflow includes river leakage, recharge from precipitation, head-dependent flux from the southern general head boundary and the interaction of the dam with the aquifer. The outflows are surface runoff, groundwater abstraction, evapotranspiration, leakage through the bottom of the dam, the head-dependent flux between the rivers and the aquifer and the discharge along the northern general head boundary (Table 7.3). Both the inflows and outflows can be expressed in terms of the following equation:

$$RCH + RIV_{in} + HDB_{in} = RIV_{out} + EVT + GHB + Abs\_wells + Surface\ runoff$$

RCH is recharge, RIV is a river, GHB is a general head boundary, EVT is evapotranspiration, while Abs_well is abstraction wells.

The results of the simulated water budget indicate the total inflow and outflow (Table 7.3). The recharge contributes to 99.6% of inflow, followed by river leakage (0.36%) and GHB (0.08%). Among the outflow components, surface runoff takes the lion's share (83.3%), followed by evapotranspiration (16.6%) and river leakage 0.02%.

Table 7.3: Water balance derived from simulation of groundwater flow.

Component	**Inflow** (m^3/d)	**Outflow** (m^3/d)
RCH	2,7599E+10	
River leakage	99403200	6552489,6
HDB	23016960	326160
EVT		4611600000
Abstraction wells		5028480
Runoff		2,3085E+10
Total	2,7722E+10	2,7708E+10

Figure 7.5 graphically displays the water balance for the calibrated model. The high evapotranspiration appears to be due to open bushes that largely cover the model area. In addition, an increase in evapotranspiration may be attributed to the shallow water table as shown by the contour map of the model in Figure 7.3. The large surface runoff can be attributed to the high topographic relief and the dominance of the crystalline lithologies that cover the southeastern part of the study area. These rocks are characterised by low permeability and they allow little rain to infiltrate and recharge groundwater.

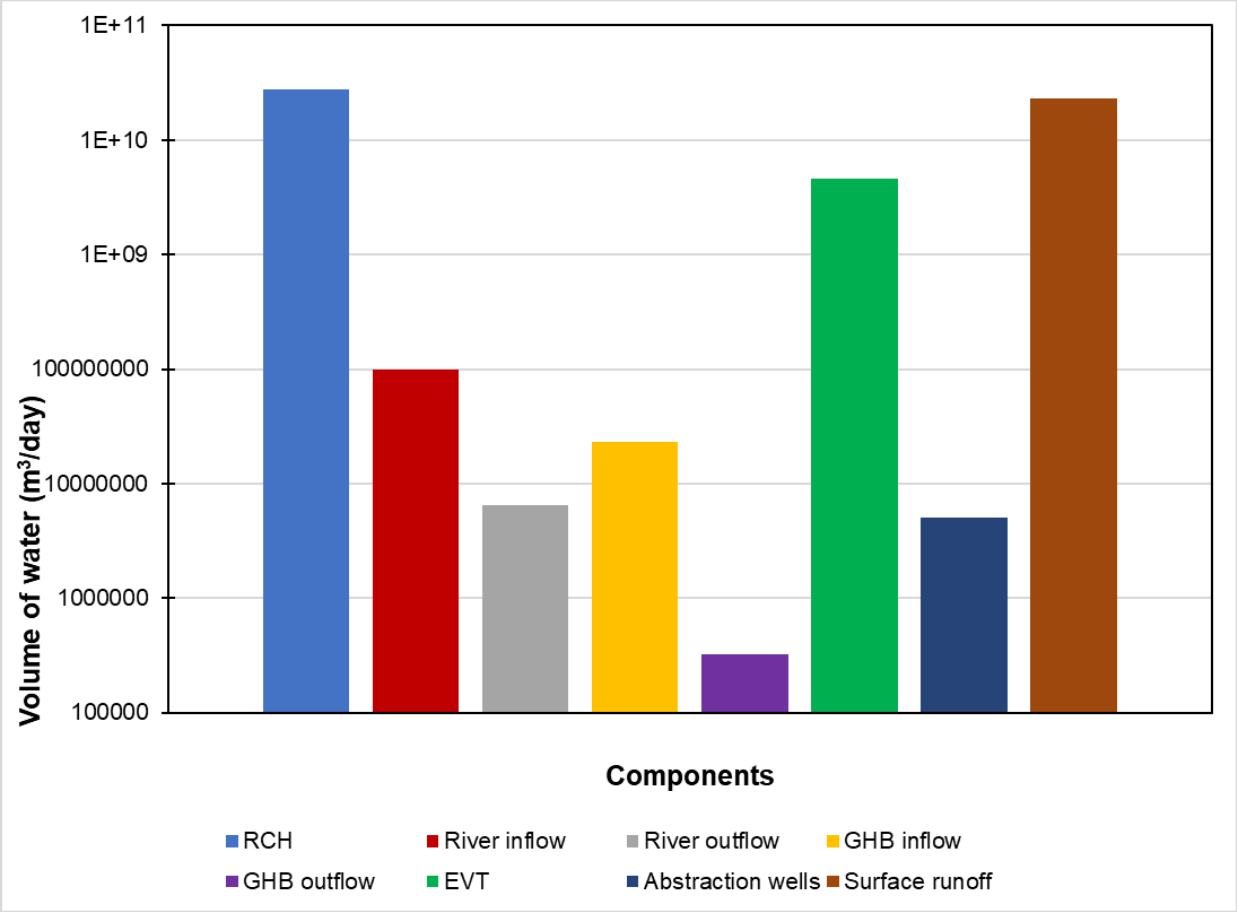

Figure 7.5: Graph display of the simulated water balance.

7.2.4 Zone Budget

The zone budget was implemented to evaluate the interaction between surface water and groundwater by quantifying the amount of water that flows from one component to the other (Abdelhalim et al., 2020). This was achieved by assigning zone numbers to the objects that represent boundary conditions (e.g., river and dam). Zone 1, 2 and 3 were assigned to the aquifer, river, and dam, respectively. Zones 2 and 3 correspond to the Mogalakwena River and Glen Alpine Dam, respectively. These two zones were used to understand the extent of flux that is taking place between the aquifer and the two zones. Table 7.4 shows the results of the zone budget.

Table 7.4: Zone budget for surface water and groundwater

Water exchange	**Inflow** (m^3/day)	**Outflow** (m^3/day)
Zone 2 to 1	170570880	
Zone 3 to 1	3622492,8	
Zone 1 to 2		1169251200
Zone 1 to 3		11490336
Total	174193372,2	1180741536

Groundwater and surface water are two interconnected systems of a single water resource and any impact/stress applied to one of these systems will eventually affect the other, either in terms of quality or quantity (Abdelhalim et al., 2020). Based on this analogy, a river can either drain water from or supply water to the aquifer or both gain and lose at different drainage points (Brunner et al., 2009). However, in a case where the water table beneath the river is deep, variations in the water table will not affect the exchange in water between the two systems, the same applies to the dam (Brunner et al., 2009). Figure 7.6 graphically shows water exchange between the aquifer, Mogalakwena River, and Glen Alpine Dam. The results suggest that the aquifer is supplying more water to the river and the dam than it receives, which is consistent with the results of the piezometer contour map shown in Figure 7.3.

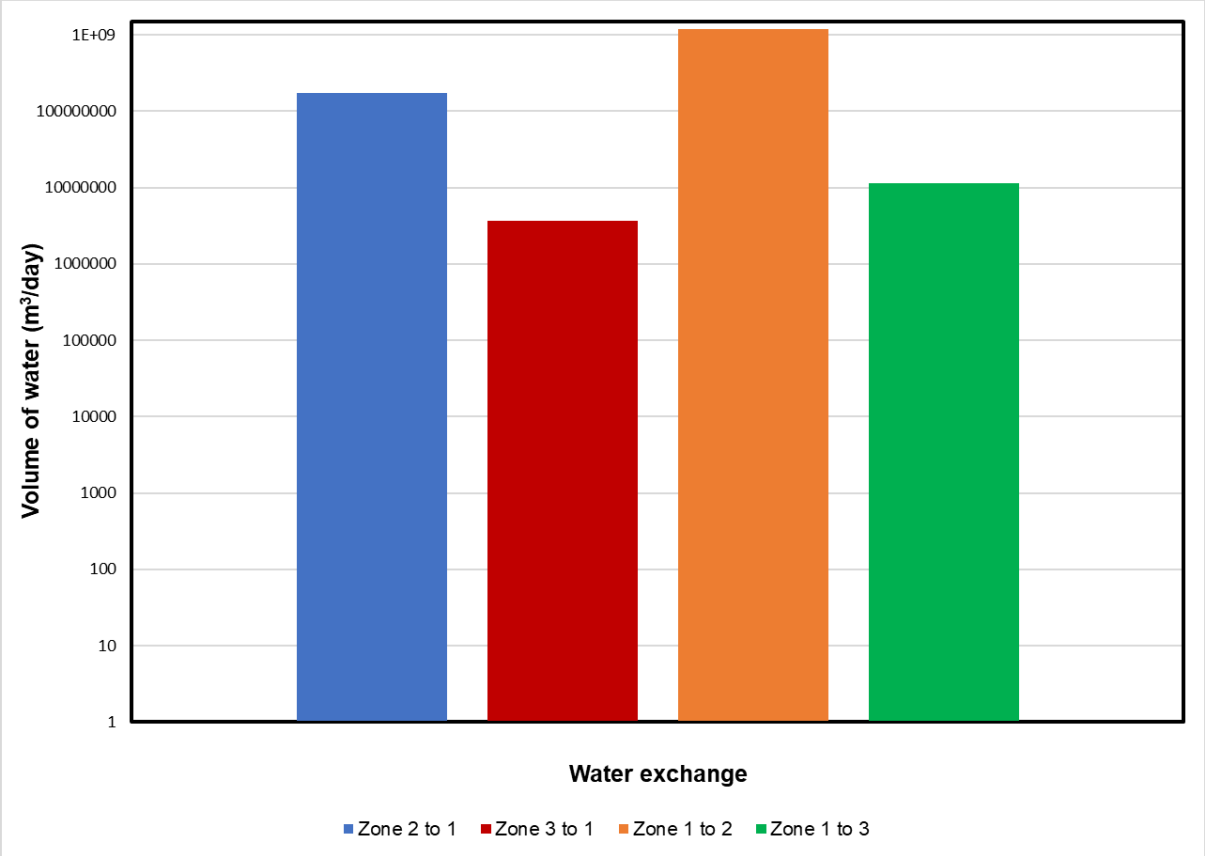

Figure 7.6: The exchange of water between the aquifer, Mogalakwena River and Glen Alpine Dam.

7.2.4.1 River-aquifer interaction

Table 7.3 shows that Mogalakwena River gains a large volume of water from the aquifer system than it supplies to the aquifer. The interaction between the river and groundwater is dominantly controlled by the conductance of the streambed and the water level in the aquifer system. Furthermore, a large areal extent of the Mogalakwena Subcatchment is covered by an unconfined intergranular aquifer of the Waterberg sandstones. The unconfined aquifers in the Mogalakwena Subcatchment are characterised by shallow water tables which may rise to the level of the river during rainy seasons making the river gain water from the aquifer system. In addition, the southern parts of the study area are characterised by high topographic relief, which may contribute to contrast in the hydraulic head or piezometric surface and the river stage. The variability in topography throughout the study area may contribute to the rise in the water table above the river stage. When the altitude of the river stage is lower than that of the groundwater level, the aquifer discharges water into the streams.

According to (Brunner et al., 2009), the interaction between the river and groundwater is dependent on the difference between the hydraulic heads. For rivers gaining water from the aquifer, the discharge rate of groundwater will decrease until an equilibrium between the heads is reached (Brunner et al., 2009). In the case that the water table is lowered, the stream may supply water to the aquifer. Based on the proportion of water the Mogalakwena River and its tributaries are supplying to the aquifer, the river may supply water to the aquifer in regions where there are high abstraction rates which result in lowering of the water table.

7.2.4.2 Dam-aquifer interaction

Though there is an interaction between the aquifer and the dam, the process of exchange of water is not as extensive as the river and the aquifer. A small volume of water exchange is observed between the two components. Unlike the drainage system, the Glen Alpine Dam occupies a small areal extent, thus the water exchange is expected to be lower than the river. Both Figure 7.6 and Table 7.3 show that the groundwater system supplies more water to the dam as compared to the amount the dam supplies to the aquifer.

7.3 Prediction of Aquifer Response

The future fate of water availability in the Mogalakwena Subcatchment was investigated by considering the impacts of changing climate and anthropogenic factors on the aquifer system. The model parameters were varied to evaluate the change in water balance considering three scenarios:

I. decrease in recharge rate,
II. increase in abstraction rate,
III. increase in evapotranspiration rate.

7.3.1 Decrease in Recharge Rate

Climate change has influenced an ongoing decrease in rainfall patterns which alters the recharge rate resulting in declining water levels. How will the aquifer respond if the recharge rate decreases due to climate change? To answer this question the recharge rate was decreased at a rate of 10% each step to evaluate the aquifer's response. The resulting groundwater budget is shown in Table 7.5.

Table 7.5: Variation in water balance as groundwater recharge declines

Components	**Recharge-10%**		**Recharge-20%**		**Recharge-30%**		**Recharge-40%**	
	Inflow (m^3/d)	Outflow (m^3/d)	Inflow (m^3/d)	Outflow (m^3/d)	Inflow (m^3/d)	Outflow (m^3/d)	Inflow (m^3/d)	Outflow (m^3/d)
RCH	2,509E+10		2,25E+10		1,99E+10		1,72E+10	
River leakage	104924160	6222701	1,11E+08	5868547	1,18E+08	5484845	1,26E+08	5075136
GGHB	23785920	308318	24615360	290606	25505280	272721,6	26507520	254707
EVT		4,4E+09		4,2E+09		3,95E+09		3,7E+09
Wells		3456000		3456000		3456000		3456000
Surface Runoff		2,1E+10		1,9E+10		1,64E+10		2,2E+10
Total	2,522E+10	2,5E+10	2,26E+10	2,3E+10	2E+10	2,04E+10	1,74E+10	2,6E+10

As the recharge decreases, the river inflow slightly increases to compensate for the declining water table due to the river stage exceeding the height of the water table (Figure 7.7). In addition, the decrease in recharge rate is accompanied by a slight decrease in both surface runoff and evapotranspiration rate. A decrease in recharge rate results in deepening of the piezometric surface relative to the evapotranspiration extinction depth, which ultimately decreases the rate of evapotranspiration. Similarly, a decrease in recharge rate lowers the depth of the water level below the river stage, which consequently triggers the flow of water from the river to the aquifer. However, the volume of flow of water from the aquifer to the river decreases considerably due to the lowering of the depth of the piezometric surface below the river stage.

The volume of UZF surface runoff is expressed as a function of the amount of rain, which is the main source of groundwater recharge. Thus, the surface runoff decreases due to a decline in the amount of rainfall. The decrease in inflows and an increase in outflows corresponding to the GHB can be similarly attributed to the decline in the amount of recharge. In general, the water balance shows that as recharge decreases by 20% or more, the outflow exceeds the inflow resulting in a continuous drop in water level, which may ultimately risk the availability of groundwater in the area.

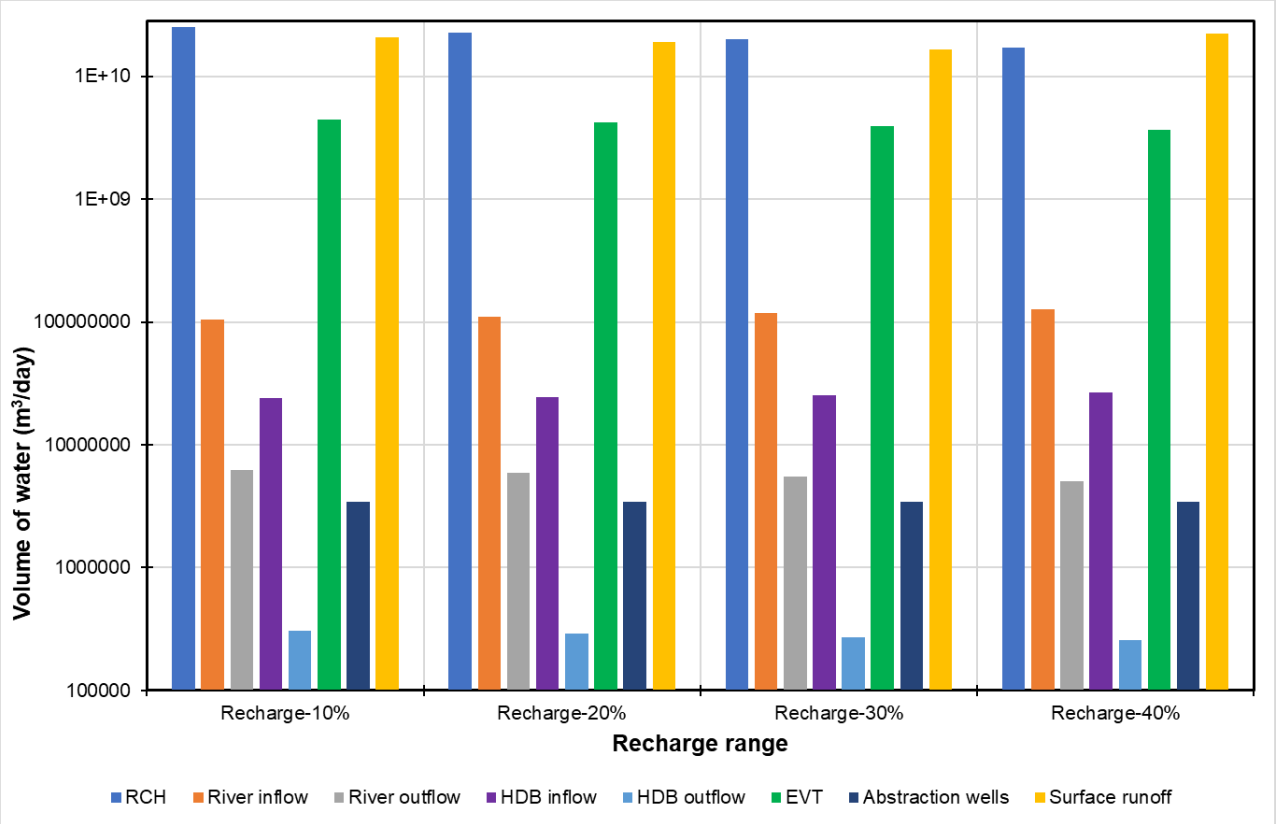

Figure 7.7: Graph showing the variation of the volume of water as groundwater recharge declines.

Figure 7.8 shows the changes in the simulated head as recharge decreases. The legend corresponding to each map indicates that the simulated head decreases with a decrease in recharge. Both the maximum and minimum simulated heads reduce as groundwater recharge declines (Figure 7.8).

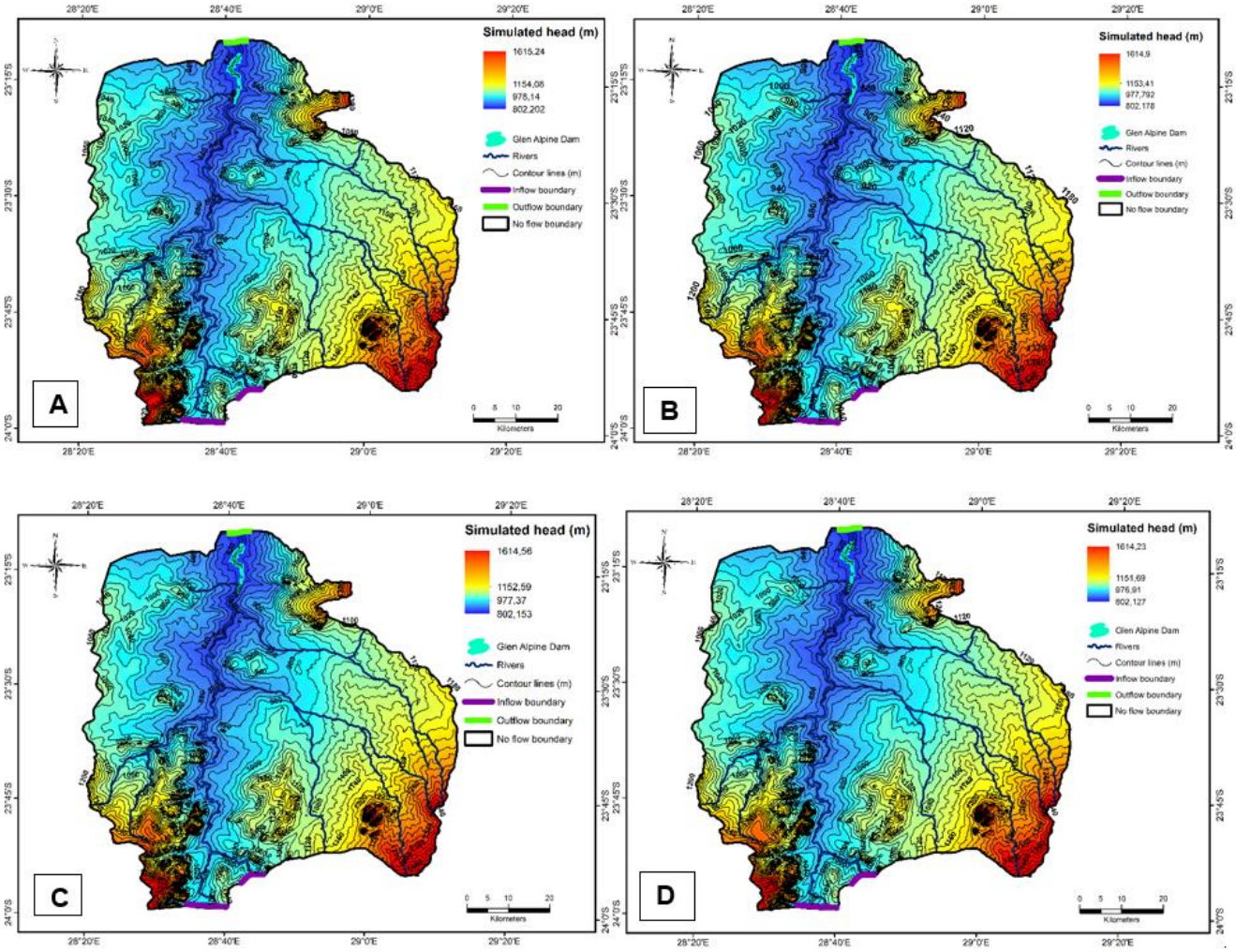

Figure 7.8: Water level contour maps of the simulated heads corresponding to decrease in recharge rates (A) recharge-10%, (B) recharge-20%, (C) recharge-30% and (D) recharge-40%.

7.3.2 Increase in Abstraction Rate

Population increase can impose pressure on the aquifer system due to increased water demand. Furthermore, economic developments such as mining and farming can project the demand for water to a higher level, which altogether put groundwater under significant stress. How will the aquifer respond if the abstraction rate increases due to population growth and/ industrialisation? To answer this question, the abstraction rate was successively increased, and the simulated water budget is presented in Table 7.6 and Figure 7.9. An increase in groundwater pumping rate results in a substantial decline in the simulated water level (Figure 7.9).

Table 7.6: Variation in water balance as abstraction rate increases. 2X, 3X and 4X represent twice, trice and quadruple increase in abstraction relative to the present groundwater use for domestic, irrigation and mining.

	2X abstraction rate		**3X abstraction rate**		**4X abstraction rate**	
Components	Inflow (m^3/d)	Outflow (m^3/d)	Inflow (m^3/d)	Outflow (m^3/d)	Inflow (m^3/d)	Outflow (m^3/d)
RCH	2,76E+10		2,76E+10		2,76E+10	
River leakage	99403200	6552489,6	99403200	6552489,6	99403200	6552489,6
GHBGHB	23016960	326160	23016960	326160	23016960	326160
EVT		4611600000		4,612E+09		4611600000
Wells		6912000		10368000		13824000
Surface Runoff		2,3085E+10		2,308E+10		2,3085E+10
Total	2,77E+10	2,771E+10	2,772E+10	2,771E+10	2,772E+10	2,7717E+10
Water Budget	11386310,4		7930310,4		4474310,4	

According to Winter et al. (1999), the increase in the pumping rate of water from shallow aquifers will result in a decline in the water quantity in the surface water bodies due to the surface water and groundwater interactions. Since the aquifer supplies most of the water to the Mogalakwena River, some of the water will be captured rather than discharged to the river due to the increased abstraction rate (Winter et al., 1999). Furthermore, the surrounding surface water bodies may be forced to supply water to the aquifer system (Winter et al., 1999). This implies that an increase in abstraction

rate in the study area has the capability of affecting both surface water and groundwater.

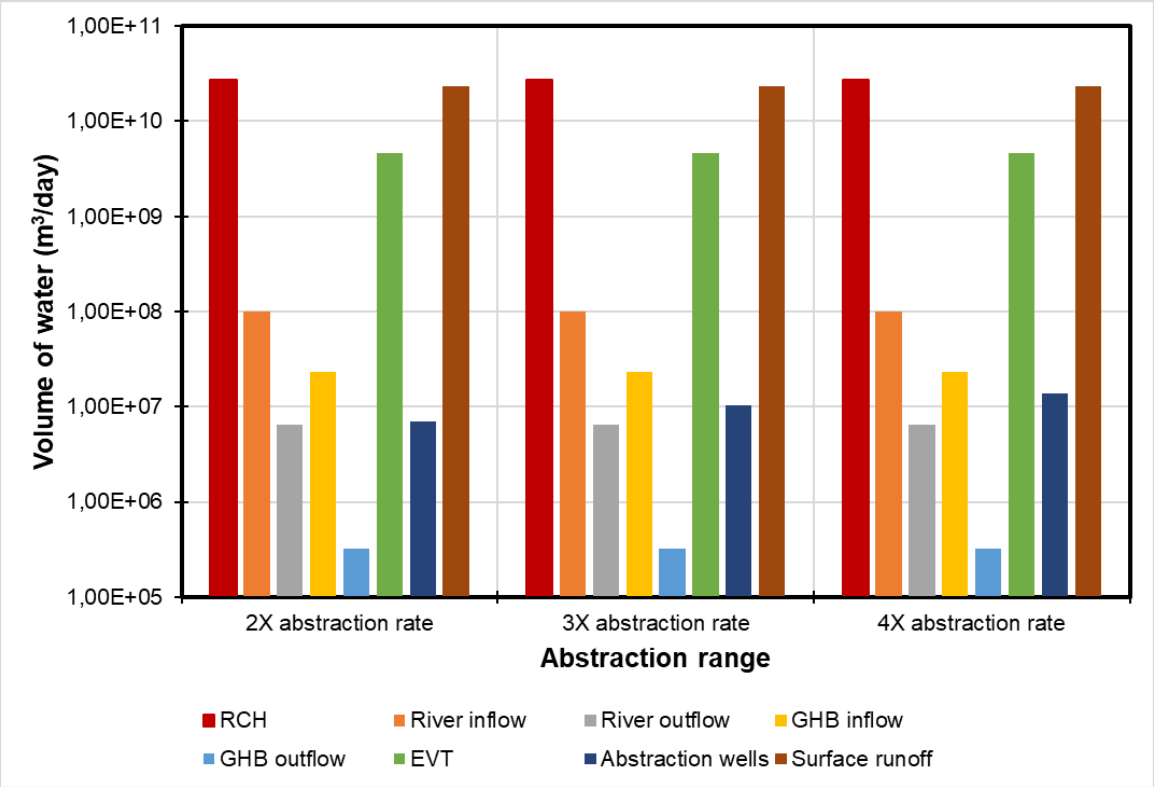

Figure 7.9: Graph showing the variation in water quantity as the groundwater abstraction rate increases.

7.3.3 Increase in Evapotranspiration Rate

Evapotranspiration rate is one of the major outflows in the model domain. The main factors contributing to a high evapotranspiration rate include climate change and anthropogenic activities, i.e., increase in temperature and plantation (e.g., emerging farms and land covered by trees that consume a large volume of water) can enhance the current evapotranspiration rate to a higher level. Table 7.7 and Figure 7.10 both show the changes in the groundwater budget as the evapotranspiration rate increases at a rate of 20% to 80% with a step of 20%. The availability of water diminishes as the rate of evapotranspiration increases (Table 7.7 and Figure 7.10).

Table 7.7: Water balance as evapotranspiration rate increases by 20%, 40%, 60% and 80%.

Com Ponent	**EVT+20%**		**EVT+40%**		**EVT+60%**		**EVT+80%**	
	Inflow (m^3/d)	Outflow (m^3/d)	Inflow (m^3/d)	Outflow (m^3/d)	Inflow (m^3/d)	Outflow (m^3/d)	Inflow (m^3/d)	Outflow (m^3/d)
RCH	2,8E+10		2,78E+10		2,8E+10		2,8E+10	
River leakage	1E+08	6421507	1,03E+08	6291475	1E+08	6164294	1,1E+08	6040742
GHB	2,3E+07	317148	23293440	308284	2,3E+07	299532	2,4E+07	291021
EVT		5,5E+09		6,4E+09		7,2E+09		8E+09
Wells		5011200		5028480		5028480		5028480
Surface Runoff		2,2E+10		2,2E+10		2,1E+10		2E+10
Total	2,8E+10	2,8E+10	2,79E+10	2,8E+10	2,8E+10	2,8E+10	2,8E+10	2,8E+10
Water balance	1,1E+07		15440881		9096814		8995596	

An increase in the evapotranspiration rate from 20% to 40%, 40% to 60% and 60% to 80% resulted in a decline in the volume of water that leaks from the aquifer to the river by 130,032 m^3/day, 127,181 m^3/day and 123,552 m^3/day. This is because an increase in evaporation rate has a direct impact by lowering the piezometers and decreasing the volume of water that flows from the aquifer to the river. This implies that an increase in abstraction rate results in lower piezometers than the river stage, which consequently initiated the flow of water from the river to the aquifer. However, the flow of water from the aquifer to the river decreases due to the piezometer being lower than the river stage. In addition, an increase in the evaporation rate from 20% to 40%, 40% to 60% and 60% to 80% resulted in a decline in the volume of water that flows from the aquifer to the GHB boundaries (dam, inflow, and outflow boundaries), which can be similarly attributed to a decline in the piezometer.

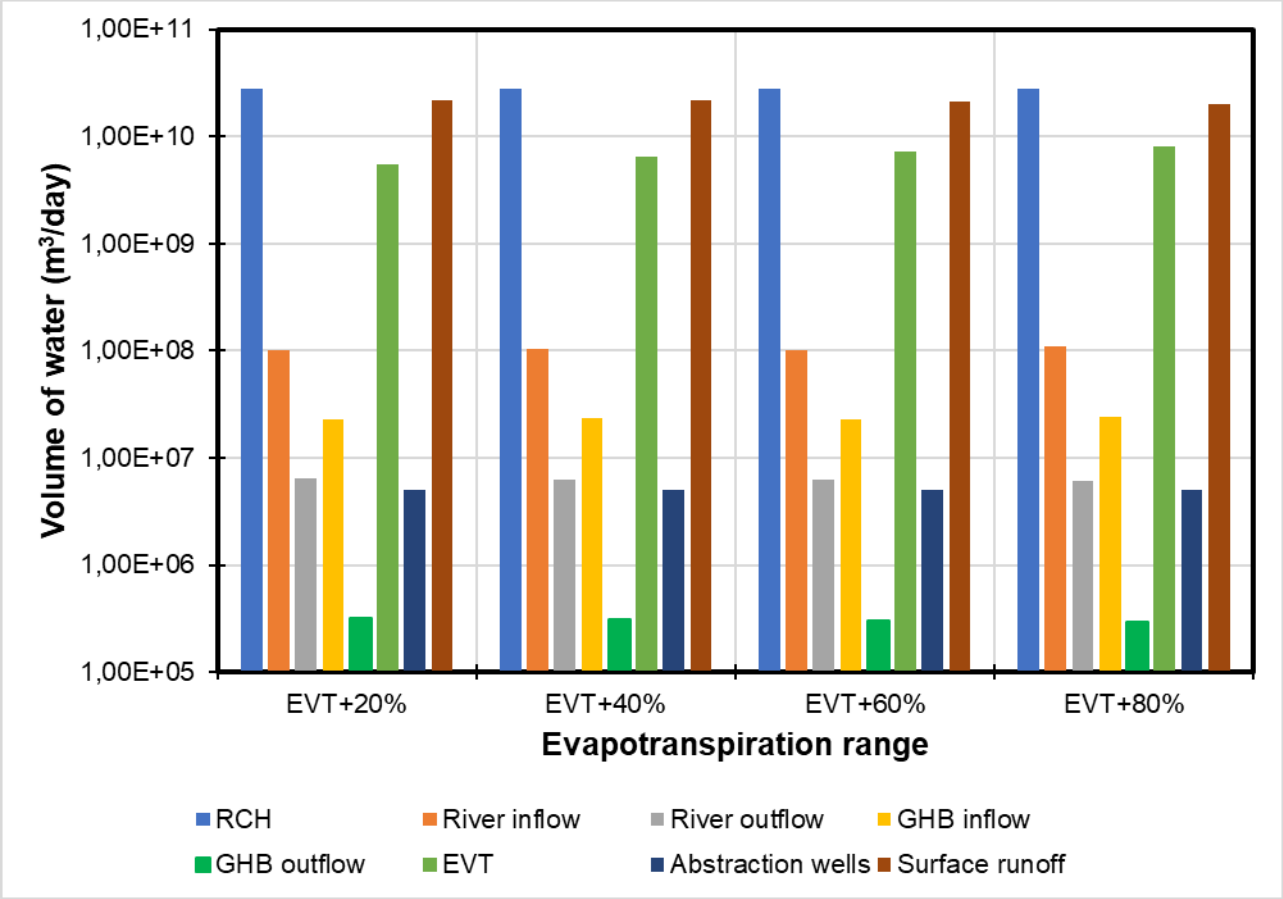

Figure 7.10: Graph showing the variation in water quantity as groundwater evapotranspiration rate increases.

7.4 Water Management

Based on the results of the three scenarios in section 7.2 and overall understanding of the study, the following measures may be important to implement to ensure the protection and sustainable use of groundwater and surface water in the Mogalakwena Subcatchment:

I. Mogalakwena Subcatchment receives rainfall mainly in summer with a negligible amount of rainfall in winter. The results of the numerical model of groundwater flow indicate that recharge is the major contributing factor to groundwater availability. Therefore, water can be conserved by rain harvesting during rainy seasons to preserve the water surplus from the surface and groundwater. This strategy will improve the availability of water during dry seasons (Jha and Gupta, 2003).

II. The surface runoff and evapotranspiration take the lion's share among the outflow components, which are 83.3% and 16.6%, respectively. Managing land cover and land use as well as eliminating alien trees that consume a large volume of water from the aquifer system may enable to reduce the water lost from the aquifer system through evapotranspiration and surface runoff.

III. The groundwater potential map can be utilised for further groundwater exploration to implement well fields which can be reliable for managing water use and protection and regulation of abstraction rate. Furthermore, the sustainable borehole yield of groundwater aquifers should be determined in order to regulate maximum daily borehole abstraction rates (Oljira, 2006).

IV. Mogalakwena Subcatchment is dominantly rural, and wastewater in the area can be reused depending on its quality for irrigation purposes, environmental and recreational uses instead of utilising freshwater for such activities (Tewari and Kushwaha, 2008).

V. The implementation of alternative water supply including large-scale water treatments and/ exploration of surrounding groundwater aquifers to supplement the declining groundwater levels (Oljira, 2006).

VI. Implementation of public awareness campaigns to educate communities about the scarcity, and deteriorating quality of both surface water groundwater at Mogalakwena Subcatchment is vital with respect to water use, protection, and management.

8. Conclusions and Recommendations

8.1 Conclusion

The main aim of the study was to understand how the dynamics of surface water-groundwater interactions affect the water balance at Mogalakwena Subcatchment. The investigation of the groundwater-surface water interactions was achieved through the implementation of steady-state numerical modelling of groundwater flow. In light of the discussion of the results, the following conclusions were drawn:

The quality of water in the Mogalakwena Subcatchment was evaluated using hydrochemical data and physical parameters. Most of the quality of water from the boreholes is within an acceptable limit of groundwater quality as prescribed by SANS241 (2015), with the exception of a few boreholes with high concentrations of nitrate, total dissolved solids (TDS) and chloride. The main hydrochemical facies in the area is Ca-Mg-HCO_3, which suggests that the presence of recently recharged fresh groundwater, though there are few wells with NaCl, Na-HCO_3 and Ca-Mg-Cl facies. In general, the hydrochemistry and physical parameters of groundwater suggest that the water in the study area is desirable for consumption with exception of a few boreholes that require treatment.

The analysis of water samples collected from shallow aquifers, Mogalakwena River and Glen Alpine Dam show enrichment in heavy isotopes which signifies the effect of extensive evaporation. However, there are water samples that show a strong correlation to the PLMWL, suggesting direct recharge from rainfall without undergoing extensive evaporation.

The present study used AHP and GIS techniques to delineate groundwater potential zones. Six thematic layers that include lineaments density, geology, land cover/land use, slope, soil and drainage density were combined to generate the groundwater potential zones of the area. The resulting map was classified into five categories depending on the favourability of the occurrence of groundwater. These are: - very low, low, moderate, high, and very high groundwater potential zones. Zones with high and very high groundwater potential are associated with sedimentary rocks (e.g., sandstone) and high lineament density, mainly in the western sector of the study area.

The water balance analysis of the calibrated steady-state model indicates that the recharge is the main inflow into the aquifer system, while surface runoff and evapotranspiration are the major outflows. The recharge contributes to 99.6% of inflow, followed by river leakage (0.36%) and GHB (0.08%). Among the outflow components, surface runoff takes the lion's share, i.e., 83.3%, followed by evapotranspiration (16.6%) and river leakage 0.02%. The results of the zone budget indicate that there is a strong interaction between the aquifer and surface water, mainly Mogalakwena River and Glen Alpine Dam. The surface water bodies gain a large volume of water from the aquifer system. The river gains more volume of water from the aquifer than the Glen Alpine Dam.

A predictive analysis of the aquifer's response to an increase in abstraction rate, evapotranspiration rate and a decrease in recharge was carried out. The results suggest that a decrease in recharge rate resulted in deepening of the piezometric surface relative to the evapotranspiration extinction depth, which ultimately decreases the rate of evapotranspiration. Similarly, a decrease in recharge rate lowers the depth of the water level below the river stage, which consequently initiates the flow of water from the river to the aquifer. However, the volume of flow of water from the aquifer to the river decreases considerably due to the lowering of the depth of the piezometric surface below the river stage.

Furthermore, the prediction of the aquifer response suggests that the surface runoff will decrease due to a decline in the amount of rainfall recharge, which consequently may have an impact on an ecosystem along the lower reaches of the Mogalakwena River Catchment, which mainly depends on surface water for their livelihood. Moreover, the results of the predictive analysis suggest that there will be a decrease in inflows and an increase in outflows corresponding to the GHB, which can be attributed to the impacts of the interaction between surface water and groundwater.

8.2 Model Limitations

A groundwater model is a simplification of a complex real hydrological system, which is usually developed based on a conceptual model that consists of numerous boundary conditions that are defined based on assumptions. For example, in this study, the inflows and outflows were defined based on assumptions. Although groundwater models are very important for predictions of future hydrological

scenarios, it is vital to note that the outcomes of the modelling exercise should be used within the scope of its limitations. The following are therefore the limitations of the present steady-state three-dimensional model of groundwater flow:

I. The hydraulic conductivity zones of the model domain were defined based on the available geological map of the area at a scale of 1:250,000. The boundary between adjacent hydraulic conductivity zones is an approximation of real boundaries, owing to the broad-scale nature of the geological map of the area that may not represent the local-scale observation of the contact between hydraulic conductivity zones. In addition, the hydraulic conductivity values assigned to each zone were based on information obtained from published articles and unpublished technical reports. The values used in this study may deviate if measured based on standard procedures that are widely used for the determination of the hydraulic conductivities of layers.

II. Groundwater recharge varies according to topographic relief, land use, land cover, soil type and type of rocks. Though the Unsaturated Zone Flow Package (UZF) provides reasonable estimates of the amount of infiltration that reaches the saturated zone, the UZF Package utilises several parameters that are implemented based on assumptions. These include Brooks-Corey epsilon, the saturated water content of soil and evapotranspiration extinction water content, etc. The infiltration rate was based on the chloride mass balance approach, while the evapotranspiration (EVT) rate was determined using Pennmann Monteith (FAO-56). Although most of the parameters used for numerical modelling were supported by field data, assumptions were implemented in the absence of observed field data.

III. The model domain was discretised at a grid cell size of 200 m by 200 m, which can be too coarse to provide a reasonable spatial resolution of the simulated hydraulic heads corresponding to the abstraction wells and the rivers. This may have partly contributed to the discrepancy between the simulated and observed hydraulic heads. Furthermore, there are several assumptions regarding the implementation of parameters such as well abstraction rate, borehole screen elevation, EVT extinction depth, the thickness of the interface between the aquifer and river, the thickness of the layer that separates the bottom of the

dam from the aquifer, etc. These parameters may not be determined with great certainty and may have partly contributed to the calibration process difficulty. Moreover, the assumptions might have partly contributed to the discrepancy between the simulated hydraulic head and the observed head.

IV. Most of the data used in this study were obtained from government organisations and public institutions. The measurements of several parameters were not reliable, and these prompted to use of assumptions during the implementation of the model. However, despite all these odds about assumptions, the results of the model are satisfactory and can be used as a frame of reference for regional-scale planning, management, protection, and sustainable use of water in the area.

8.3 Recommendations

The following recommendations are made based on the limitations highlighted in the above section:

I. Fieldwork that involves aquifer tests at selected boreholes may improve the uncertainties related to the hydraulic conductivities of the rocks. Furthermore, a transient model can be recommended subject to the availability of reliable spatial data to further understand the aquifer's response to temporal variation of boundary conditions and hydrological stresses.

II. Observation wells in the study area are limited and not evenly distributed. In addition, there is a gap in recordings of water levels at several monitoring wells. It is therefore recommended that future work should ensure the availability of an optimum number of observation heads (e.g., at least 25) that are preferably evenly distributed throughout the model area.

III. There is a wide gap in recordings of the abstraction rates corresponding to the abstraction wells used for modelling. Regular recording of the abstraction wells ensures groundwater management, protection, and sustainable use. In addition, the data improves the reliability of the results of numerical modelling of groundwater flow.

IV. There are only two river gauging stations located upstream and downstream of the Mogalakwena River. The stations are insufficient as there is a gap in understating the fluctuations of the river stage and discharge rates at the middle reach of the river. Additional gauging stations can improve the outcome of numerical simulation of groundwater flow.

V. Due to the fluctuation of groundwater level in response to climate change, the surface water recharges the aquifer, which may result in contamination of groundwater. Thus, regular monitoring of groundwater quality can be recommended to ensure the availability of safe and freshwater for domestic and other uses.

VI. The hydrogeological system of the Mogalakwena Subcatchment is very complex and requires field experience to understand and mitigate the prevailing water crisis in the area. Therefore, each municipality requires to permanently hire at least two qualified hydrogeologists who will be responsible for periodically monitoring groundwater level, aquifer test, sampling, chemical analysis of water, drilling site selection and supervision of borehole drilling. These will ensure groundwater protection, management, and the sustainable supply of water. Furthermore, the municipalities shall not rely on incompetent private contractors who usually fail to mitigate the prevailing water crisis in the area.

References

Abdelhalim, A., Sefelnasr, A. and Ismail, E., 2020. Response of the interaction between surface water and groundwater to climate change and proposed megastructure. Journal of African Earth Sciences, 162, pp.103-723.

Ahokpossi, D.P., 2017. Quantification and modelling of heterogeneities in aquifers (Doctoral dissertation, University of the Free State).

Anderson, M.P. and Woessner, W.W., 1992. The role of the postaudit in model validation. Advances in Water Resources, 15(3), pp.167-173.

Anderson, M.P., Woessner, W.W. and Hunt, R.J., 2015. Applied groundwater modelling: simulation of flow and advective transport. Academic press.

Aral, M.M. and Taylor, S.W. eds., 2011. Groundwater quantity and quality management. American Society of Civil Engineers.

Arulbalaji, P., Padmalal, D. and Sreelash, K., 2019. GIS and AHP techniques based delineation of groundwater potential zones: a case study from southern Western Ghats, India. Scientific reports, 9(1), pp.1-17.

Ashton, P.J., Love, D., Mahachi, H. and Dirks, P.H.G.M., 2001. An overview of the impact of mining and mineral processing operations on water resources and water quality in the Zambezi, Limpopo and Olifants Catchments in Southern Africa. Contract Report to the Mining, Minerals and Sustainable Development (Southern Africa) Project, by CSIR-Environmentek, Pretoria and Geology Department, University of Zimbabwe-Harare. Report No. ENV-PC, 42, pp.1-362.

Banejad, H., Mohebzadeh, H., Ghobadi, M.H., and Heydari, M., 2014. Numerical simulation of groundwater flow and contamination transport in Nahavand Plain aquifer, west of Iran. Journal of the Geological Society of India, 83(1), pp.83-92.

Banks, E.W., Simmons, C.T., Love, A.J., Cranswick, R., Werner, A.D., Bestland, E.A., Wood, M. and Wilson, T., 2009. Fractured bedrock and saprolite hydrogeologic controls on groundwater/surface-water interaction: a conceptual model (Australia). Hydrogeology Journal, 17(8), pp.1969-1989.

Barker, O.B., Brandl, G., Callaghan, C.C., Eriksson, P.G. and van Der Neut, M., 2006. The Soutpansberg and Waterberg groups and the Blouberg formation. The Geology of South Africa, pp.301-318.

Barratt, J.C., 2018. Episodic recharge of groundwater due to cyclonic events within the Limpopo province, South Africa (Doctoral dissertation, North-West University (South Africa), Potchefstroom Campus).

Bear, J., Beljin, M.S. and Ross, R.R., 1992. Fundamentals of ground-water modeling. Ground-water issue (No. PB-92-232354/XAB; EPA-540/S-92/005). Environmental Protection Agency, Ada, OK (United States). Robert S. Kerr Environmental Research Lab.

Broadhurst, J., 2019. The Contribution of Mining to Clean Water and Sanitation (SDG 6): Case Studies from South Africa. Sustainable Development in Africa: Case Studies, pp.220.

Brunner, P., Cook, P.G. and Simmons, C.T., 2009. Hydrogeologic controls on disconnection between surface water and groundwater. Water Resources Research, 45(1), pp.1-13.

Bumby, A.J., 2007. The geology of the Blouberg Formation, Waterberg and Soutpansberg Groups in the area of Blouberg mountain, Northern Province, South Africa (Doctoral dissertation, University of Pretoria).

Bumby, P., Eriksson, G., and Van Der Merwe R., 2004, The early Proterozoic sedimentary record in the Blouberg area, Limpopo Province, South Africa; implications for the timing of the Limpopo orogenic event, pp.123-131.

Busari, O., 2008. Groundwater in the Limpopo Basin: occurrence, use and impact. Environment, Development and Sustainability, 10(6), pp.943-957.

Busari, O., 2009. Groundwater use in parts of the Limpopo Basin, South Africa. In Proceedings of the 3rd International Conference of Energy and Development-Environment-Biomedicine, Athens, Greece, pp.29-31.

Cai, X., Magidi, J., Nhamo, L. and van Koppen, B., 2017. Mapping irrigated areas in the Limpopo Province, South Africa (Vol. 172). International Water Management Institute (IWMI).

Clark, I.D. and Fritz, P., 1997. Environmental isotopes in hydrogeology. CRC press.

Cook, P.G. and Herczeg, A.L. eds., 2012. Environmental tracers in subsurface hydrology.

Cook, P.G., 2003. A guide to regional groundwater flow in fractured rock aquifers Henley Beach, South Australia: Seaview Press, pp.151.

Craig, H., 1961. Isotopic variations in meteoric waters. Science, 133(3465), pp.1702-1703.

Dar, M.A., Sankar, K. and Dar, I.A., 2011. Fluorine contamination in groundwater: a major challenge. Environmental monitoring and assessment, 173(1), pp.955-968.

De Giglio, O., Quaranta, A., Barbuti, G., Napoli, C., Caggiano, G. and Montagna, M.T., 2015. Factors influencing groundwater quality: towards an integrated management approach. Ann Ig, 27, pp.52-57.

Department of Water Affairs & Forestry (DWAF)., 1996. In Holms S. Ed., South African water quality guidelines, 2nd ed., vol. 1: Domestic use, Pretoria: Department of Water Affairs & Forestry.

Dippenaar, M.A., Witthüser, K.T. and Van Rooy, J.L., 2009. Groundwater occurrence in Basement aquifers in Limpopo Province, South Africa: model-setting-scenario approach. *Environmental Earth Sciences*, *59*(2), pp.459-464.

Dube, T., Shoko, C., Sibanda, M., Baloyi, M.M., Molekoa, M., Nkuna, D., Rafapa, B. and Rampheri, B.M., 2020. Spatial modelling of groundwater quality across a land use and land cover gradient in Limpopo Province, South Africa. Physics and Chemistry of the Earth, Parts A/B/C, 115, pp.102-820.

El Alfy, M., 2014. Numerical groundwater modelling as an effective tool for management of water resources in arid areas. Hydrological Sciences Journal, 59(6), pp.1259-1274.

Elango, L., 2005. Numerical simulation of groundwater flow and solute transport. Chennai: Allied Publishers.

Ely, D.M. and Kahle, S.C., 2012. Simulation of groundwater and surface-water resources and evaluation of water-management alternatives for the Chamokane Creek basin, Stevens County, Washington. US Geological Survey Scientific Investigations Report, 5224, pp.74.

Eriksson, P., Long, D., Bumby, A., Eriksson, K., Simpson, E., Catuneanu, O., Claassen, M., Mtimkulu, M., Mudziri, K., Brümer, J. and van der Neut, M., 2008. Palaeohydrological data from the c. 2.0 to 1.8 Ga Waterberg Group, South Africa: discussion of a possibly unique Palaeoproterozoic fluvial style. South African Journal of Geology, 111(2-3), pp.281-304.

Eriksson, P.G., Hattingh, P.J. and Altermann, W., 1995. An overview of the geology of the Transvaal Sequence and Bushveld Complex, South Africa. Mineralium Deposita, 30(2), pp.98-111.

Feng, X., Faiia, A.M. and Posmentier, E.S., 2009. Seasonality of isotopes in precipitation: A global perspective. Journal of Geophysical Research: Atmospheres, 114(D8), pp.1-13.

Fourie, J., 2016. 179 Mogalakwena villages in water crisis with no end in sight. Review,15 January 2016.

Freeze, R.A., and Cherry, J.A., 1979, Groundwater: New Jersey, Prentice Hall.

Futornick, Z.O., 2015. Using MODFLOW to Predict Impacts of Groundwater Pumpage to Instream Flow: Upper Kittitas County, Washington, Master's thesis.

Gebere, A., Kawo, N.S., Karuppannan, S., Hordofa, A.T. and Paron, P., 2021. Numerical modeling of groundwater flow system in the Modjo River catchment, Central Ethiopia. *Modeling Earth Systems and Environment*, *7*(4), pp.2501-2515.

Gupta, S.K. and Deshpande, R.D., 2005. Groundwater isotopic investigations in India: What has been learned? Current Science, 89 (5). pp.825-835.

Hahn, N., 2011. Refinement of the Soutpansberg Geomorphic Province, Limpopo, South Africa. Transactions of the Royal Society of South Africa, 66(1), pp.32-40.

Harbaugh, A.W., Banta, E.R., Hill, M.C. and McDonald, M.G., 2000. Modflow-2000, the u. s. geological survey modular ground-water model-user guide to modularization concepts and the ground-water flow process. Open-file report. U. S. Geological Survey, (92), pp.134.

Hartzer, F.J., 1995. Transvaal Supergroup inliers: geology, tectonic development and relationship with the Bushveld Complex, South Africa. Journal of African Earth Sciences, 21(4), pp.521-547.

Harvey, K., 1995. A descriptive framework for compensation. The Translator, 1(1), pp.65-86.

Healy, R.W. and Cook, P.G., 2002. Using groundwater levels to estimate recharge. Hydrogeology journal, 10(1), pp.91-109.

Hentati, I., Triki, I., Trablesi, N. and Zairi, M., 2016. Piezometry mapping accuracy based on elevation extracted from various spatial data sources. Environmental Earth Sciences, 75(9), pp.802.

Holland, M. and Witthüser, K., 2009. Factors that control sustainable yields in the Archean basement rock aquifers of the Limpopo Province. The Basement Aquifers of Southern Africa, pp.67.

Holland, M. and Witthüser, K.T., 2011. Evaluation of geologic and geomorphologic influences on borehole productivity in crystalline bedrock aquifers of Limpopo Province, South Africa. Hydrogeology Journal, 19(5), pp.1065-1083.

Holland, M., 2011. Hydrogeological characterisation of crystalline basement aquifers within the Limpopo Province, South Africa (Doctoral dissertation, University of Pretoria).

Holland, M., 2012. Evaluation of factors influencing transmissivity in fractured hard-rock aquifers of the Limpopo Province. Water SA, 38(3), pp.379-390.

https://www.usgs.gov

Kareem, H., 2018. Study of water resources by using 3D groundwater modelling in Al-Najaf region, Iraq (Doctoral dissertation, Cardiff University).

Kinoti, I.K., 2018. Integraded hydrological modelling of surface and groundwater interactions in Heuningnes catchment (South Africa) (Master's thesis, University of Twente).

Kinzelbach, W. and Aeschbach, W., 2002. A survey of methods for analysing groundwater recharge in arid and semi-arid regions (Vol. 2). Division of Early Warning and Assessment, United Nations Environment Programme.

Konikow, L.F., 1996. Use of numerical models to simulate groundwater flow and transport. US Geological Survey, Reston, Virginia, USA, pp.75-116.

Krishan, G., 2019. Groundwater Salinity. Current World Environment, 14(2), pp.186.

Kumar, C.P., 2013. Numerical modelling of ground water flow using MODFLOW. Indian Journal of Science, 2(4), pp.86-92.

Kumar, P.S., 2013. Interpretation of groundwater chemistry using piper and Chadha's diagrams: a comparative study from Perambalur Taluk. Elixir Geosci, 54, pp.12208-12211.

Kramers, J.D., McCourt, S. and Van Reenen D.D. 2006. Limpopo Belt. The Geology of South Africa, pp.209-236.

Lombaard, J., Pieterse, H.S., Rossouw, J.R. and Nditwani, T., 2015. Project Name: Limpopo Water Management Area North Reconciliation Strategy.

Loudyi, D., 2005. 2D finite volume model for groundwater flow simulations: integrating non-orthogonal grid capability into modflow. Cardiff University (United Kingdom).

Machavaram, M.V. and Krishnamurthy, R.V., 1995. Earth surface evaporative process: a case study from the Great Lakes region of the United States based

on deuterium excess in precipitation. Geochimica et Cosmochimica Acta, 59(20), pp.4279-4283.

Magesh, N.S., Chandrasekar, N. and Soundranayagam, J.P., 2012. Delineation of groundwater potential zones in Theni district, Tamil Nadu, using remote sensing, GIS and MIF techniques. Geoscience frontiers, 3(2), pp.189-196.

McCarthy, T. S. and Rubidge, B., 2005. The story of Earth and Life A southern African perspective on a 4.6-billion-year journey. Published by Struik. Cape Town.

McCarthy, T.S., Rowberry, M.D., Brandt, D., Hancox, P.J., Marren, P.M., Tooth, S., Jacobs, Z., Thompson, M., Woodborne, S. and Ellery, W.N., 2011. The origin and development of the Nyl River floodplain wetland, Limpopo Province, South Africa: trunk-tributary river interactions in a dryland setting. South African Geographical Journal, 93(2), pp.172-190.

Merz, S.K., 2012. Australian groundwater modelling guidelines, Waterlines report, National Water Commission, Canberra

Moalafhi, D.B., Sharma, A. and Evans, J.P., 2017. Reconstructing hydro-climatological data using dynamical downscaling of reanalysis products in data-sparse regions–Application to the Limpopo catchment in southern Africa. Journal of Hydrology: Regional Studies, 12, pp.378-395.

Mohsin, M., Safdar, S., Asghar, F. and Jamal, F., 2013. Assessment of drinking water

Naidoo, K., 2005. The Anthropogenic impacts of Urbanization and Industrialisation on the Water Quality, Ecology and Health status of the Palmiet River catchment in Durban, KwaZulu-Natal (Doctoral dissertation).

Nasr, M. and Zahran, H.F., 2014. Using of pH as a tool to predict salinity of groundwater for irrigation purpose using artificial neural network. The Egyptian Journal of Aquatic Research, 40(2), pp.111-115.

Netshiendeulu, N. and Motebe, N., 2012. Nitrate contamination of groundwater and it's implications in the Limpopo Water Management Area. Water Practice and Technology, 7(4).

Nistor, M.M., 2019. Climate change effect on groundwater resources in South East Europe during 21st century. Quaternary International, 504, pp.171-180.

Niswonger, R.G., Panday, S. and Ibaraki, M., 2011. MODFLOW-NWT, a Newton formulation for MODFLOW-2005. US Geological Survey Techniques and Methods, 6(A37), pp.44.

Niswonger, R.G., Prudic, D.E. and Regan, R.S., 2006. Documentation of the unsaturated-zone flow (UZF1) package for modeling unsaturated flow between the land surface and the water table with MODFLOW-2005 (No. 6-A19).

Nthunya, L.N., Maifadi, S., Mamba, B.B., Verliefde, A.R. and Mhlanga, S.D., 2018. Spectroscopic determination of water salinity in brackish surface water in Nandoni Dam, at Vhembe District, Limpopo Province, South Africa. Water, 10(8), pp.990.

Odiyo, J.O. and Makungo, R., 2012. Water quality problems and management in rural areas of Limpopo Province, South Africa. WIT Transactions on Ecology and the Environment, 164, pp.135-146.

Oljira, E., 2006. Numerical groundwater flow modeling of the Akaki River catchment. Addis Ababa University, Ethiopia (MSc thesis).

Phungula, P. P. (2018). The use of diatoms in assessing water quality in the Nyl and Mogalakwena River system, in the Limpopo, South Africa (Doctoral dissertation, University of Johannesburg).

Preeja, K.R., Joseph, S., Thomas, J. and Vijith, H., 2011. Identification of groundwater potential zones of a tropical river basin (Kerala, India) using remote sensing and GIS techniques. Journal of the Indian Society of Remote Sensing, 39(1), pp.83-94.

Rankoana, S.A., 2016. Perceptions of climate change and the potential for adaptation in a rural community in Limpopo Province, South Africa. Sustainability, 8(8), pp.672.

Rao, N.S., 2006. Groundwater potential index in a crystalline terrain using remote sensing data. Environmental geology, 50(7), pp.1067-1076.

Regli, C., Rauber, M. and Huggenberger, P., 2003. Analysis of aquifer heterogeneity within a well capture zone, comparison of model data with field experiments: A case study from the river Wiese, Switzerland. Aquatic Sciences, 65(2), pp.111-128.

Reilly, T.E. and Harbaugh, A.W., 2004. Guidelines for evaluating ground-water flow models. US Department of the Interior, US Geological Survey. Scientific investigations report 2004-5058.

Robb, L.J., Brandl, G., Anhaeusser, C.R., Poujol, M., Johnson, M.R. and Thomas, R.J., 2006. Archaean granitoid intrusions. The Geology of South Africa, pp.57-94.

Roefs, M., 2001. Mogalakwena municipality: assessment of information: access & quality. Draft report prepared for the UNDP.

Roy, S., Hazra, S., Chanda, A. and Das, S., 2020. Assessment of groundwater potential zones using multi-criteria decision-making technique: a micro-level case study from red and lateritic zone (RLZ) of West Bengal, India. Sustainable Water Resources Management, 6(1), pp.1-14.

Rwanga, S.S., 2018. Modelling groundwater flow under recharge uncertainty: an application to central Limpopo (Doctoral dissertation, Tshwane University of Technology).

SANS, 2015. South African National Standard 241-1: Drinking water. Part 2: Application of SANS 241-1.

Schwartz, M.O., 2006. Numerical modelling of groundwater vulnerability: the example Namibia. Environmental Geology, 50(2), pp.237-249.

Sener, E., Davraz, A. and Ozcelik, M., 2005. An integration of GIS and remote sensing in groundwater investigations: a case study in Burdur, Turkey. Hydrogeology Journal, 13(5-6), pp.826-834.

Shamuyarira, K.K., 2017. Determination of recharge and groundwater potential zones in Mhinga area, South Africa (Doctoral dissertation).

Sharp, J.M., 2010. The impacts of urbanization on groundwater systems and Nkhonjera, G.K. and Dinka, M.O., 2017. Significance of direct and indirect impacts of climate change on groundwater resources in the Olifants River basin: A review. Global and Planetary Change, 158, pp.72-82.

Singh, A.K. and Kumar, S.R., 2015. Quality assessment of groundwater for drinking and irrigation use in semi-urban area of Tripura, India.

Siosemarde, M., Kave, F., Pazira, E., Sedghi, H. and Ghaderi, S.J., 2010. Determine of constant coefficients to relate total dissolved solids to electrical conductivity. World Academy of Science, Engineering and Technology, 46, pp.258-260.

Stober, I. and Bucher, K., 1999. Origin of salinity of deep groundwater in crystalline rocks. Terra Nova-Oxford, 11(4), pp.181-185.

Tessema, A., Nzotta, U. and Chirenje, E., 2014. Assessment of Groundwater Potential in Fractured Hard Rocks around Vryburg, North West Province, South Africa. Water Research Commission, Pretoria, WRC Report, (2055/1), pp.13.

Tewari, D.D. and Kushwaha, R.L., 2008. Socio-economics of groundwater management in Limpopo, South Africa: poverty reduction potential and resource management challenges. Water International, 33(1), pp.69-85.

Titus, R., Witthüser, K. and Walters, B., 2009. Groundwater and mining in the Bushveld Complex. In Proceedings of the international mine water conference, Pretoria, South Africa (pp.178-184).

Tooth, S., McCarthy, T.S., Hancox, P.J., Brandt, D., Buckley, K., Nortje, E. and McQuade, S., 2002. The geomorphology of the Nyl River and floodplain in the semi-arid Northern Province, South Africa. South African Geographical Journal, 84(2), pp.226-237.

Tshikolomo, K.A., Walker, S. and Nesamvuni, A.E., 2013. Prospect for Developing Water Storage through Analysis of Runoff and Storage Capacity of Limpopo and Luvuvhu-Letaba Water Management Areas of South Africa. International Journal of Applied Science and Technology, 3(3), pp.70-79.

Vatsala, P.M. and Ramakrishnaiah, C.R., 2021. Delineation of groundwater potential zones in Kolar District using remote sensing and GIS technology.

Vermeulen, P. and Bester, M., 2009, October. Assessment of how waste quality and quantity will be affected by mining of the Waterberg coal reserves. In International Mine Water Conference, pp.113-123.

Vinger, B., Hlophe, M. and Selvaratnam, M., 2012. Relationship between nitrogenous pollution of borehole waters and distances separating them from pit latrines and fertilized fields. Life Science Journal, 9(1), pp.402-407.

Vogel, H., Mokokwe, K. and Setloboko, T., 2004. Nitrate hotspots and salinity levels in groundwater in the Central District of Botswana. Environmental Geology Division Report, Department of Geological Survey, Lobatse, Botswana.

Wimalawansa, S.J., 2016. Effect of Water Hardness on Non-Communicable Diseases. Including Chronic Kidney Dis-ease of Multifactorial Origin (CKDmfo/CKDuo), pp.1-11.

Winter, T.C., Harvey, J.W., Franke, O.L. and Alley, W.M., 1999. Ground water and surface water. A single resource. USGS Circular, 1139.

Yang, Q., Mu, H., Guo, J., Bao, X. and Martín, J.D., 2019. Temperature and rainfall amount effects on hydrogen and oxygen stable isotope in precipitation. Quaternary international, 519, pp.25-31.

Zdechlik, R., 2016. A review of applications for numerical groundwater flow modeling. International Multidisciplinary Scientific GeoConference: SGEM, 3, pp.11-18.

Zhang, Y.K. and Schilling, K.E., 2006. Effects of land cover on water table, soil moisture, evapotranspiration, and groundwater recharge: a field observation and analysis. Journal of Hydrology, 319(1-4), pp.328-338.

Zhou, P., Li, M. and Lu, Y., 2017. Hydrochemistry and isotope hydrology for groundwater sustainability of the coastal multilayered aquifer system (Zhanjiang, China). Geofluids, 2017.

Zhu, T. and Ringler, C., 2012. Climate change impacts on water availability and use in the Limpopo River Basin. Water, 4(1), pp.63-84.

Zotarelli, L., Dukes, M.D., Romero, C.C., Migliaccio, K.W. and Morgan, K.T., 2010. Step by step calculation of the Penman-Monteith Evapotranspiration (FAO-56 Method). Institute of Food and Agricultural Sciences. University of Florida.